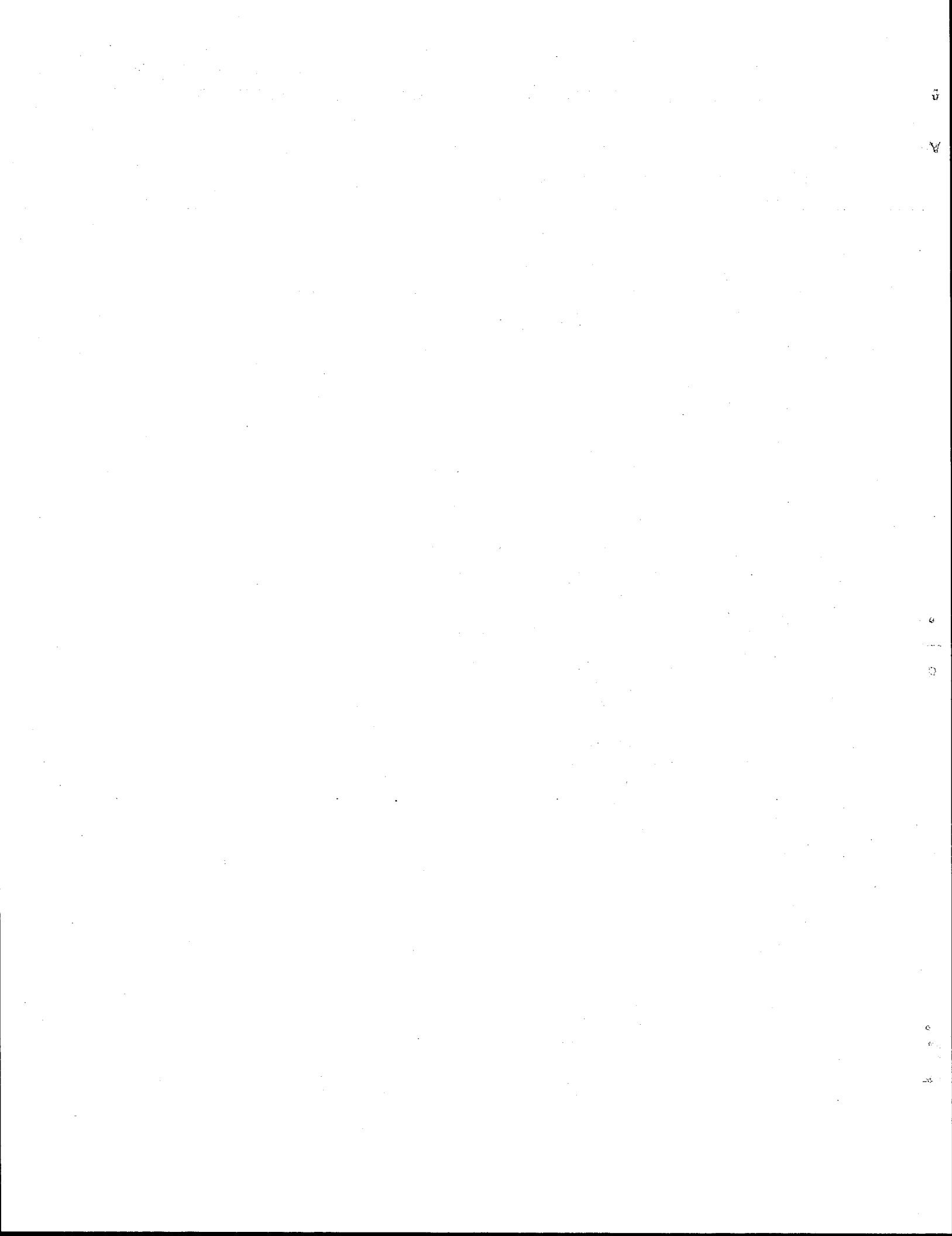


## TECHNICAL REPORT STANDARD TITLE PAGE

1. Report No. FHWATX78-211-2	2. Government Accession No.	3. Recipient's Catalog No.	
4. Title and Subtitle  Field Test and Preliminary Design Method for Laterally Loaded Drilled Shafts in Clay		5. Report Date September 1978	
6. Performing Organization Code			
7. Author(s) George L. Holloway, Harry M. Coyle, Richard E. Bartoszewitz and William G. Sarver		8. Performing Organization Report No. Research Report 211-2	
9. Performing Organization Name and Address Texas Transportation Institute Texas A&M University College Station, Texas 77843		10. Work Unit No.	
		11. Contract or Grant No. Study No. 2-5-77-211	
		13. Type of Report and Period Covered Interim-September, 1976 September, 1978	
12. Sponsoring Agency Name and Address State Department of Highways and Public Transportation; Transportation Planning Division P. O. Box 5051 Austin, Texas 78763		14. Sponsoring Agency Code	
15. Supplementary Notes Research performed in cooperation with DOT, FHWA. Study Title: Design of Drilled Shafts to Support Precast Panel Retaining Walls			
16. Abstract The behavior of a laterally loaded drilled shaft in clay has been investigated by conducting a second lateral load test on an instrumented shaft. For each increment of the applied lateral load, the shaft rotation, the soil resistance, and the lateral deflection were measured. Pneumatic pressure cells were used to measure the soil resistance along the shaft. Dial gages located at the top of the shaft were used to measure the lateral deflection, and an inclinometer was used to measure the rotation of the shaft. The lateral load was measured with a strain gaged load cell. The ultimate lateral load for this test was defined as the load where the amount of lateral movement which occurred was enough to develop the limiting soil resistance. Using this definition for ultimate lateral load, it was possible to compare the ultimate soil reaction predicted by several analytical procedures with the soil reaction calculated from the soil resistance measured at the ultimate lateral load. Also, the ultimate lateral load for the test shaft was predicted using various analytical methods, and a comparison was made between the predicted ultimate loads and the measured ultimate load. Finally, a comparison was made between the measured ultimate loads obtained from six other load tests reported in the technical literature and the ultimate loads predicted by the different analytical methods. Based upon the comparison of measured versus predicted ultimate loads a preliminary design procedure for the design of rigid laterally loaded drilled shafts is presented. However, additional load tests are needed before this preliminary design procedure can be finalized.			
17. Key Words Drilled shaft, lateral load test, pressure cells, soil reaction, ultimate load, deflection, rotation, soil creep.		18. Distribution Statement No Restrictions. This document is available to the public through the National Technical Information Service, Springfield, Virginia 22161	
19. Security Classif. (of this report) Unclassified	20. Security Classif. (of this page) Unclassified	21. No. of Pages 109	22. Price



FIELD TEST AND PRELIMINARY DESIGN METHOD  
FOR LATERALLY LOADED DRILLED SHAFTS IN CLAY

by

George L. Holloway  
Research Assistant

Harry M. Coyle  
Research Engineer

Richard E. Bartoszewitz  
Engineering Research Associate

and

William G. Sarver  
Research Associate

Research Report No. 211-2

Design of Drilled Shafts to Support Precast Panel Retaining Walls  
Research Study Number 2-5-77-211

Sponsored by  
State Department of Highways and Public Transportation  
in Cooperation with the  
U.S. Department of Transportation  
Federal Highway Administration

September 1978

TEXAS TRANSPORTATION INSTITUTE  
Texas A&M University  
College Station, Texas

### **Disclaimer**

The contents of this report reflect the views of the authors who are responsible for the facts and accuracy of the data presented herein. The contents do not necessarily reflect the views or policies of the Federal Highway Administration. This report does not constitute a standard, specification or regulation.

There was no invention or discovery conceived or first actually reduced to practice in the course of or under this contract, including any art, method, process, machine, manufacture, design or composition of matter, or any new and useful improvement thereof, or any variety of plant which is or may be patentable under the patent laws of the United States of America or any foreign country.

## ABSTRACT

The behavior of a laterally loaded drilled shaft in clay has been investigated by conducting a second lateral load test on an instrumented shaft. For each increment of the applied lateral load, the shaft rotation, the soil resistance, and the lateral deflection were measured. Pneumatic pressure cells were used to measure the soil resistance along the shaft. Dial gages located at the top of the shaft were used to measure the lateral deflection, and an inclinometer was used to measure the rotation of the shaft. The lateral load was measured with a strain gaged load cell.

The ultimate lateral load for this test shaft was defined as the load where the amount of lateral movement which occurred was enough to develop the limiting soil resistance. Using this definition for ultimate lateral load, it was possible to compare the ultimate soil reaction predicted by several analytical procedures with the soil reaction calculated from the soil resistance measured at the ultimate lateral load. Also, the ultimate lateral load for the test shaft was predicted using various analytical methods, and a comparison was made between the predicted ultimate loads and the measured ultimate load. Finally, a comparison was made between the measured ultimate loads obtained from six other load tests reported in the technical literature and the ultimate loads predicted by the different analytical methods.

Based upon the comparison of measured versus predicted ultimate loads a preliminary design procedure for the design of rigid laterally loaded drilled shafts is presented. However, additional load tests are needed before this preliminary design procedure can be finalized.

KEY WORDS: Drilled Shaft, Lateral Load Test, Pressure Cells, Soil Reaction, Ultimate Load, Deflection, Rotation, Soil Creep.

## SUMMARY

This report presents the results of the second year of a four-year study on drilled shafts (piers) that are used to support precast panel retaining walls. The objective of the study is to develop rational criteria for the design of foundations for this purpose.

During the first year it was determined that many drilled shafts that are used in this manner can be designed or analyzed as rigid structural members. The first part of this report briefly summarizes some of the work that has been done by others within recent years relating to the design of rigid shafts, the prediction of lateral load capacities, and the measurement of lateral soil pressures.

A field test was conducted on a 36-in. diameter shaft embedded 15-ft in clay. Passive lateral pressures in the longitudinal direction on the shaft were measured with 6-in. square pressure cells. At one point on the shaft three cells were mounted along a circumferential line to measure the horizontal pressure distribution. Lateral displacement of the shaft was measured at one point located about 9-in. above ground level. Rotation of the shaft was measured by an inclinometer and also by horizontal offsets from a plumb line to several points on the shaft. An electric strain gage type load cell was used to measure the lateral load that was applied by means of a hydraulic winch connected to a block and tackle.

A comparison was made between the ultimate soil reaction computed from the test data and the values predicted by several analytical methods. A comparison was also made between (1) the measured ultimate load and the loads predicted by several analytical techniques, and (2) the ultimate loads obtained from six load tests reported in the literature and the corresponding loads predicted by the same analytical techniques.

A preliminary design procedure for rigid laterally loaded drilled shafts is presented. The procedure is based upon the comparison of the measured versus predicted ultimate loads.

## IMPLEMENTATION STATEMENT

A preliminary procedure has been developed for the design of laterally loaded drilled shafts in clay to support precast panel retaining walls. The procedure was developed from the results of lateral load tests conducted on two shafts similar in size to those that would be used in practice. It was found that the ultimate lateral load in each case exceeded the load that could be reasonably expected to occur in a normal service structure. However, in each case the shaft rotation at the ultimate load was too great to be aesthetically acceptable. Recognizing this fact, it appears that the design of drilled shafts for this purpose may be realistically designed on the basis of a limiting value of rotation in conjunction with a required lateral load capacity. Moreover, it is not known at this time what effect, if any, the phenomenon of time-dependent soil creep will have on the interrelationship between load and rotation. A "creep-test" is planned for the third year of this study in order to possibly resolve this question. Therefore, it is recommended that implementation of the study findings to date should not be carried out until all test data relative to shafts in clay are obtained and the results have been thoroughly analyzed.

## ACKNOWLEDGEMENTS

The combined efforts of many people were required to successfully complete the objectives of the second year of this research study. Sincere gratitude is expressed to all who participated in the study, especially to the State Department of Highways and Public Transportation (SDHPT) and the Federal Highway Administration (FHWA) whose cooperative sponsorship made the research possible.

The authors are grateful to Mr. H. D. Butler of the SDHPT Bridge Division who served as the contact representative, and to Mr. Robert E. Long of the SDHPT Materials and Test Division who was the assistant contact representative for the study. Their cooperation and suggestions were most helpful to the research staff. Gratitude is also expressed to Mr. Charles Duncan, contact representative with the Federal Highway Administration, for his continued interest in the study.

Sincere appreciation is extended to Messrs. Eddie Denk and Bill Ray of the Engineering and Construction section of the Texas Transportation Institute research support services group, and to the men under their supervision. The successful completion of the field portion of this study would not have been possible without their dedicated cooperation.

## TABLE OF CONTENTS

INTRODUCTION . . . . .	1
Drilled Shaft Characteristics . . . . .	1
Rigid Behavior of Laterally Loaded Cylindrical Foundations . . . . .	2
Objectives of This Study . . . . .	7
FIELD LOAD TEST . . . . .	10
Soil Conditions . . . . .	10
Loading System . . . . .	17
Test Shaft . . . . .	19
Instrumentation . . . . .	21
Test Shaft Construction . . . . .	27
Loading Procedure . . . . .	29
TEST RESULTS . . . . .	35
Pressure Cell Data . . . . .	35
Load-Deflection Characteristics . . . . .	52
Load-Rotation Characteristics . . . . .	52
Ultimate Soil Reaction . . . . .	56
Ultimate Load on Rigid Shafts . . . . .	61
PRELIMINARY DESIGN PROCEDURE . . . . .	67
Force Acting on Retaining Wall . . . . .	67
Application Point of Resultant Force . . . . .	68
Soil Shear Strength . . . . .	68
Allowable Shaft Rotation . . . . .	69
Soil Creep . . . . .	71
Drilled Shaft Design Method . . . . .	71

Proposed Design Procedure . . . . .	74
Example of Design Procedure . . . . .	75
CONCLUSIONS AND RECOMMENDATIONS . . . . .	80
Conclusions . . . . .	80
Recommendations . . . . .	81
APPENDIX I - REFERENCES . . . . .	83
APPENDIX II - NOTATION . . . . .	87
APPENDIX III - EXPLANATION OF SPECIAL LOADING PROCEDURES . . . . .	89

## LIST OF TABLES

Table	Page
1. Initial Pressure Cell Readings . . . . .	35
2. Rotation Point Below the Groundline . . . . .	57
3. Comparisons of Measured Ultimate Loads with Predicted Ultimate Loads . . . . .	63
III-1 Deflections for Constant Time Interval (Reload 120 kips) . . . . .	90
III-2 Deflections for Constant Time Interval (Load 125 kips) . . . . .	91
III-3 Deflections for Constant Time Lateral (Load 125 kips) . . . . .	92
III-4 Deflections for Constant Time Interval (Load 130 kips) . . . . .	93
III-5 Deflections for Constant Time Interval (Reload 130 kips) . . . . .	94
III-6 Deflections for $\pm$ 50 Microstrain Range (Reload 130 kips) . . . . .	96

## LIST OF FIGURES

Figure		Page
1	PRECAST PANEL RETAINING WALL . . . . .	8
2	LOCATION OF BORINGS . . . . .	11
3	BORING - S1 . . . . .	12
4	BORING - S2 . . . . .	13
5	BORING - S3 . . . . .	14
6	BORING - S4 . . . . .	15
7	BORING - S5 . . . . .	16
8	TEXAS CONE PENETROMETER TEST . . . . .	18
9	LOADING SYSTEM . . . . .	20
10	STEEL REINFORCING CAGE . . . . .	22
11	TERRA TEC PRESSURE CELL (ROUND PLATE) . . . . .	23
12	TERRA TEC PRESSURE CELL (SQUARE PLATE) . . . . .	24
13	STRAIN GAGED LOAD CELL . . . . .	26
14	POSITION OF DEFLECTION DIAL GAGES . . . . .	28
15	LOCATION OF PRESSURE CELLS . . . . .	30
16	LATERAL LOAD VS DEFLECTION AT GROUNDLINE . . . . .	33
17	LATERAL LOAD VS LATERAL PRESSURE, CELL 885 . . . . .	38
18	LATERAL LOAD VS LATERAL PRESSURE, CELL 890 . . . . .	39
19	LATERAL LOAD VS LATERAL PRESSURE, CELL 893 . . . . .	40
20	LATERAL LOAD VS LATERAL PRESSURE, CELL 878 . . . . .	41
21	LATERAL LOAD VS LATERAL PRESSURE, CELL 886 . . . . .	42
22	LATERAL LOAD VS LATERAL PRESSURE, CELL 888 . . . . .	43
23	LATERAL LOAD VS LATERAL PRESSURE, CELL 898 . . . . .	44
24	LATERAL LOAD VS LATERAL PRESSURE, CELL 892 . . . . .	45

Figure	Page
25 LATERAL LOAD VS LATERAL PRESSURE, CELL 875 . . . . .	46
26 LATERAL LOAD VS LATERAL PRESSURE, CELL 876 . . . . .	47
27 LATERAL PRESSURE VS DEPTH BELOW GROUNDLINE . . . . .	50
28 HORIZONTAL PRESSURE VS LATERAL LOAD . . . . .	51
29 LATERAL LOAD VS DEFLECTION AT GROUNDLINE . . . . .	53
30 LATERAL DEFLECTION VS TIME . . . . .	54
31 LATERAL LOAD VS ROTATION . . . . .	55
32 ULTIMATE SOIL REACTION VS DEPTH BELOW GROUNDLINE . . . .	60
33 DESIGN CHART FOR COHESIVE SOILS . . . . .	73

## INTRODUCTION

### Drilled Shaft Characteristics

Drilled shafts are cylindrical foundation elements that serve essentially the same function as piles. The only significant difference between the two is the method of installation. Drilled shafts are usually constructed by placing concrete in an excavated cylindrical hole, whereas, piles are driven directly into the soil. The purpose of these types of foundation elements is to transfer structural loads from the surface to a depth in the soil where a more adequate bearing strata is found. Other terms which are used to describe the drilled shaft foundation element are drilled pile, bored piles, and drilled caisson (38). The term "drilled shaft" will be used in this study.

The manner in which a drilled shaft resists an axial load varies according to the subsurface material and physical dimensions of the shaft. The bearing capacity is derived from a combination of frictional resistance and end-bearing resistance. Drilled shafts are usually designed for end-bearing in the case where the shaft is placed through soft or compressible deposits and supported on dense soil or rock. A drilled shaft may also be constructed with an enlarged base in order to provide additional end-bearing capacity (7).

Widespread use of drilled shafts began near the end of World War II. The increased use of shafts was the result of the need by the Army for rapid construction of light service buildings. Today, truck or crane

---

Numbers in parentheses refer to the references listed in Appendix I.

mounted drilling rigs are capable of producing holes with diameters ranging from 12 in. to 20 ft (30 cm to 6.1 m) and shaft depths in excess of 200 ft (61.0 m). Battered shafts, those which are skewed from the vertical, can also be constructed if the contractor has suitable drilling equipment (38).

Drilled shafts have some distinct advantages over piles. The most important one is that the shaft can be drilled to the anticipated bearing stratum, whereas, a pile may seek refusal in dense sand layers, in weathered rock, or in soil with obstructions. Shafts are drilled with virtually no displacement to the foundation soil. On the other hand, pile driving with its associated vibrations, remolds and displaces the adjacent soil (3). Shafts which have been underreamed provide additional advantages over driven piles. Two advantages which are obtained by underreaming are increased bearing capacity of the shaft and uplift resistance.

#### Rigid Behavior of Laterally Loaded Cylindrical Foundations

In 1932 Sieler (32) suggested that a parabolic stress distribution was developed along the buried length of a timber pole subjected to lateral loads. From this early work with timber poles a design chart was developed for calculating the required embedment depth for poles subjected to lateral loads. This parabolic stress distribution, which was later confirmed by Rutledge (26), Osterberg (25) and Shilts et al. (33), satisfied statics and included the distributed effect of the soil resistance. However, several arbitrary assumptions were made in these studies. The most notable assumption was that the point of rotation

occurred at a depth of two thirds the embedment depth and that the soil resistance was zero.

J. Brinch Hansen (12) developed a method for the design of rigid foundations based on theoretical earth pressure coefficients,  $k_c$  and  $k_q$ . The coefficient,  $k_c$  is determined from the product of the bearing capacity factor and a depth factor. The coefficient  $k_q$  is the product of the at rest earth pressure coefficient, the tangent of the angle of shearing resistance, and the bearing capacity factor. Hansen's method requires an iterative process for the summation of moments about an assumed point of rotation. The process is quickly converging and usually only 2 or 3 trials are necessary before a solution is achieved. However, this method is not easily adaptable to chart solutions for routine designs.

In two related publications, Broms (4, 5) discussed the lateral resistance and the design of piles in cohesive soils. From studies conducted on short rigid piles Broms determined that the ultimate lateral soil resistance is equal to nine times the undrained cohesive strength of the soil multiplied by the pile diameter. The soil resistance was neglected from the ground surface to a depth of one and a half times the pile diameter. As a result of this work, a dimensionless design chart was developed from which deflections, embedment depths, and maximum bending moments could be obtained.

In 1966, Ivey and Hawkins (17) proposed a method to calculate the embedment depth of drilled shafts for the support of sign structures. The method utilizes the same parabolic soil pressure distribution as that suggested by Sieler (32) in 1932. However, the Rankine passive

earth pressure formula (35) is used to determine the maximum allowable passive pressures. The maximum allowable passive pressure is then reduced to an average allowable pressure by an appropriate geometric reduction factor to fit to the parabolic soil pressure distribution. Since Rankine's formula is based on a theoretically frictionless medium, the presence of friction in an actual case introduces an error on the safe side for this design procedure. In later studies directed by Ivey (11, 15, 16, 18) a three dimensional analysis of the laterally loaded drilled shaft problem was developed. This analysis takes into account all shear forces acting on the shaft when determining the ultimate resistance due to overturning loads. A series of model and full scale tests were conducted which indicated that a modifying factor should be introduced into the calculation of the coefficients of passive and active earth pressure. Using the theory developed in this study, predicted values of ultimate load are unconservative. However, the theory gives conservative results for rotations up to  $3^{\circ}$ .

Numerous other authors (1, 7, 14, 19, 22, 35) have conducted studies which involve the measurement of soil pressure on cylindrical foundations by the use of pressure cells or pressure gages. In addition to direct measurements of soil pressure, several investigators have reported soil reactions that were determined indirectly from instrumented piles or drilled shafts (9, 21, 23, 30, 31, 39). The soil reactions were determined by double-differentiation of the bending moments that were obtained from strain gage measurements. However, before either method of measurement was employed, the researcher had to decide whether to use an elastic or rigid behavior analysis in determining the relative

flexibility of the shaft.

The determination of whether a drilled shaft behaves either elastically or rigidly is dependent upon the relationship between the soil stiffness and the shaft flexural stiffness. Methods of determining drilled shaft behavior have been proposed by Broms (4), Vesic (37), Matlock and Reese (24), Davisson and Gill (8), and Lytton (20). Most of these methods require the use of a stiffness ratio in order to determine the relative stiffness of the shaft with respect to the soil. A comparison of the results obtained by the different methods shows that they give similar results, and therefore, it makes little difference which method is used.

Hays et al. (13) developed two methods of solution for the rigid pile problem. The first, being a more analytical approach, was a discrete element solution utilizing the Winkler assumption and load deformation curves. Using this analytical approach it was observed that the point of rotation was not located at a constant distance below the ground surface but shifted from somewhere below the middle of the pile embedment depth for light loads to a depth below the three quarters point for failure loads. The point of rotation varied at ultimate loads for different soils and for different ratios of applied moment to shear. It should also be noted that this solution assumed that premature material failure did not occur and that the load-deformation curves experienced continued deflection at the maximum value of soil reaction.

The second method for the solution of rigid pile behavior was called the Ultimate Load Solution. The assumption used in this method was that the soil resistance is at its maximum value along the whole

length of the pile, even though the maximum resistance will never be reached around the rotation point. The solution is a quickly converging iterative process involving the selection of trial embedment depths. It is greatly enhanced by the development of design charts.

In 1977, Kasch (19) measured the pressure distribution in the soil along a drilled shaft subjected to large lateral loads. The measurement system used to measure soil pressure consisted of a series of pressure cells placed vertically along the shaft. A load cell instrumented with strain gages was used to measure the lateral load applied to the shaft. The ultimate soil resistance was never developed during this test because the test shaft failed structurally prior to soil failure. However, a tentative design procedure was developed on the results of this test and other existing design methods.

Although there are a number of methods which are available for predicting lateral load behavior of drilled shafts, relatively few full-scale field tests have been conducted which could be used to determine the best method. Bhusham, Haley, and Fang (2) have reported on 12 drilled shaft tests. The test shafts varied in size from 2 to 4 ft (0.6 to 1.2 m) in diameter and 9 to 22 ft (2.7 to 6.7 m) in length. Detailed laboratory investigations of the soil parameters were included for each site. A computer program (29) entitled "Analysis of Laterally Loaded Piles by Computer," (Code name - COM622) was used to predict lateral deflections and the results were compared with field measurements. Using this method, the soil properties are characterized by load-deflection curves (21, 23, 24, 31) and the flexural stiffness of the pile is characterized in an appropriate manner to obtain compatibility

between the pile and soil deflection. The results of these investigations indicated that for laterally loaded drilled shafts in clay the agreement between the measured and predicted lateral deflections was good for deflections up to 0.5 in. (1.3 cm). However the agreement became progressively worse at larger deflections.

### Objectives of This Study

The State Department of Highways and Public Transportation (SDHPT) has in recent years developed a new concept in retaining wall design and construction. The new type of retaining wall makes use of precast panels that are placed between T-shaped pilasters. The pilasters are spaced approximately twelve feet on centers, and are supported by drilled shafts as shown in Fig. 1. The precast panel derives its restraining ability from the pilasters, which are located at the edges of the panel. The active earth pressures acting on the panel are transmitted to the pilasters and must be resisted by the soil in contact with the drilled shafts. Both passive and active pressures may be developed in the soil which is in contact with the shaft. Since the magnitude and distribution of these pressures are not well known and understood at this time, shaft designs have been necessarily conservative to ensure the long-term stability of the walls.

Wright, Coyle, Bartoskewitz, and Milberger (39) have developed design criteria for determining the lateral earth pressures developed in the cohesionless backfill acting on precast panel walls. As part of this study on precast panel retaining walls, Wright, et al., instrumented one drilled shaft with pressure cells in order to verify that this method

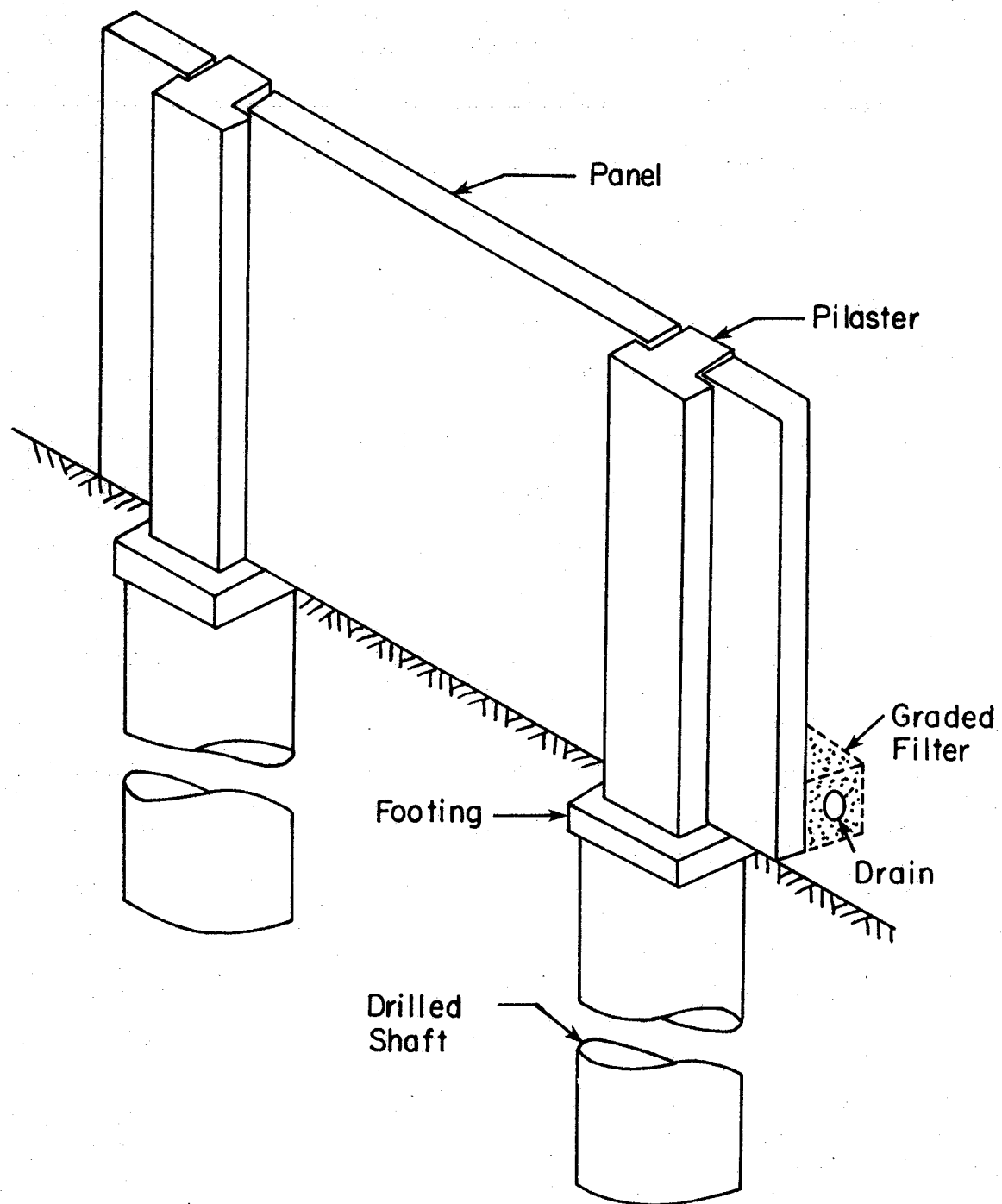


FIG. 1 - PRECAST PANEL RETAINING WALL

could be used to measure pressure distribution on the shaft. It was determined that the method could be used in future research studies.

A three-year research study was begun at Texas A&M University in 1977 to develop a rational design criteria for the design of drilled shafts supporting precast panel retaining walls. The first year of the study was devoted to the testing of one drilled shaft and the results have been reported by Kasch et al. (19). The test shaft for the first year had the same dimensions as those used in the related studies by Prescott (27) and Wright (39) on precast panel walls. As mentioned previously, this test shaft failed structurally and some minor problems were encountered with the loading system. Consequently, a soil failure was not attained during the 1977 test program. However, the use of pressure cells to measure soil pressure reaction was successful, and their use was continued in future test programs.

During the second year of this study a test shaft was constructed and tested in order to insure a failure in the soil. The shaft contained enough reinforcing steel to insure that a structural failure would not occur, and the loading system was redesigned for the anticipated higher failure loads. Also, pressure cells were placed on the horizontal as well as the vertical axis of the test shaft in order to study pressure distributions in both directions. The test procedure followed by Kasch (19) during the 1977 test was used during the initial phase of this test program. The results of the test program which was conducted during the second year of this research study are reported herein.

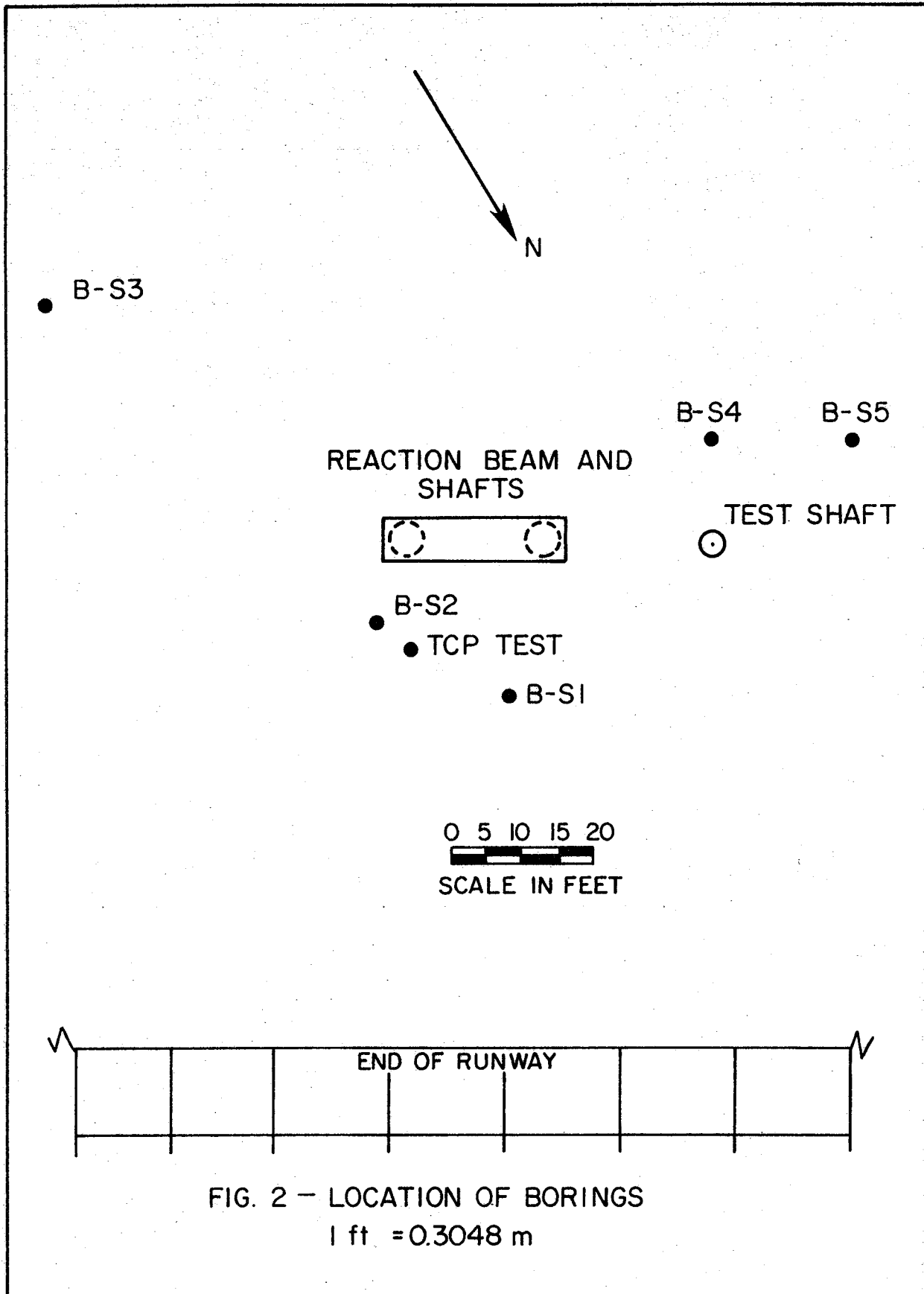
## FIELD LOAD TEST

The drilled shaft which was tested during the second year of this research program was also tested in a cohesive soil. The test site was located at the Southwest end of the Northeast runway at the Texas A&M Research Annex. Not only did the test site contain a suitable cohesive soil but also the beam-shaft reaction system was already in place from the previous test conducted by Kasch (19) in 1977.

### Soil Conditions

Soil conditions at the test site were investigated by making two additional soil borings. Three soil borings had been made and one Texas Cone Penetrometer (TCP) test had been conducted previously in the general test area by Kasch (19). The two new soil borings were made on January 6, 1978. These borings were designated as B-S4 and B-S5. Their location, along with the location of the borings previously made (B-S1, B-S2 and B-S3) are shown in Fig. 2. Undisturbed soil samples were taken with a 1.5 in. (3.8 cm) thin-wall tube sampler. The location of the TCP test which was conducted previously is also shown in Fig. 2.

Laboratory tests were performed on the undisturbed samples in order to determine Atterberg limits, moisture content, and total unit weight. The undrained shear strength,  $C_u$ , of the cohesive samples was determined from unconfined compression tests. The results of laboratory tests for each soil boring are given in Figs. 3 thru 7. These test results indicate that the soil properties at the test site are fairly uniform. The soil consists of stiff to very stiff clay with an average undrained shear strength of 1.4 tsf (134 kPa). To a depth of approximately



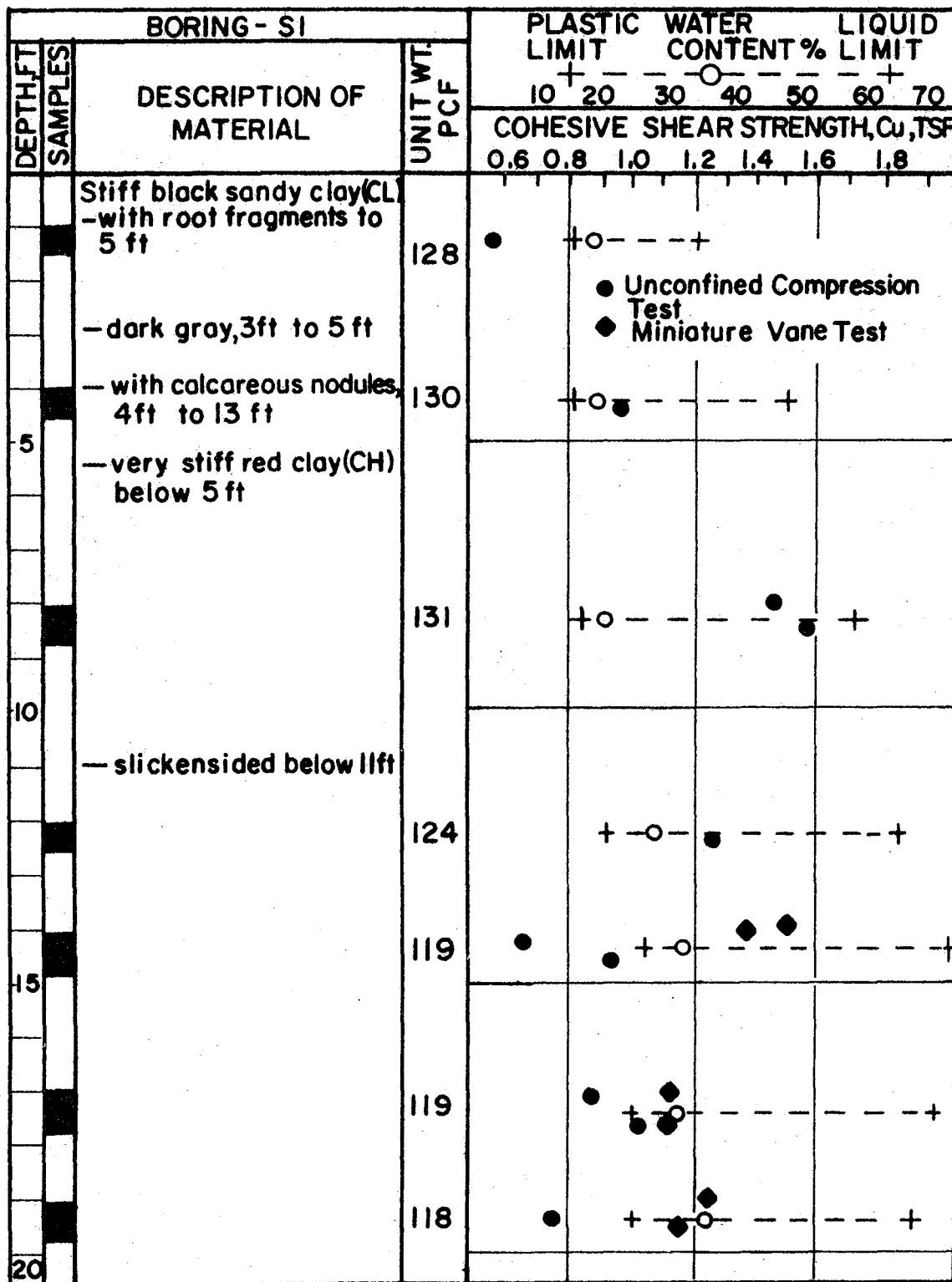


FIG. 3 - BORING- SI

1ft = 0.3048m, 1tsf = 95.8 kPa, 1pcf = 0.157 kN/m<sup>3</sup>

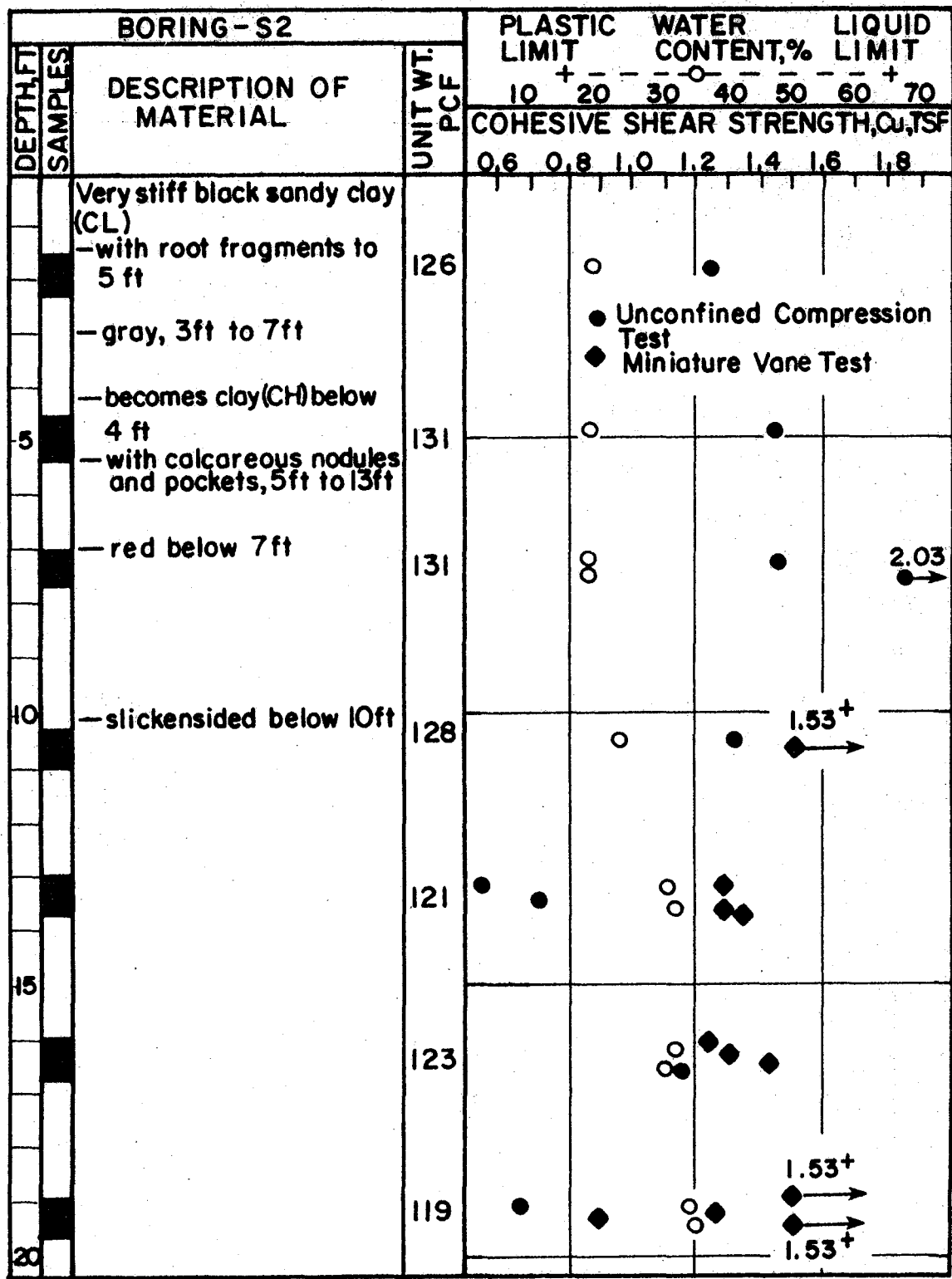


FIG. 4 — BORING-S2  
1ft = 0.3048m, 1tsf = 95.8 kPa, 1pcf = 0.157 kN/m<sup>3</sup>

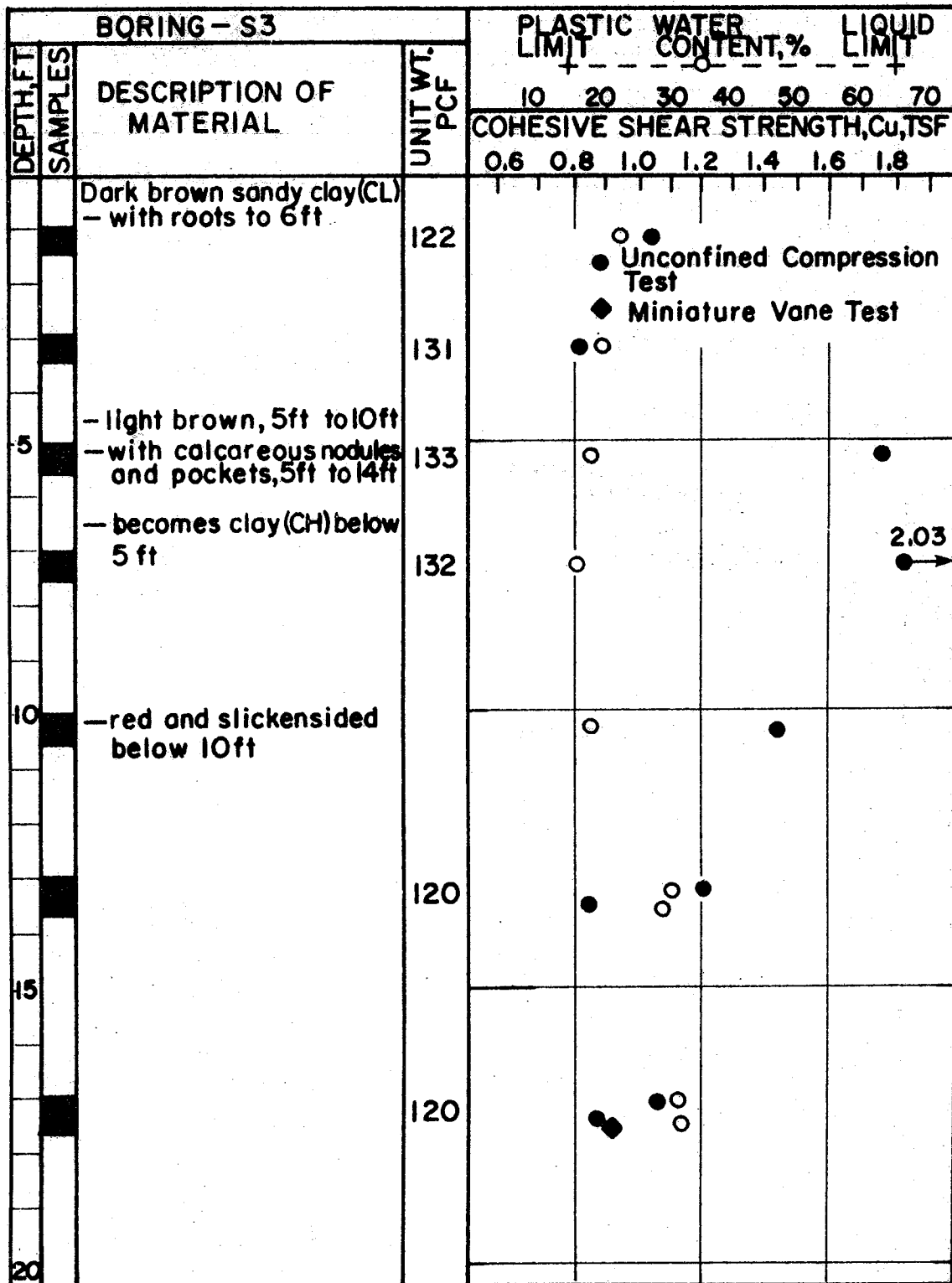


FIG. 5 — BORING—S3  
 $1\text{ft} = 0.3048\text{m}$ ,  $1\text{tsf} = 95.8 \text{ kPa}$ ,  $1\text{pcf} = 0.157 \text{ kN/m}^3$

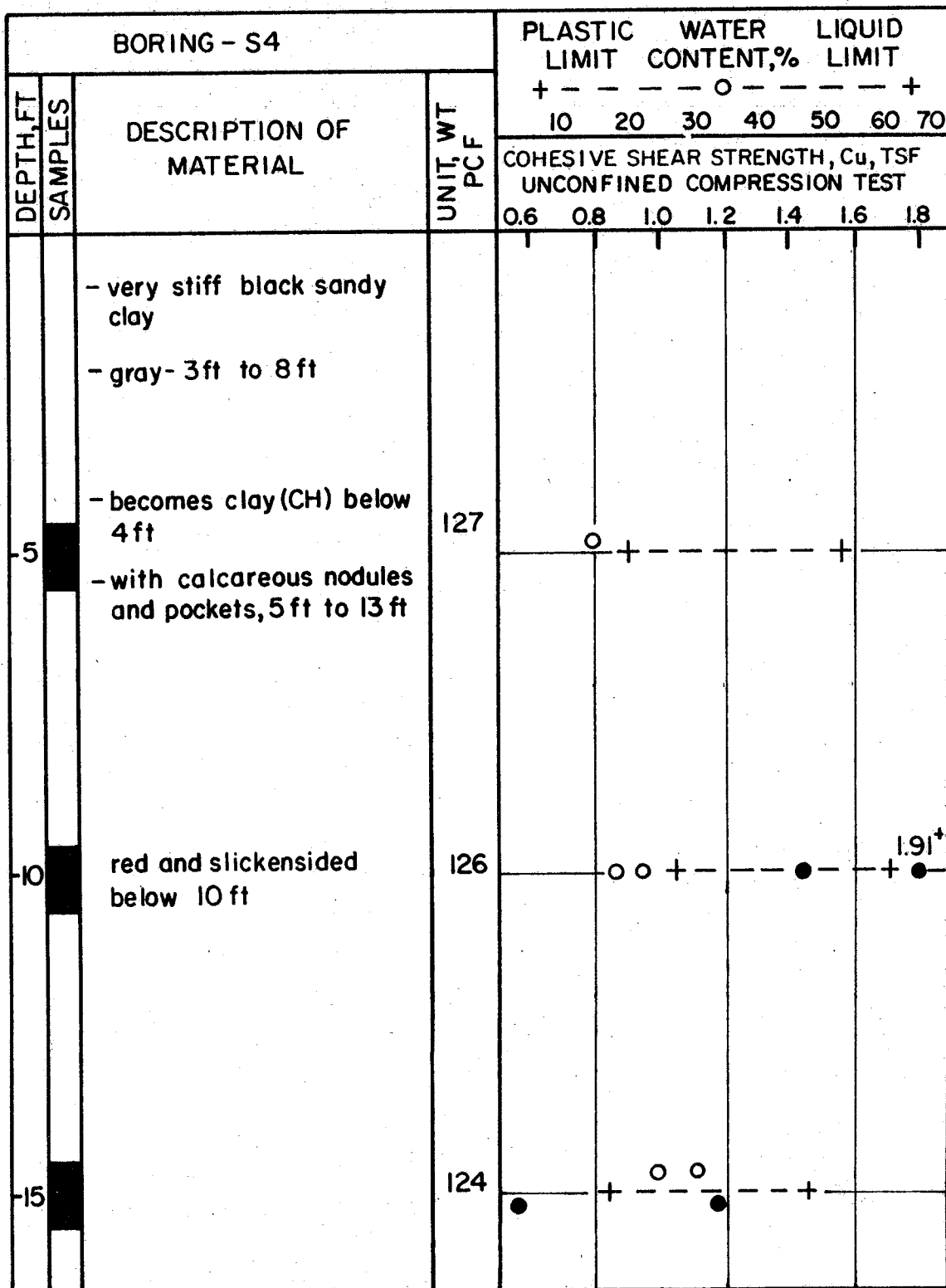


FIG. 6 - BORING - S4

1 ft = 0.3048 m, 1 tsf = 95.8 kPa,

1 pcf = 0.157 k N/m<sup>3</sup>

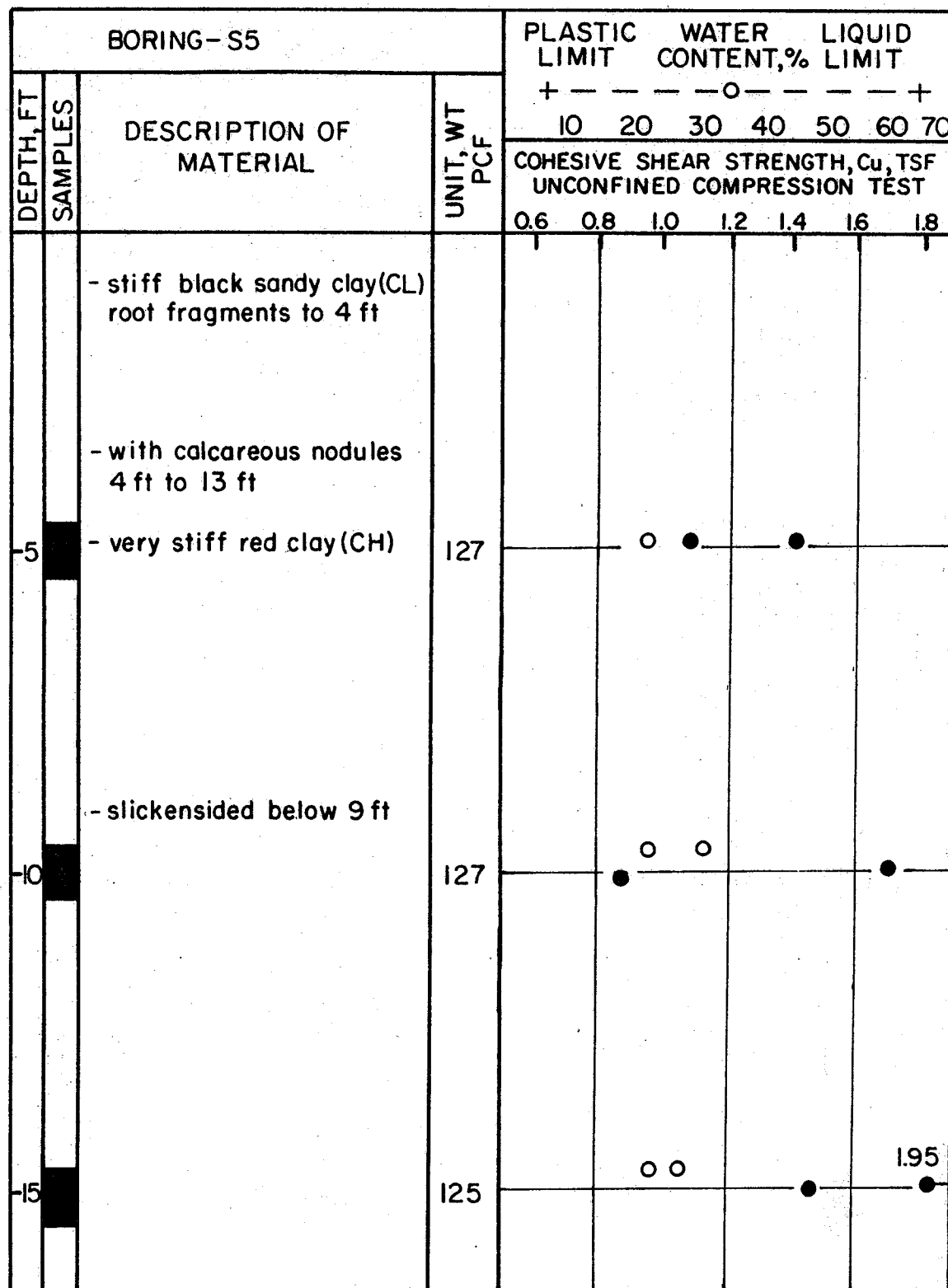


FIG. 7 - BORING- S5

$1\text{ft} = 0.3048\text{ m}$ ,  $1\text{tsf} = 958\text{ kPa}$ ,  $1\text{pcf} = 0.157\text{ k N/m}^3$

5 ft (1.5 m), the clay was classified as a CL according to the Unified Soil Classification System. The clay immediately below the 5-ft (1.5 m) depth was classified as a CH. A slickensided structure was noted in the clay at depths below 10 ft (3.0 m). The average undrained cohesive shear strength determined by the Duderstadt (10) methods which involves the use of the N-value (blow count) from the TCP test, was 1.15 tsf (110.2 kPa). The TCP shear strength data are given in Fig. 8. The average of 1.15 tsf (110.2 kPa) compares well with the average of 1.4 tsf (134 kPa) obtained from the unconfined compression test.

Upon completion of the boring B-S3 in July 1977, an open end stand pipe was installed at the site in order to make ground water observations. A perforated PVC pipe, covered with screen wire was placed in the bore hole and surrounded with clean gravel. The water level readings recorded throughout the year indicated that the level was steady at a depth of 18.8 ft (5.73 m).

#### Loading System

As stated previously, the test site is the same as the one used by Kasch (19) for the twenty foot deep drilled shaft test conducted during the first year of this study. Therefore, only a few modifications needed to be made in the existing loading system to accommodate the new test shaft.

The loading mechanism was moved to the opposite end of the reaction slab, so that the load could be applied in the opposite direction from the earlier test. The reason for repositioning was to insure that the new test shaft would not be tested in disturbed soil.

TEXAS CONE PENETROMETER TEST				
DEPTH, FT	TEST DEPTH	N. BLOWS	C <sub>u</sub> , TSF	UNDRAINED COHESIVE SHEAR STRENGTH, C <sub>u</sub> , TSF
20		20	1.34	
5		14	0.94	●
10		18	1.21	●
10		18	1.21	●
15		17	1.14	●
15		16	1.07	▽
20		15	1.01	●
20		16	1.07	●

FIG. 8 — TEXAS CONE PENETROMETER TEST  
 1 ft = 0.3048 m, 1 tsf = 95.8 k Pa, 1 pcf = 0.157 kN/m<sup>3</sup>

The pulley blocks used for this second test consisted of two six sheave, 100-ton (890 kN) capacity blocks with an equalizer attached. This gave the loading system a 14:1 mechanical advantage. The use of the equalizer on the blocks not only added two additional strands of wire cable but also decreased the tension in the individual strands. Another factor which influenced the decision to use a greater number of strands was the capacity of the hydraulic winch. It was observed from the first test that it was very near its maximum capacity when the structural failure occurred. The complete loading system is shown in Fig. 9.

#### Test Shaft

The test shaft was located approximately 20 ft (6.1 m) center to center on line from the reaction slab. The shaft was nominally 3 ft (0.9 m) in diameter by 15 ft (4.6 m) in depth. Due to some wobble of the auger bit during drilling, the first few feet of the shaft was slightly larger than 36-in. (91 cm) in diameter. The final depth of drilling was recorded as 15.1 ft (4.61 m).

The amount of steel was increased substantially for this test in order to insure that a structural failure would not occur. The reinforcing cage consisted of 12 No. 11 bars (grade 60) with a No. 3 spiral at a 2-in. (5 cm) pitch for the first 6 ft (1.8 m), and a 6-in. (15 cm) pitch for the remaining depth. Inside the 32-in. (81 cm) diameter cage, twelve additional bars were spaced equally at a 24-in. (61 cm) diameter. Each bar was 15.5 ft (4.72 m) long and 1.5 in. (3.8 cm) in diameter, and the top 6-in. (15 cm) was threaded with a

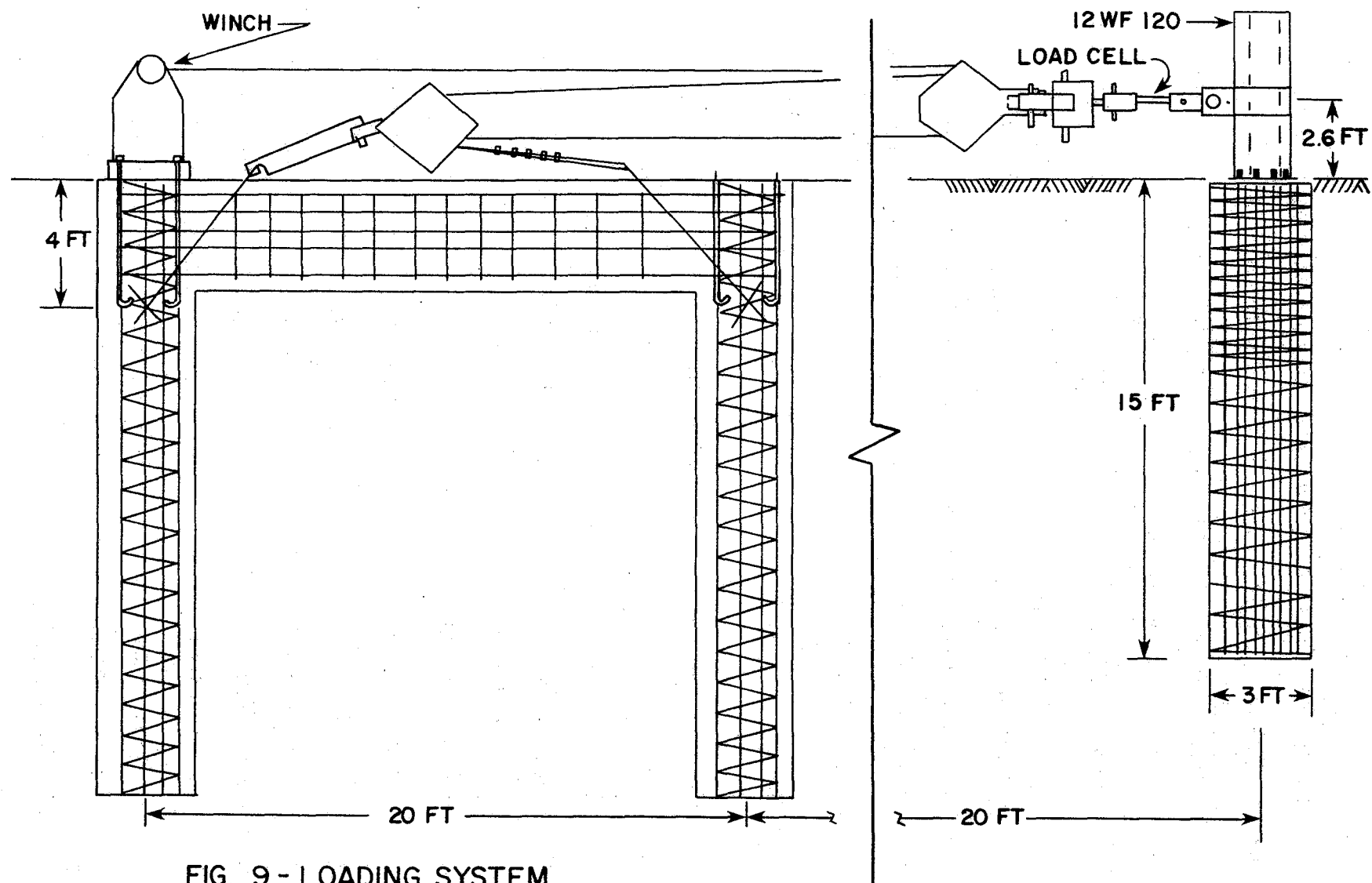


FIG. 9 - LOADING SYSTEM

1 ft = 0.3048 m

1.375 in. (3.492 cm) universal thread. The reinforcing steel configuration is shown in Fig. 10.

A 12 WF 120 steel column was bolted to the test shaft using the threaded reinforcing bars. The steel column served the purpose of not only allowing the lateral load to be applied at a reasonable distance above the ground surface but it also served as a reference point for making inclination measurement during the testing program.

#### Instrumentation

Pressure Cells. - The test shaft was instrumented with Terra Tec pressure cells. These cells were used successfully during the related studies by Wright et al. (39) and Kasch (19). Three cells were retrieved from the test shaft used in 1977 and were reused along with seven new cells for this test. The newer cells have a different shape than the older cells but the basic principal of operation is the same. The older cells (round plate) and the newer cells (square plate) are shown in Figs. 11 and 12 respectively. Before the cells were installed in the test shaft, they were individually calibrated in a pressure chamber. The zero reading of each cell was determined and no malfunctions were observed in any of the cells. The installation of the pressure cells was greatly enhanced by the use of a template. This template was lightly tapped against the soil to produce a flat surface for the face of the cell to rest against. Metal pins were then driven into the soil to hold the cells in place.

Load Cell. - The load applied to the test shaft was measured by a 200-kip (890 kN) capacity strain gaged load cell. This load cell, which

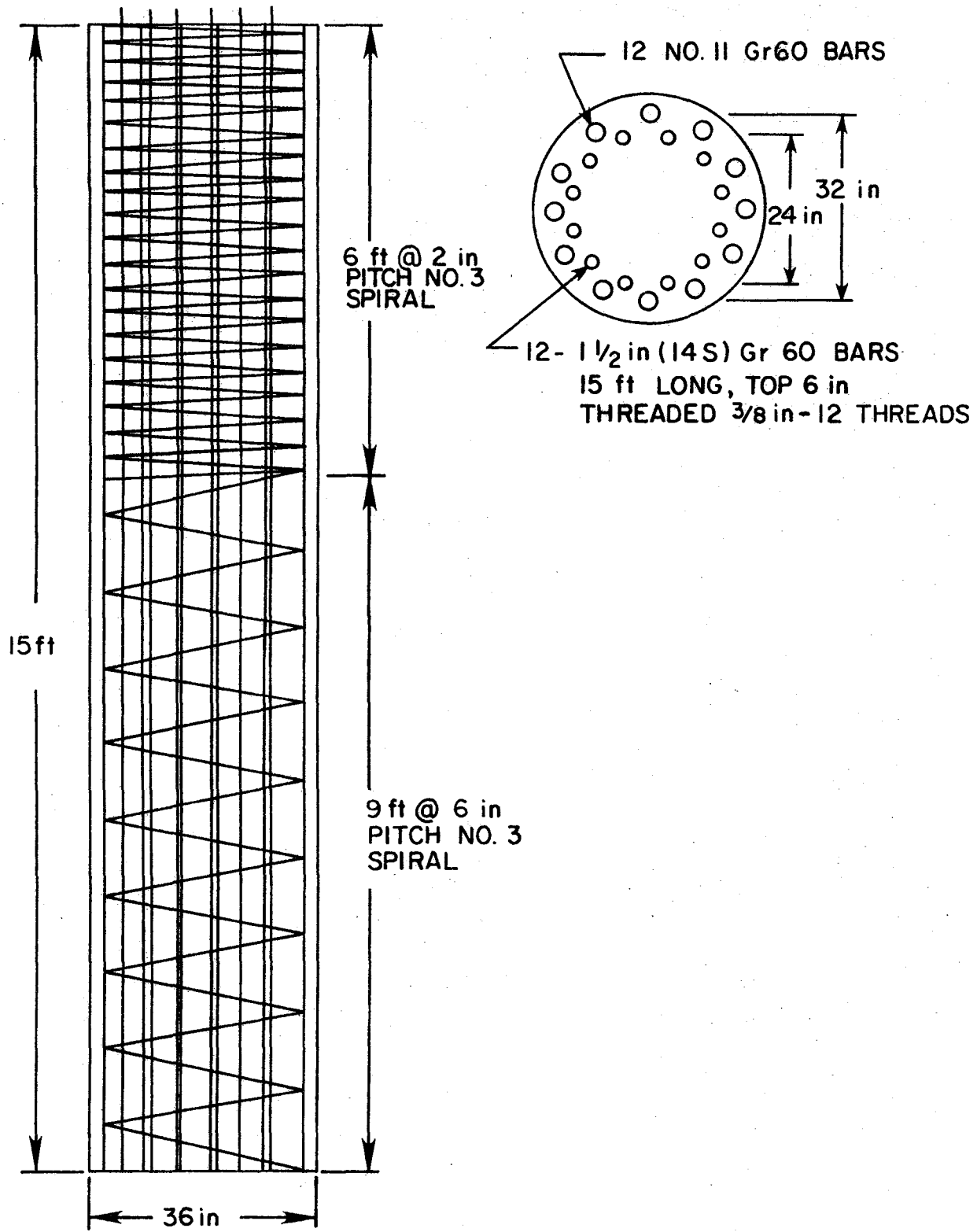


FIG. 10- STEEL REINFORCING CAGE  
1 ft = 0.3048 m

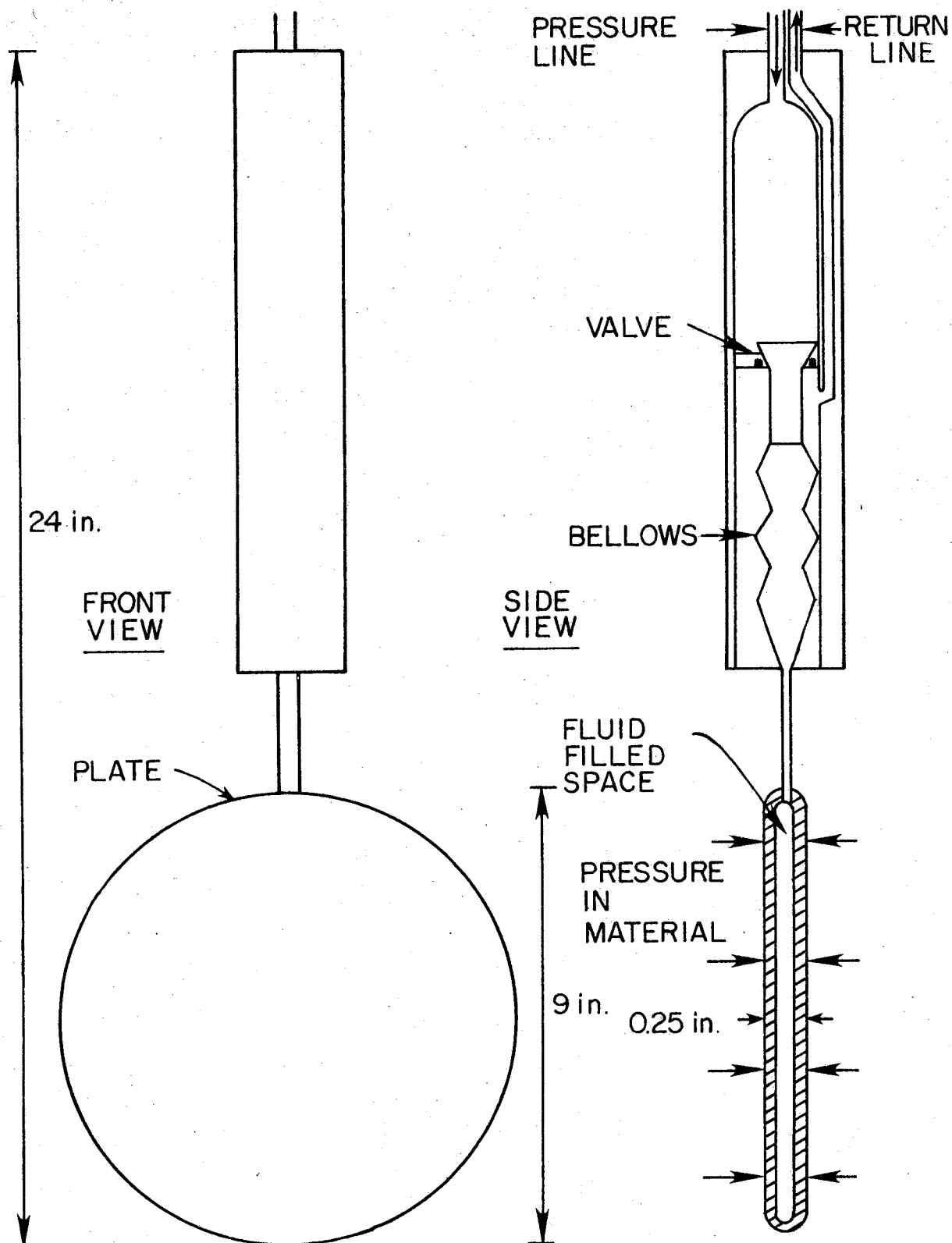


FIG. II—TERRA TEC PRESSURE CELL (ROUND PLATE)  
1 in. = 2.54 cm

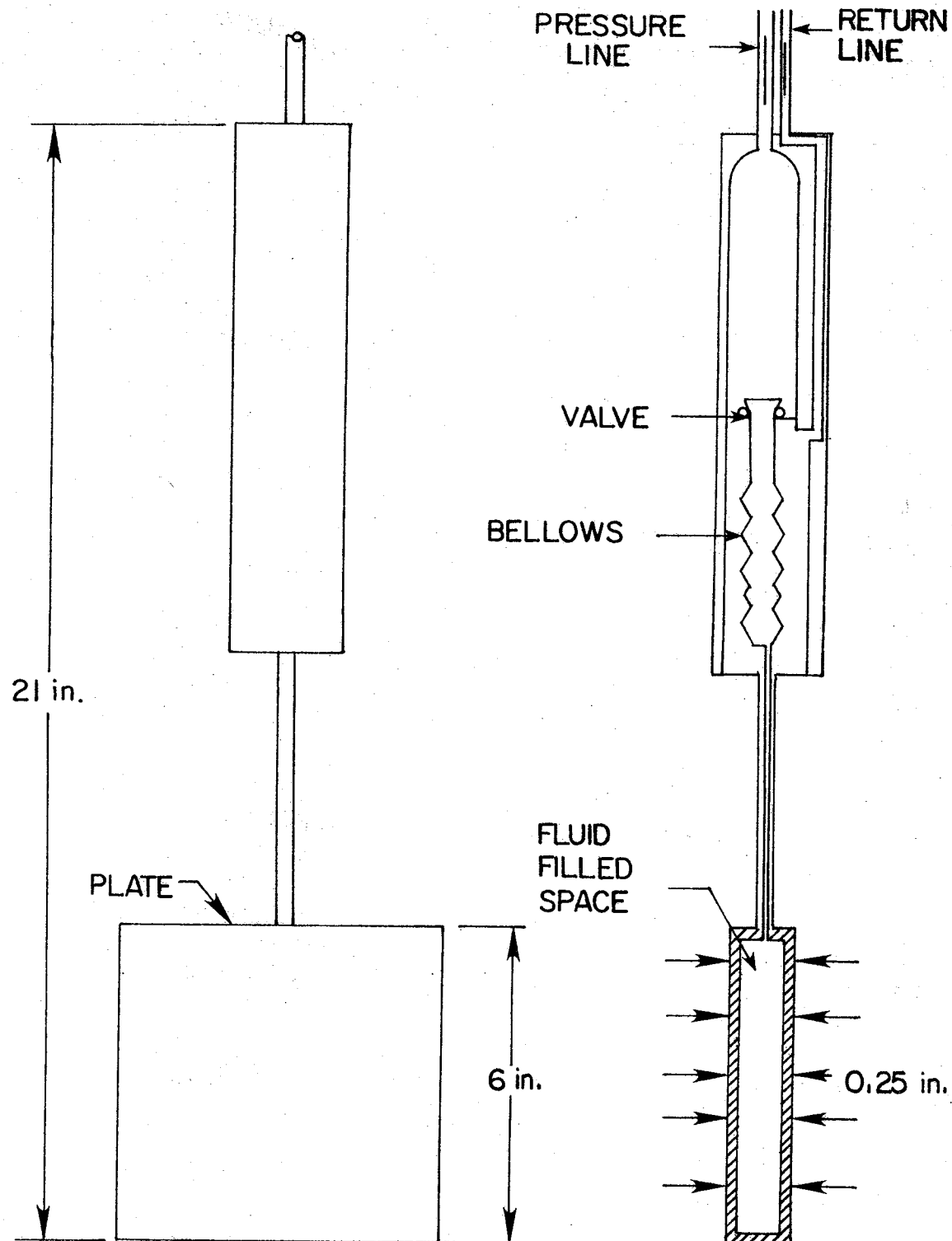


FIG. 12 - TERRA TEC PRESSURE CELL (SQUARE PLATE)    1 in. = 2.54 cm.

was the same one used by Kasch in 1977 (19), had to be modified because an elongation had occurred in the connecting pin holes. This elongation occurred from a chain reaction of events after the connecting plate material yielded. This yielding introduced a moment into the connecting pins and caused a failure of the pins. After the pins failed, the yoke expanded due to movement of the pins and this caused the connecting pin holes to elongate. The modifications were accomplished by increasing the diameter of the connecting pin holes from 1.00 in. (2.54 cm) to 1.50 in. (3.81 cm) diameter. The connecting pins were threaded on the outside of the load cell with a 1.25-in. (3.18 cm) coarse thread before being heat treated. These measures were taken so that the pins would be in double shear and would not allow moment to be transferred into them. A schematic of the load cell is shown in Fig. 13.

The load was measured with a Budd P350 indicator in units of micro-strain and converted to kips by a predetermined calibration constant. The accuracy of the load cell and Budd indicator was approximately  $\pm .04$  kips (0.18 kN).

Inclinometer. - The rotation of the shaft was determined using a Hilger & Watts TB108-1 inclinometer. The rotation was measured in degrees to an accuracy of approximately plus or minus one minute. Rotational measurements were made by placing the inclinometer at five predetermined locations on the steel column. A back-up system was also devised for the determination of the shaft rotation. A horizontal measurement from a vertical reference line to the five points on the steel column allowed the determination of the relative movement of the points. A reference line was established by a plumb-bob suspended from

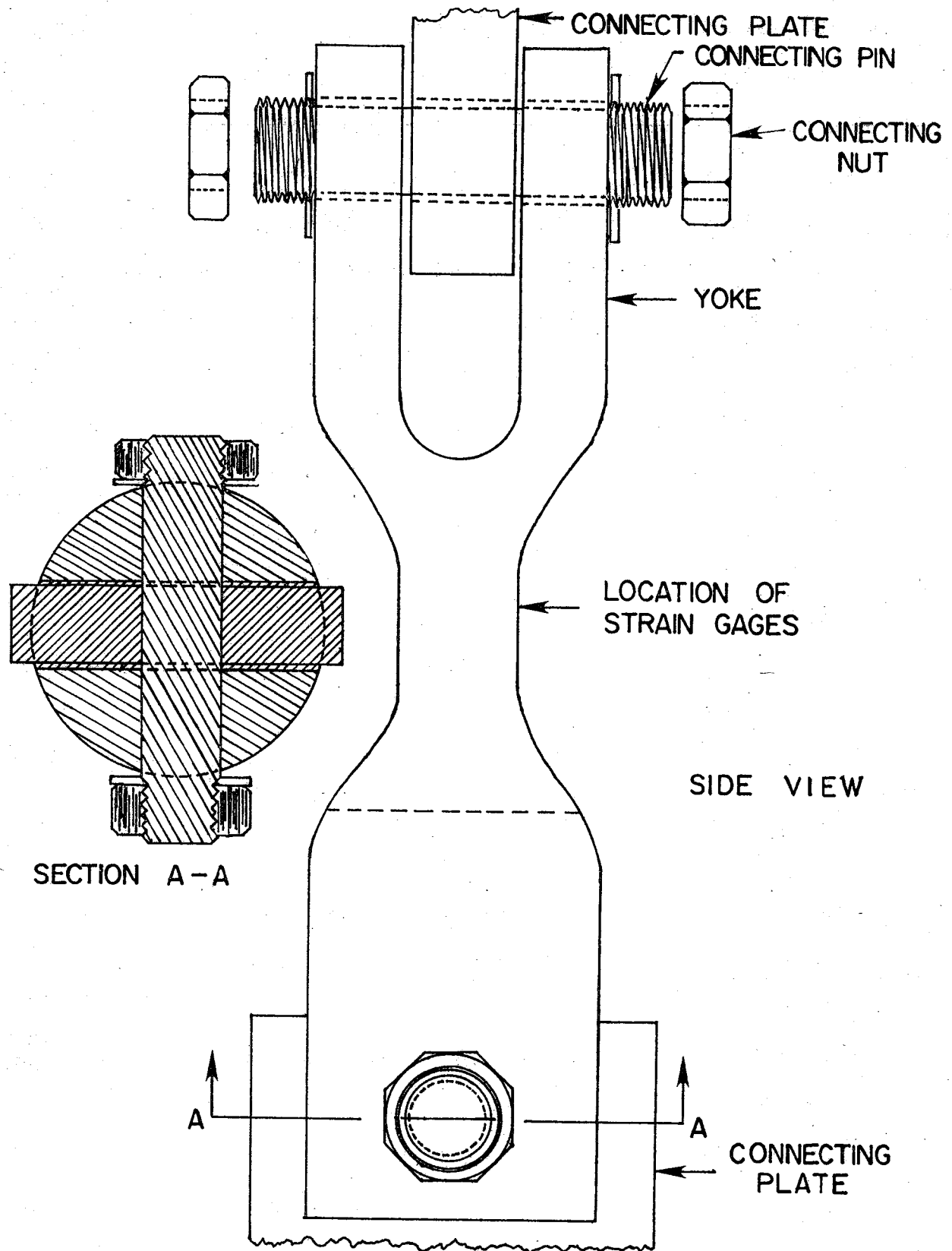


FIG. 13 - STRAIN GAGED LOAD CELL

a frame welded to the top of the column. Initial measurements were made before the lateral load was applied. The initial measurements were subtracted from subsequent measurements in order to obtain the movement relative to the initial position of the plumb line.

Dial Gages. - The deflection of the shaft at the ground line was measured using two 0.001 in. (0.03 mm) dial gages. The gages were attached to threadable rods which were mounted on a steel beam that was located 18 in. (46 cm) behind the shaft. The beam was supported by two footings which were placed approximately 7.5 ft (2.29 m) on each side of the shaft. An overhead view showing the position of the dial gages is given in Fig. 14.

#### Test Shaft Construction

The construction of the test shaft was accomplished in March 1978. Experience gained during construction of the test shaft in 1977 indicated that shoring would be needed after the soil excavation. Shoring was accomplished by tying 2 in. x 4 in. (5 cm x 10 cm) boards 15 ft (4.6 m) long to the outside of the reinforcing cage. A metal flashing was also attached to the cage on the front and back in line with the applied load. Holes had been cut in the flashing to indicate the location of the pressure cells with respect to depth. This served the purpose of reducing working time during location and installation of the pressure cells. The reinforcing cage, with the shoring and metal flashing attached, was lowered into the excavation in the proper position. After the cage was in position the tie wires were cut, and the boards and metal flashing were forced against the side of the excavation using wooden

TOP VIEW

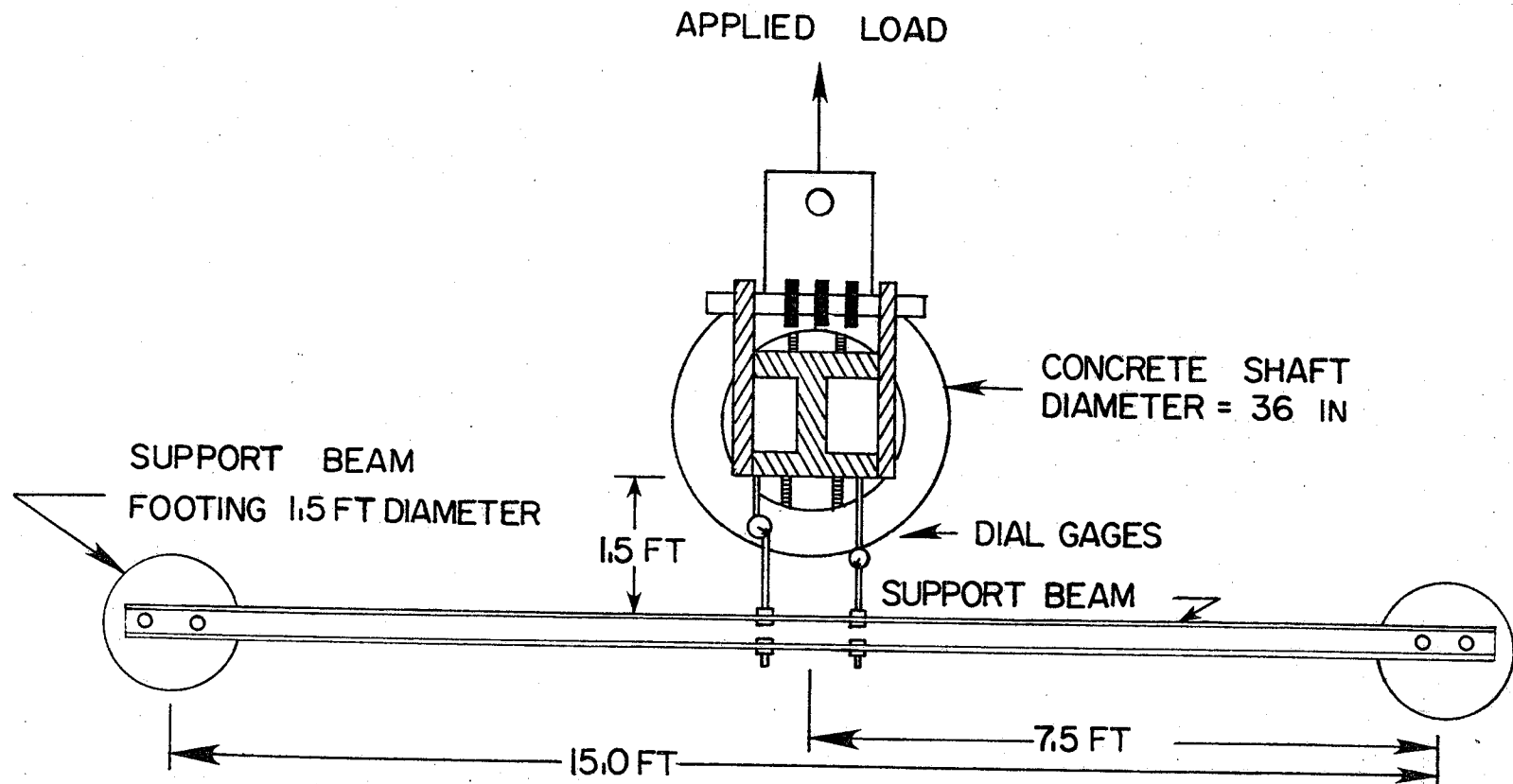


FIG. 14 - POSITION OF DEFLECTION DIAL GAGE    1 ft = 0.3048 m

blocks.

The location of the pressure cells on the test shaft is shown in Fig. 15. Eight of the cells were installed along a vertical line in the plane of the applied load, and the remaining two cells were installed in the horizontal plane perpendicular to the vertical plane at a depth of 4.5 ft (1.37 m). Seven of the pressure cells were placed on the front of the shaft facing the loading system and the remaining three cells were placed on the back of the shaft. The cells were placed in the soil along the side of the excavation and held in place by steel pins. Care was taken to insure that each cell was implanted firmly in the soil. The shoring was removed and the concrete was placed in six consecutive layers. A vibrator was used to insure consolidation of each layer. Concrete cylinders taken during the construction of the test shaft had an average 28-day strength of 4130 psi (28,480 kPa). The shaft was allowed to cure for 62 days before the first load was applied on May 24, 1978. Cylinders tested at this time had an average compressive strength of 4570 psi (31,510 kPa).

#### Loading Procedure

The loading procedure for this test shaft was a combination of two previous procedures reported by Wright et al. (39) and Kasch (19). Wright et al. developed a method for calculating the maximum resultant force of the backfill acting on a retaining wall. Kasch (19) simulated, on the shaft tested in 1977, the backfilling process of the retaining wall and the overburden pressure imposed by the backfill on the retaining wall, during a six-day period. At the conclusion of the six-day

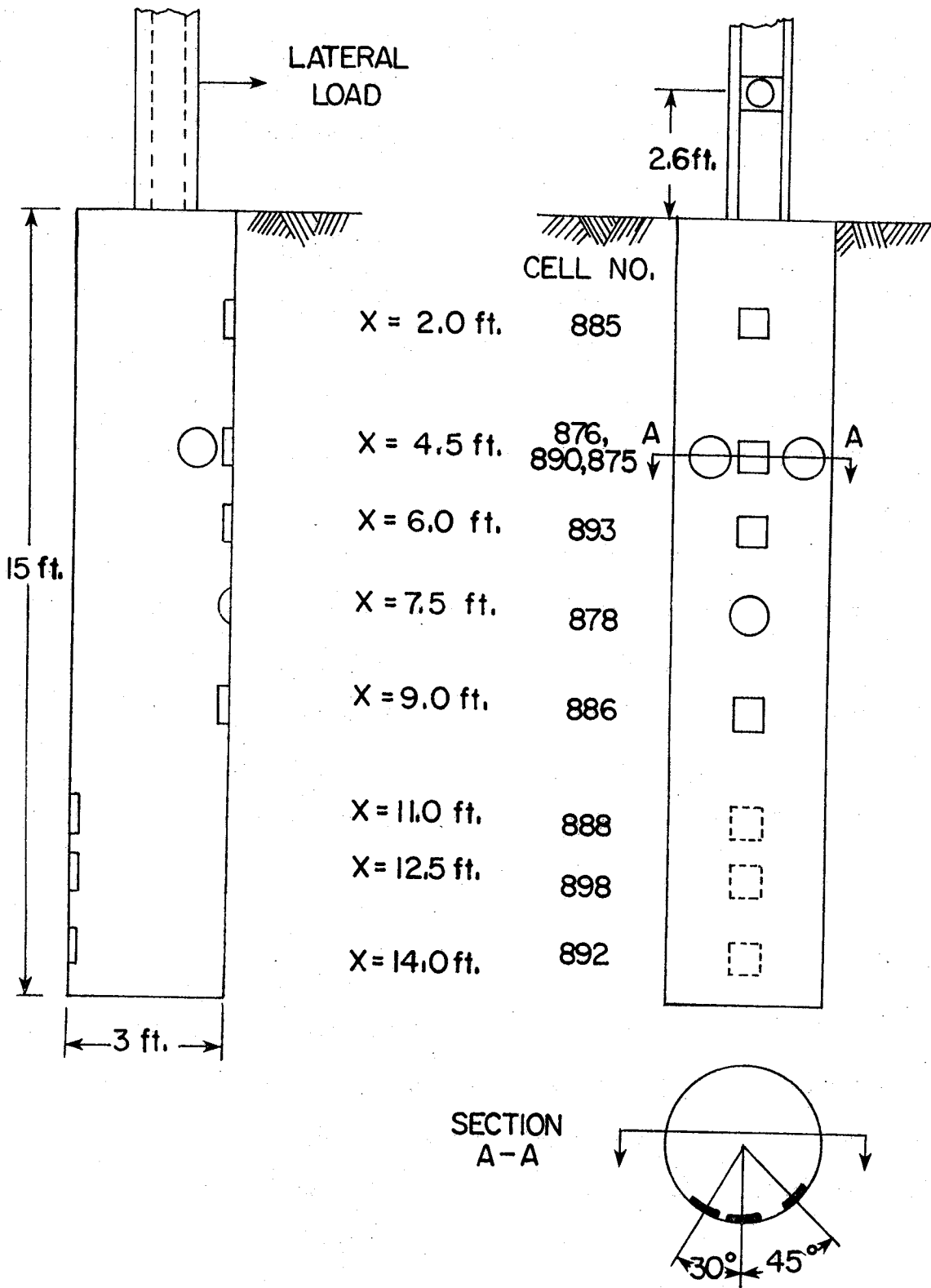


FIG. 15—LOCATION OF PRESSURE CELLS X= DEPTH  
BELOW GROUND LINE; 1ft. = 0.3048m

period, a 13-day period of "constant load" was maintained. This was done in order to determine if any creep was occurring in the soil along the front of the shaft. However, neither of these two simulations produced any significant results at this relatively low load level. The simulation of the overburden pressure did not cause any noticeable changes in the pressure cell readings and consequently was not used in this latest test.

The lateral loading procedure began with a 5-kip (22 kN) incremental load being applied four times each day for the first two days. The loads were applied, readings were made on the pressure cells, and inclinations were measured after each load movement stabilized. The stabilization time was usually 10 to 15 minutes after the load was applied. During the first two days of the loading procedure an attempt was made to simulate the loading schedule that occurred on the shaft reported by Wright et al. (39). The total lateral load was equal to 40 kips (178 kN) at the end of the first two days of loading. No large movements or unusual rotations were observed. At this point, it was decided to continue this 5-kip (22 kN) incremental loading procedure.

At the 60-kip (267 kN) level the load-deflection curve was deviating significantly from the one presented by Kasch (19) as shown in Fig. 16. Therefore, the decision was made to slow the loading procedure to 5 kips (22 kN) only twice a day. A large crack was beginning to form along the back of the drilled shaft at this time in the loading program and deflections at the top of the shaft at ground level were beginning to take longer to stabilize. It was also noted that

some creep was beginning to occur during the 24-hour period between loadings. After four days of twice a day loading the load-deflection curve was continuing to deviate from Kasch's (19) curve as shown in Fig. 16 for the 100-kip (445 kN) level.

The new curve almost paralleled the earlier curve but at a much lower load. After projecting the trend of the new data on the load-deflection graph, the decision was made to slow the loading procedure down even further. There were two reasons for this. First, it was necessary to establish the ultimate resistance of the soil, and secondly, small deflections were occurring for hours after the load was applied. By the time the new load increment was to be applied the following day, the previous load had usually fallen off approximately 15 kips (67 kN). Therefore, instead of beginning with this lower load and adding a new load of 5-kips (22 kN), the load was first brought back to where it had been the previous day. Pressure readings were made and then an additional load of 5-kips (22 kN) was added so as to limit the amount of differential load being applied to the test shaft at any given time. Bringing the load back to the previous load each day before the new load was added was considered necessary so that the ultimate resistance of the soil could be established.

Beginning at the 115-kip (512 kN) load level, large deflections were observed when the load was brought to the previous level. In addition, small deflections were continuing as the load was returned to its previous value in order to establish a stabilization point. Two different methods were used to determine if and when the movement ceased at a given constant load. These methods are outlined in detail

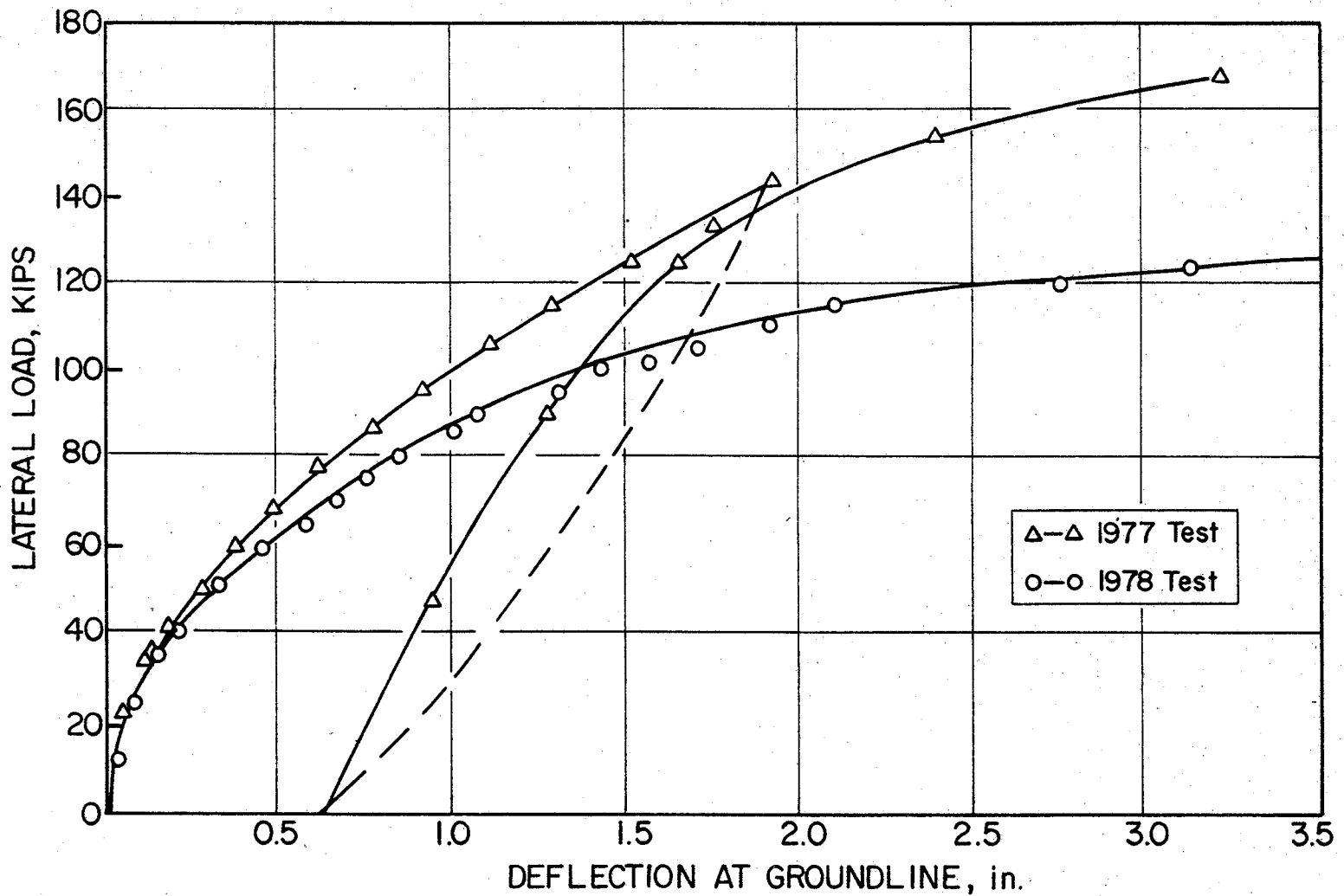


FIG. 16 - LATERAL LOAD VS DEFLECTION AT GROUNDLINE  
1 kip = 4.45 kN; 1 in. = 2.54 cm

and the corresponding data are presented in Appendix III.

It was believed that from the 115-kip (512 kN) load level to the end of the loading program the deflections were both a function of the time the load was held and the amount of load on the shaft. This value of 115-kips (512 kN) will be considered the ultimate load for this test and will be used for comparison with other methods (4, 12, 13, 16, 17) of determining ultimate soil reaction. However, it was decided to continue loading the shaft so additional pressure measurement could be taken at higher loads. Loading was continued up to 150-kips (668 kN) to determine if the shape of the pressure distribution along the shaft might change with respect to depth below the surface.

## TEST RESULTS

The data obtained from the full-scale lateral load test conducted during May and June 1978 are given in this section. Pressure cell data are presented and analyzed along with the test shaft deflection and rotation results. A comparison of the ultimate soil reaction predicted by different theories with the actual behavior of this test shaft is discussed. Also, a comparison is made between methods which predict the ultimate load on rigid shafts.

### Pressure Cell Data

**Initial Pressures.** - Three sets of pressure cell readings were made before the first lateral load was applied on May 25, 1978. These readings are shown in Table 1.

TABLE 1. - Initial Pressure Cell Readings

Cell	Zero Reading From Lab March 1978 psi	In Shaft Before Concrete March 23, 1978 psi	In Shaft Before Lateral Load May 24, 1978 psi
875	7.5	7.5	8.1
876	15.0	16.0	18.2
878	8.0	8.5	6.1
885	3.5	3.0	2.4
886	4.0	5.0	1.3
888	3.25	3.9	3.0
890	3.0	3.5	1.05
892	3.0	4.5	4.5
893	1.0	1.0	3.6
898	3.0	4.0	8.6

NOTE: 1 psi = 6.895 kPa

The readings presented are: (1) the zero readings from the laboratory calibration; (2) the initial readings taken after the cells were installed in the shaft, but before the concrete was placed; and (3) the readings taken 30 days after the concrete was placed and before the first lateral load was applied. These pressure measurements (before concrete and before load) were used for determining the total pressure change of the shaft and the amount of pressure change due to the lateral load applied. As shown in Table 1, the initial zero readings taken in the shaft differed from the zero readings obtained from the laboratory calibration. The pressures in the shaft ranged from 0.5 psi to 1.5 psi (3.4 to 10.3 kPa) higher than the laboratory calibrations except for one pressure cell. This cell (No. 885) was located two feet below the ground surface and recorded a pressure of 0.5 psi (3.4 kPa) lower than the laboratory calibrations. The reason for the pressure being lower is not known. However, this general trend of an increased pressure was expected because of the way the pressure cells were attached to the wall of the shaft during installation.

The cells were read again 30 days after the concrete was placed. There is not a consistent trend for this set of readings. Four of the pressure cells recorded pressures ranging from 0.6 to 4.6 psi (4.1 to 31.7 kPa) higher than the in shaft before concrete measurements and the remaining six cells recorded pressures ranging from 0.6 to 3.7 psi (4.1 to 25.5 kPa) lower than the in shaft before concrete measurements. The placement of the concrete or the concrete shrinkage during the 30-day curing time could have caused these fluctuations in the initial pressure cell readings.

Pressures During Lateral Loading. - The lateral soil pressures that resulted from the lateral loading of the drilled shaft were obtained by subtracting the initial cell readings from the cell readings for a particular lateral load. The initial cell readings were obtained on May 24, 1978, just prior to the application of the first lateral load. The lateral soil pressures obtained for each cell throughout the test are plotted on Figs. 17 thru 26. Most of the curves show a gradual increase in pressure as the lateral load was increased. However, cells 878 and 888 (see Fig. 15) showed an erratic pressure behavior. This behavior could possibly be explained by the point of rotation shifting downward during the increase of the lateral loading which could cause lower pressures than previously recorded. The two bottom cells (898 and 892) indicated negative pressures at the beginning of the test and did not begin to show positive pressures until the 80-kip (356 kN) and 40-kip (178 kN) load levels, respectively. A possible reason for the occurrence of negative pressures could be that some of the clay may have fallen out from behind the cells during installation and created an insufficient bearing area for the cell plate. The reason these cells did not begin to indicate any significant pressure increase as soon as the other cells did, may be because of their location on the shaft. Since these cells were the two bottom cells, it would probably take longer for the load to be felt at these depths. It is also important to note, that cell 898 did not indicate a positive pressure as soon as cell 892. This behavior would be expected, because cell 898 was 1.5 ft (.46 m) above cell 892 (see Fig. 15) and the distance to the point of rotation was greater for cell 892. Thus, cell 892 experienced positive

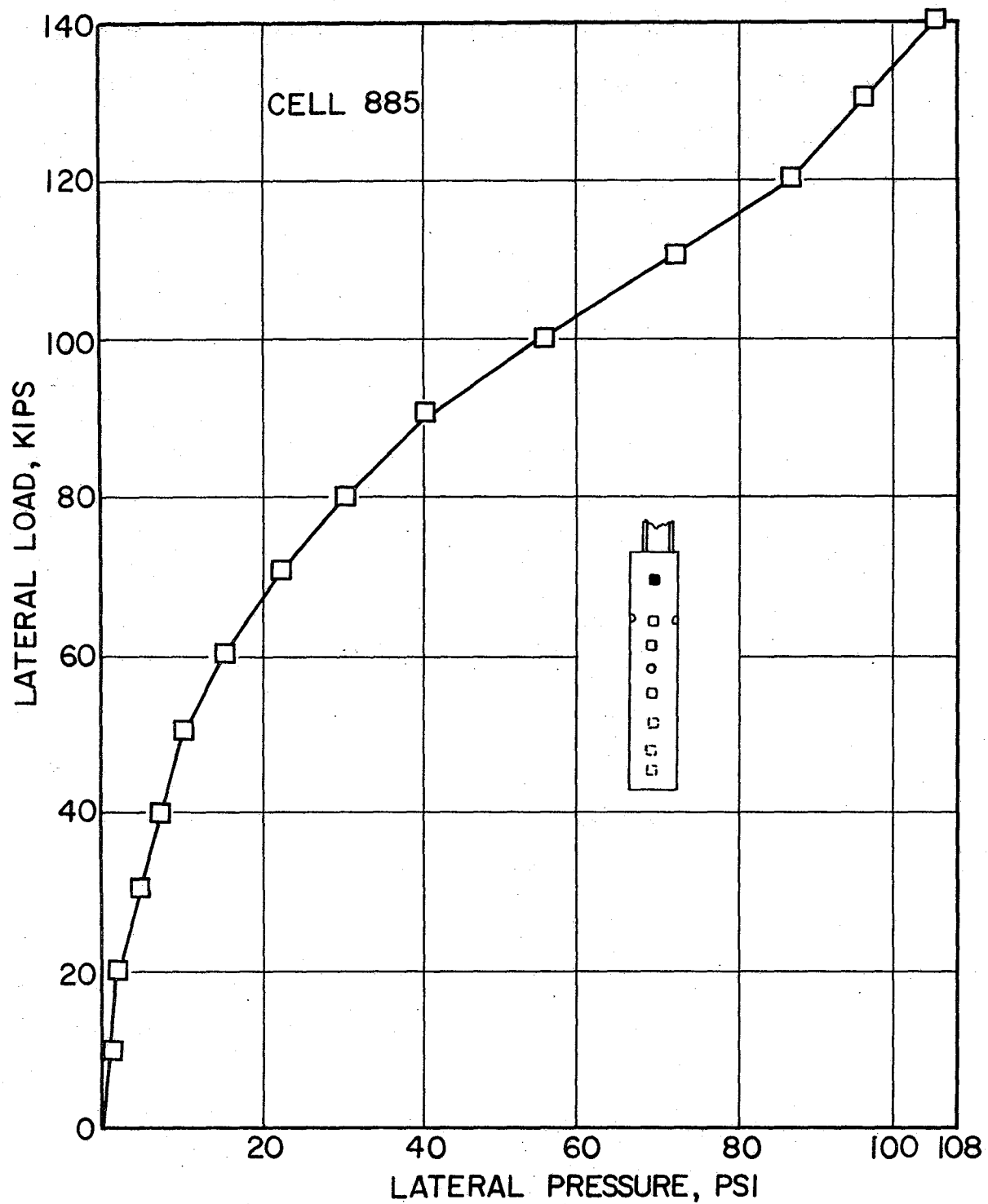


FIG. 17 - LATERAL LOAD VS LATERAL PRESSURE, CELL 885  
1 kip = 4.45 kN; 1 psi = 6.89 kPa

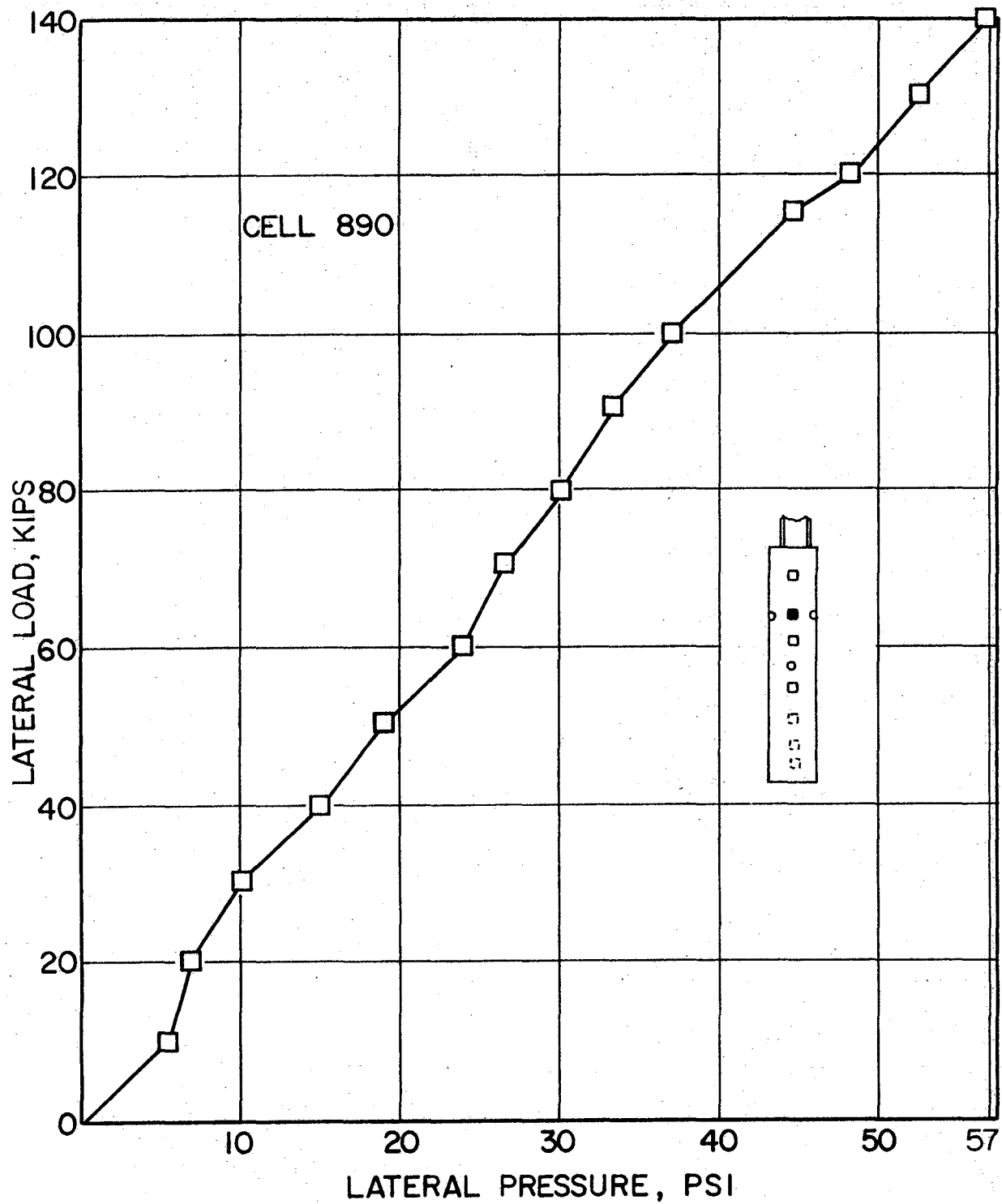


FIG. 18 - LATERAL LOAD VS LATERAL PRESSURE, CELL 890  
1 kip = 4.45 kN; 1 psi = 6.89 kPa

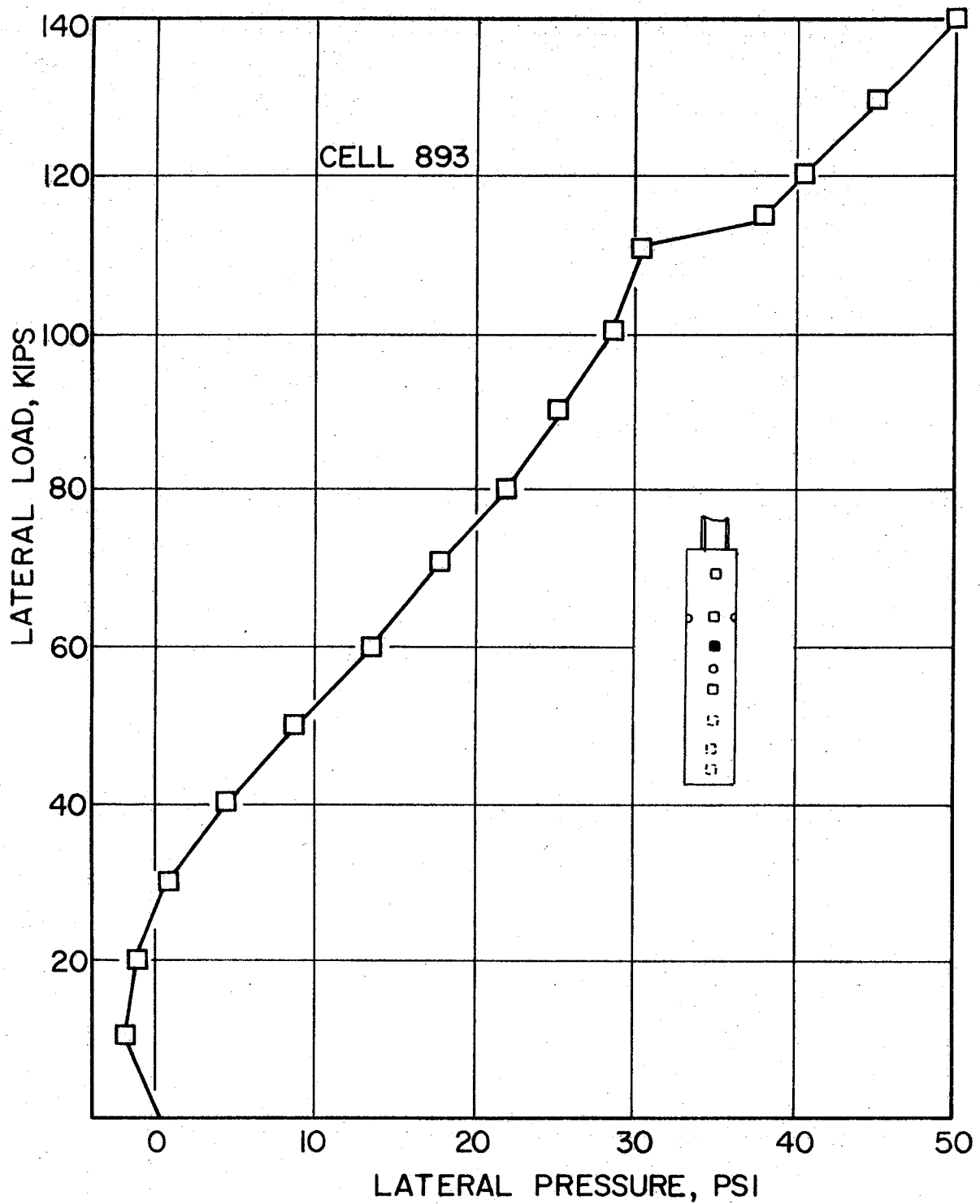


FIG. 19 - LATERAL LOAD VS LATERAL PRESSURE , CELL 893  
 1 kip = 4.45 kN; 1 psi = 6.89 kPa

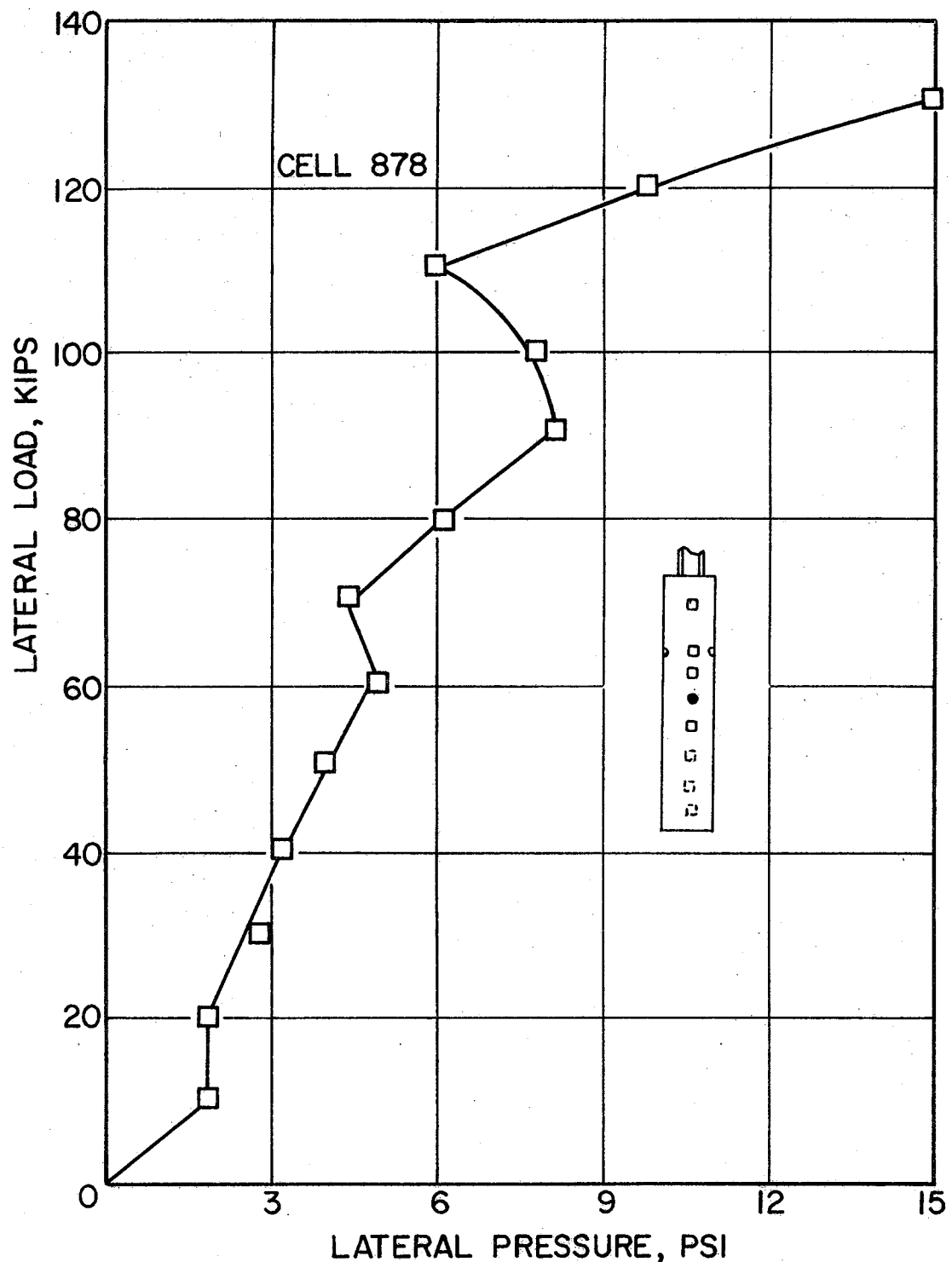


FIG. 20 - LATERAL LOAD VS LATERAL PRESSURE, CELL 878  
 1 kip = 4.45 kN; 1 psi = 6.89 kPa

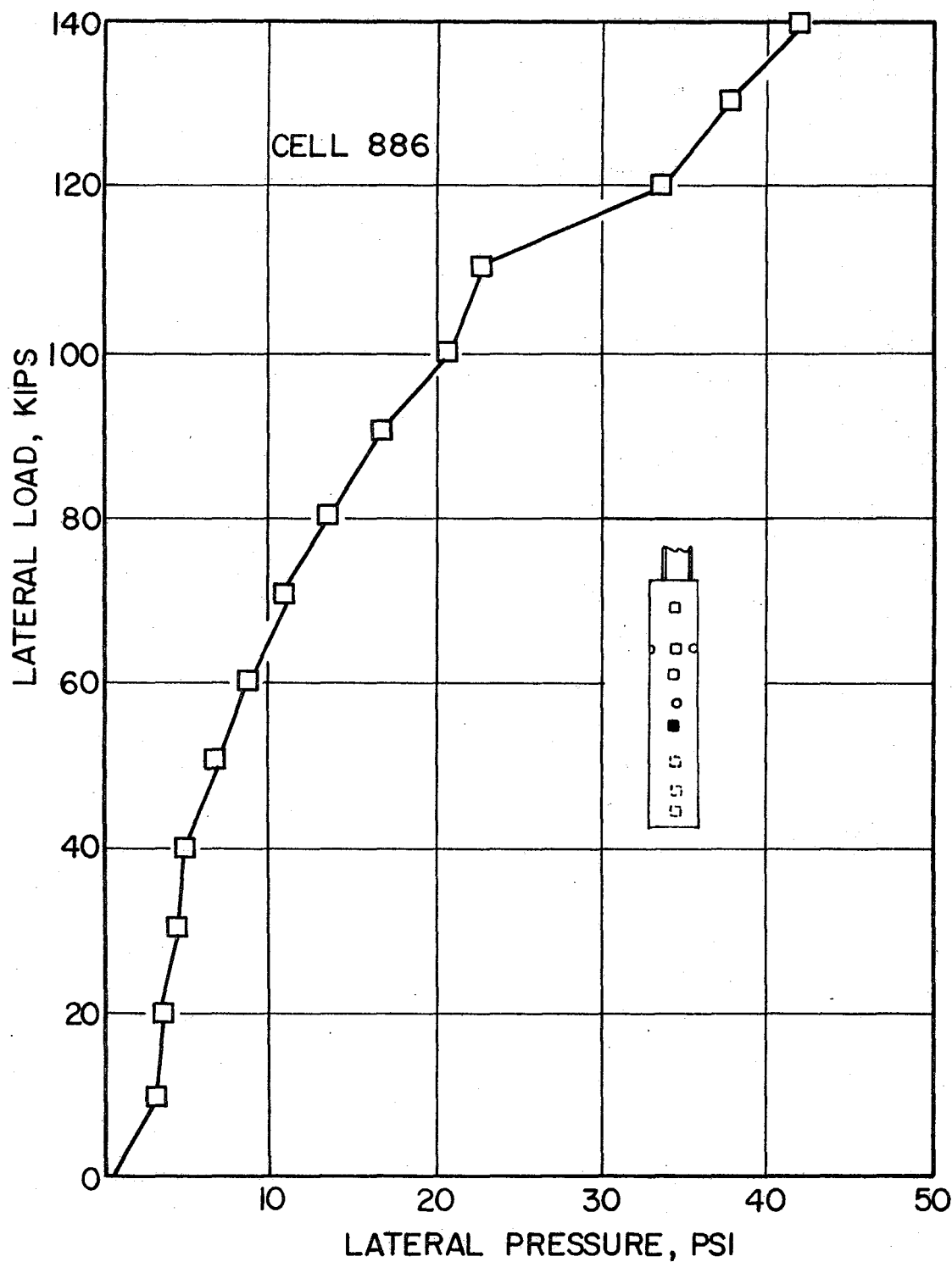


FIG. 21 - LATERAL LOAD VS LATERAL PRESSURE, CELL 886  
 1 kip = 4.45 kN; 1 psi = 6.89 kPa

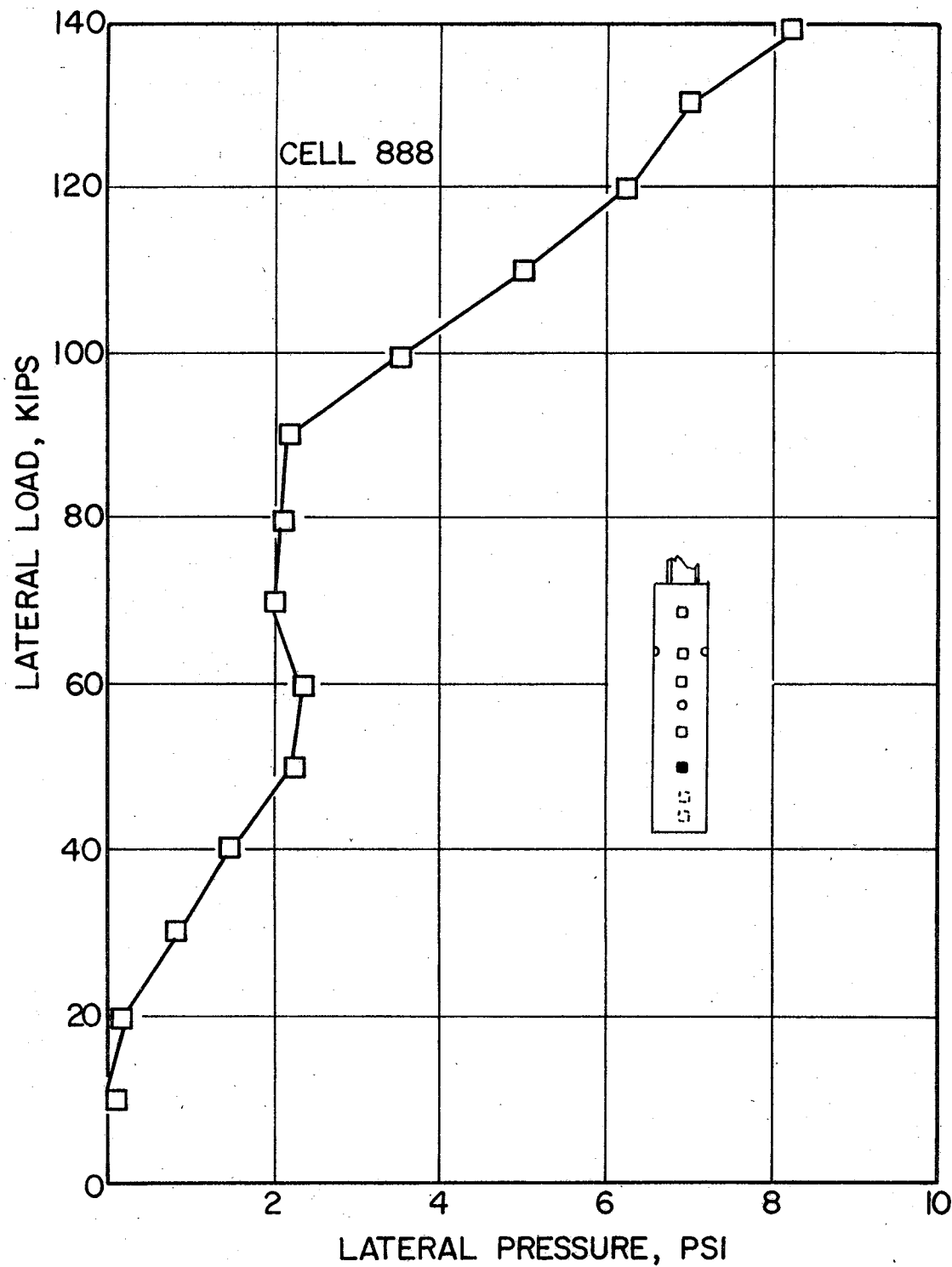


FIG. 22 - LATERAL LOAD VS LATERAL PRESSURE, CELL 888  
 1 kip = 4.45 kN ; 1 psi = 6.89 kPa

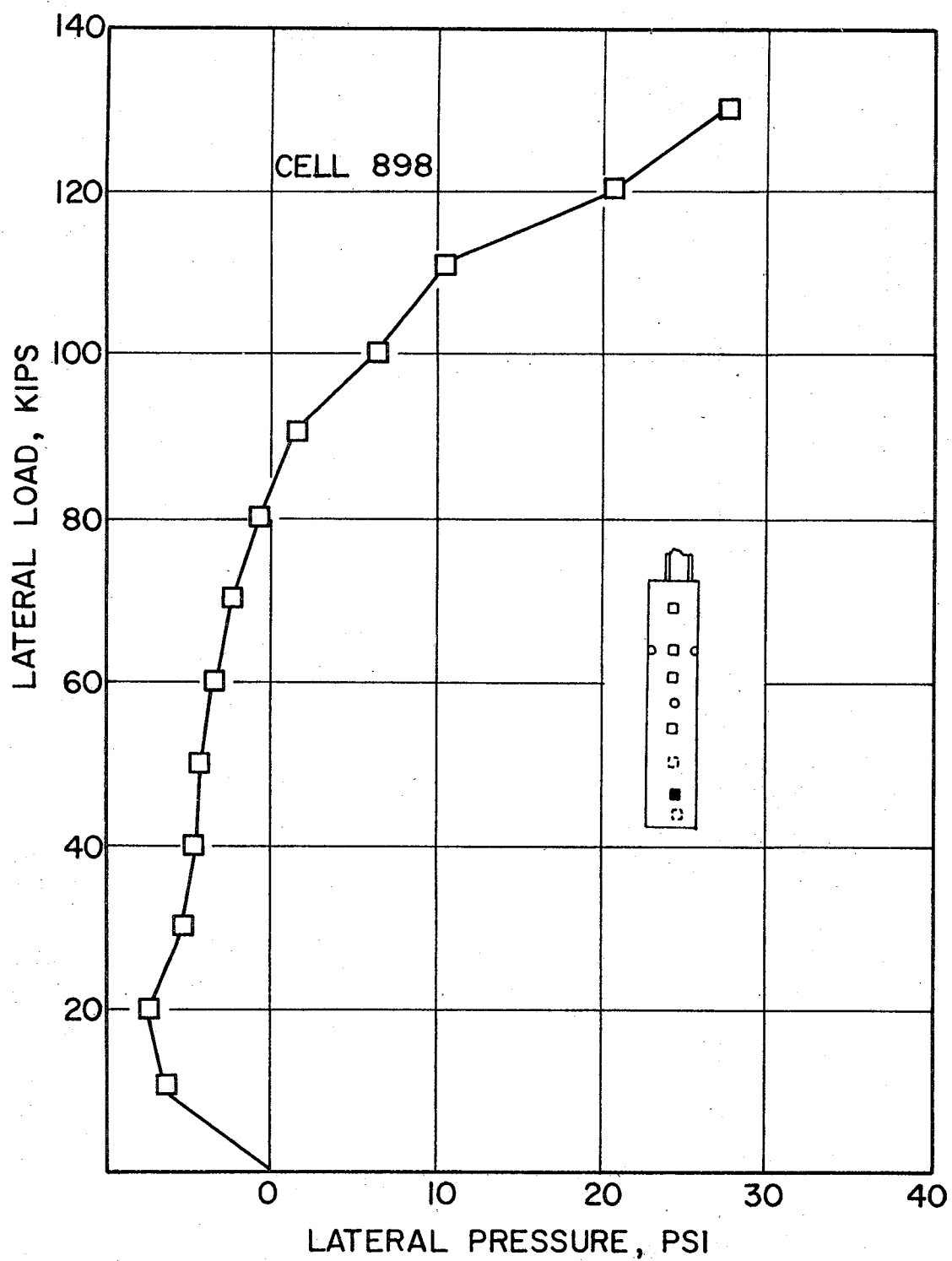


FIG. 23 - LATERAL LOAD VS LATERAL PRESSURE, CELL 898  
 1 kip = 4.45 kN ; 1 psi = 6.89 kPa

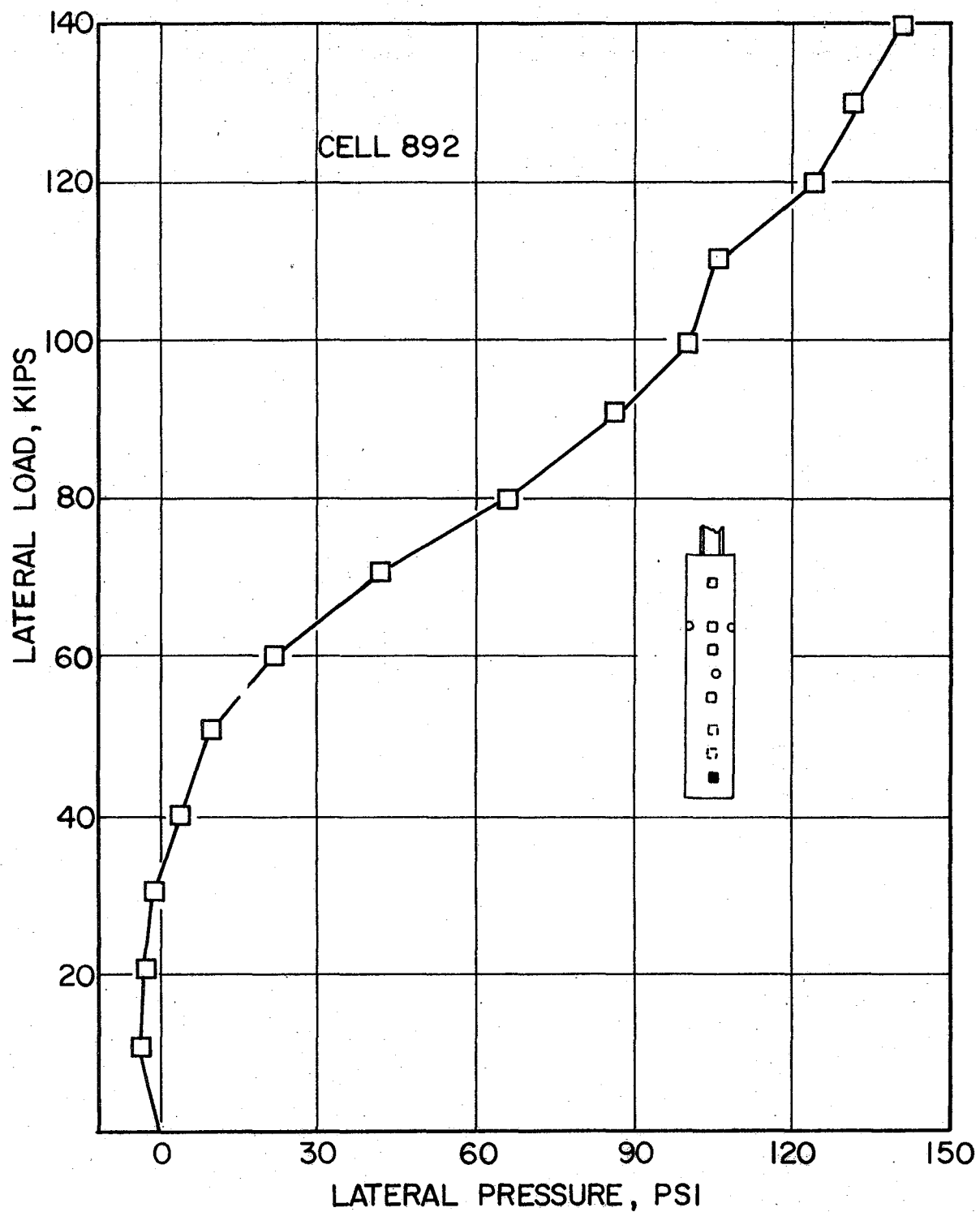


FIG. 24 - LATERAL LOAD VS LATERAL PRESSURE, CELL 892  
1 kip = 4.45 kN; 1 psi = 6.89 kPa

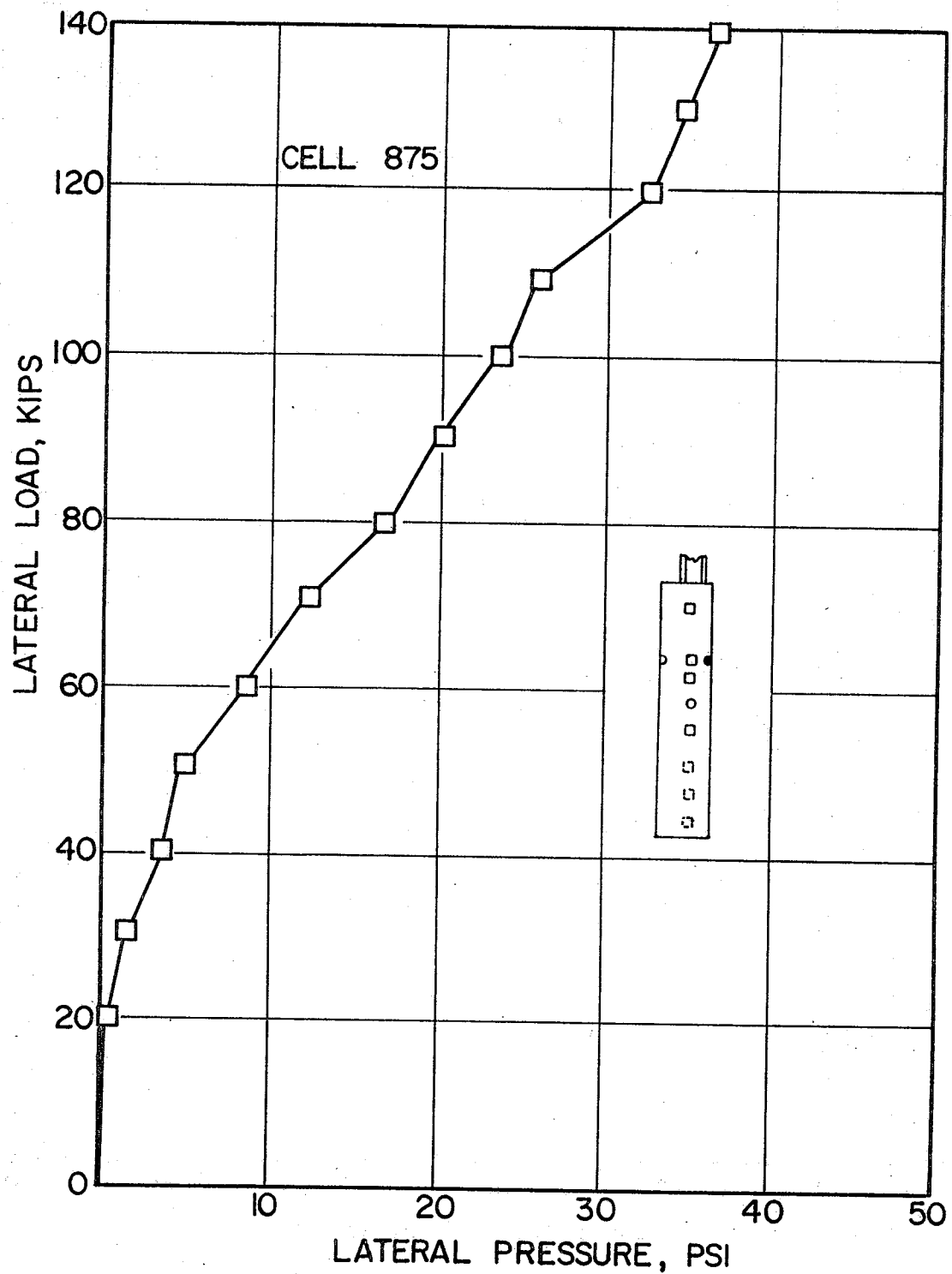


FIG. 25 - LATERAL LOAD VS LATERAL PRESSURE, CELL 875  
1 kip = 4.45 kN; 1 psi = 6.89 kPa

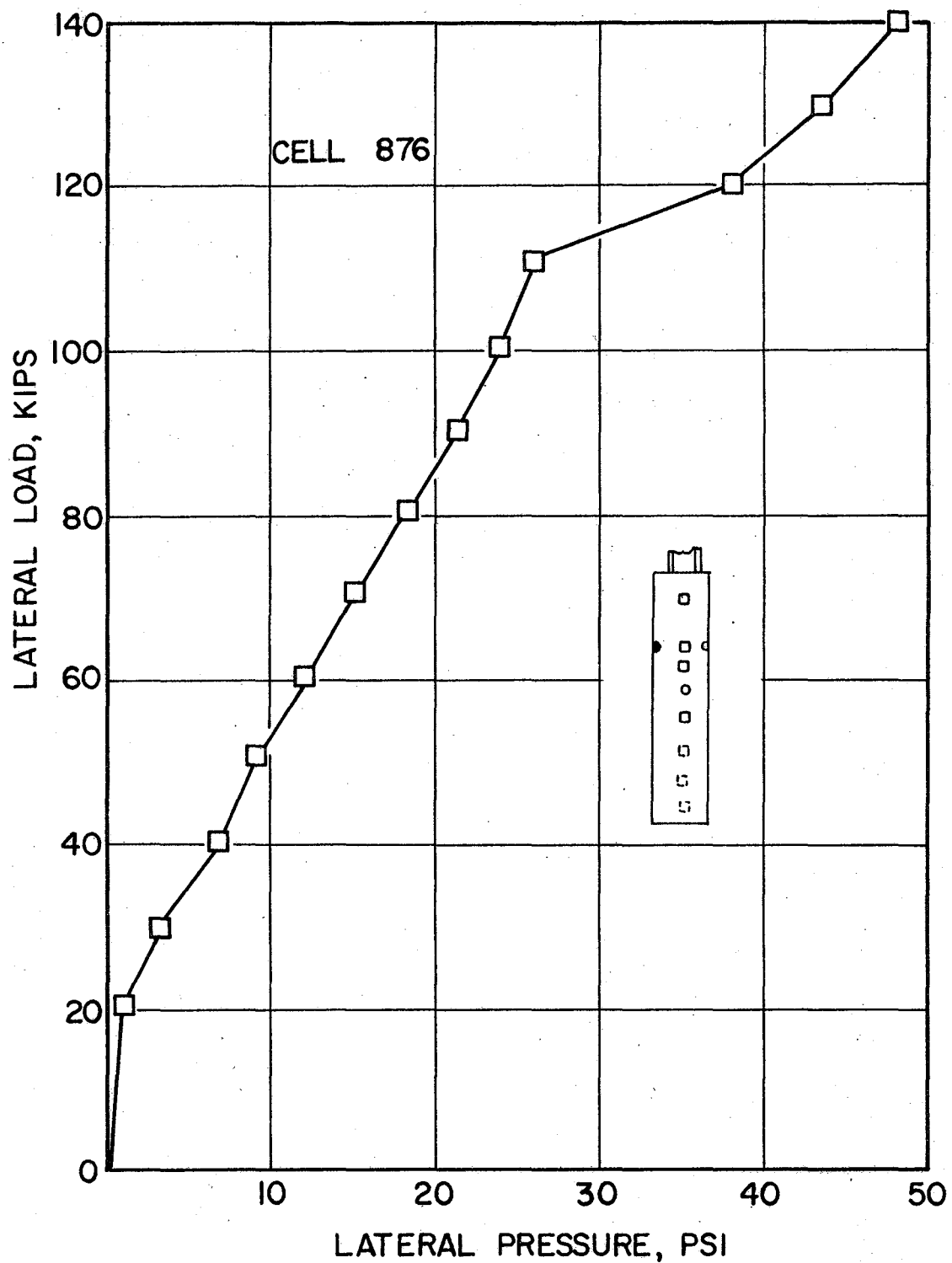


FIG. 26 - LATERAL LOAD VS LATERAL PRESSURE, CELL 876  
1 kip = 4.45 kN; 1 psi = 6.89 kPa

pressures sooner than cell 898 because larger movement into the soil occurred sooner at cell 892.

Initially it was assumed that the point of rotation caused by the lateral loading would be between 8.5 and 12.0 ft (2.59 m and 3.66 m) below the ground surface. Therefore, the cells located on the front side of the shaft in the direction of the applied load and the cells located on the back side of the shaft would all be recording passive pressures. The cell which recorded the highest pressure on the applied load side was the top cell (cell 885), and the highest pressure recorded on the back side in the direction away from the applied load was the bottom cell (cell 892).

The pressure cell data indicate that of the five cells which were in line with the applied load on the front of the shaft, the top three cells (885, 890 and 893) along with cell 886 exhibited considerable pressure increases while only a slight increase was recorded on the fifth cell (cell 878). The two cells (875 and 876) which were placed on the horizontal axis (see Fig. 15) with cell 890 also indicated some pressure increase but of a lesser magnitude than that recorded by cell 890. Of the three cells on the back side of the shaft, only the bottom cell (cell 892) indicated a significant increase in pressure. The remaining two cells (888 and 898) indicated only a slight increase in pressure.

The lateral pressures indicated by cells 885, 890, 893, 886, 888 and 892 when plotted with depth below the ground surface for the various lateral loads are shown in Fig. 27. It is interesting to note that the second cell from the top on the front side of the shaft (cell 890) recorded the highest pressures up to the 85-kip (378 kN) level.

Thereafter, the pressures indicated by the top cell (cell 885) were the highest pressures. Cell 885 recorded pressures nearly twice the amount recorded by the second cell (cell 890) as the loads reached the 120-kip (534 kN) level. Kasch (19) recorded similar pressure distributions in that the second cell below the ground surface recorded the highest pressure until the structural failure occurred and the test was terminated. The highest pressure for this test was recorded on the lowest cell (892) on the back side of the shaft at a depth of 14.0 ft (4.27 m) below the ground surface. The pressure on cell 888 remained essentially constant at less than 2.50 psi (17.25 kPa) until the latter stages of the test where it eventually increased to 8.0 psi (55.2 kPa). These data would seem to indicate that the rotation point of the shaft was in the general area of this cell. The pressures recorded from cells 878 and 898 did not correlate well with those cells positioned above and below. The complete data for cells 878 and 898 have already been presented and possible reasons for the erratic behavior have been given. Therefore, it was felt that the pressures recorded on cells 878 and 898 were questionable and these data have not been included in Fig. 27.

The pressures recorded by the three cells (875, 890 and 876) which were placed horizontally in the shaft at the 4.5-ft (1.37 m) depth are shown in Fig. 28. Since only one cell was placed on either side of cell 890, a complete pressure distribution could not be drawn. However, both cell (875 and 876) pressures were plotted on the opposite side corresponding to the same angle of rotation from the direction of applied load by assuming that these pressures would be the mirror image. The data presented in Fig. 28 illustrate the fact that the pressures

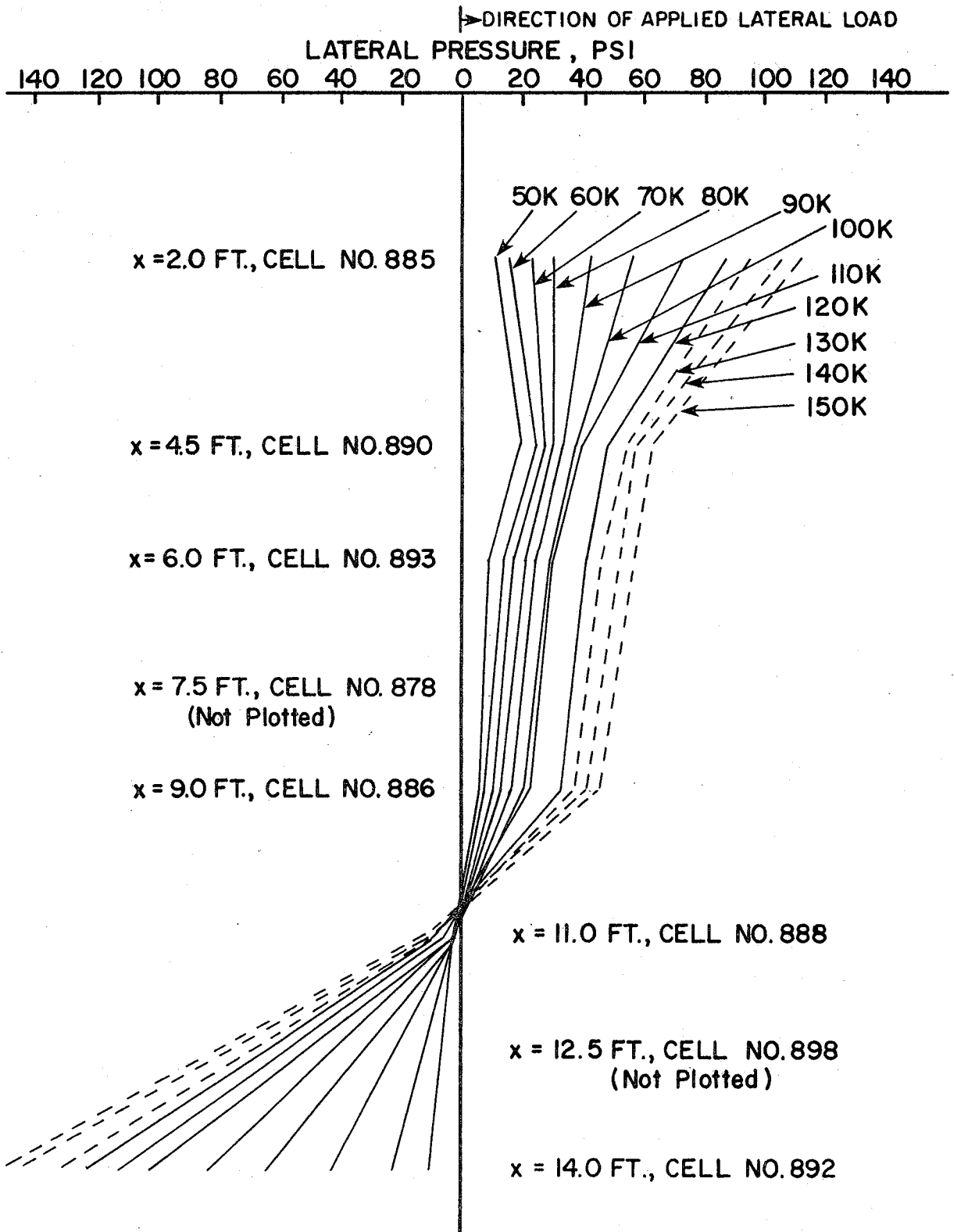


FIG. 27 - LATERAL PRESSURE VS DEPTH BELOW GROUNDLINE  
 $x = \text{DEPTH BELOW GROUNDLINE} ; 1 \text{ ft} = 0.3048 \text{ m} ;$   
 $1 \text{ kip} = 4.45 \text{ kN} ; 1 \text{ psi} = 6.89 \text{ kPa}$

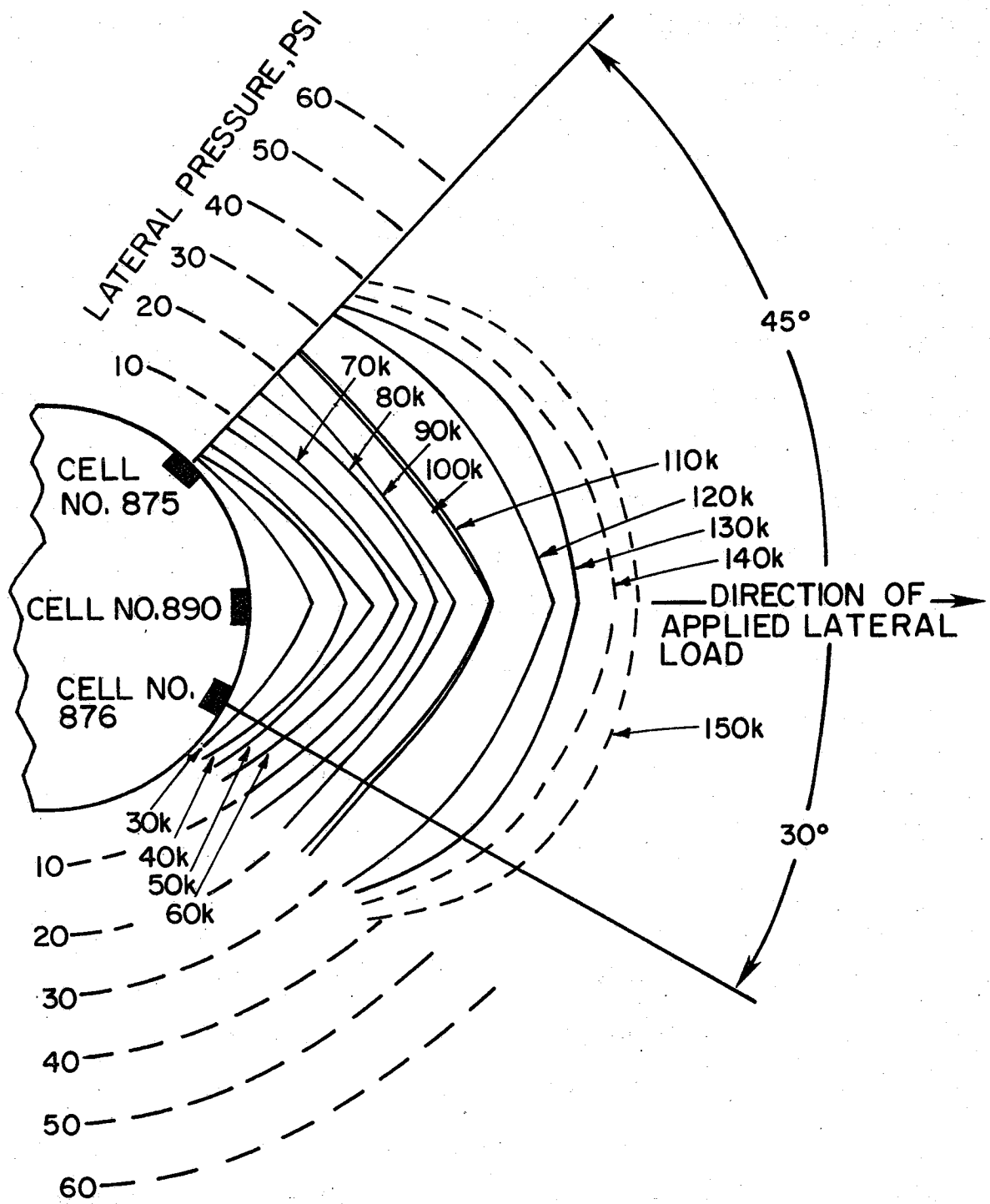


FIG. 28— HORIZONTAL PRESSURE VS LATERAL LOAD. 1 kip = 4.45 kN; 1 psi = 6.89 kPa

begin to drop significantly beyond an angle of  $30^{\circ}$  from the direction of the applied load.

#### Load-Deflection Characteristics

The measured values of lateral load versus groundline deflection for this test shaft are shown in Fig. 29. The groundline deflections were obtained by averaging the two dial gauge readings at a height of 9 in. (23 cm) above the ground surfaces. The deflection readings were taken immediately after each load was applied or at the time the deflection rate decreased to .001 in./min. (0.02 mm/min.) for loads below the 115-kip (512 kN) level. The readings where this rate was exceeded are shown as dashed lines in Fig. 29. These readings were taken when a constant rate of movement was obtained (see Appendix III). Deflection versus time curves for the test shaft are shown in Fig. 30. The dashed lines represent the time the load was held before a constant rate of movement was obtained.

#### Load-Rotation Characteristics

The load-rotation curve is shown in Fig. 31. If a value of 115 kips (512.0 kN) is taken as the ultimate load on the test shaft (see page 34), then the corresponding angle of rotation is approximately  $1.1^{\circ}$ . This is considerably less than the  $5^{\circ}$  rotation which Ivey and Dunlap (16) indicated that was needed to develop the ultimate soil resistance for minor service footings. It should be noted that this  $5^{\circ}$  rotation is based on measurements where the ratio of the height of the applied load above the ground surface to the depth of the shaft is approximately 2.0. The ratio for this study pertaining to retaining walls with much smaller

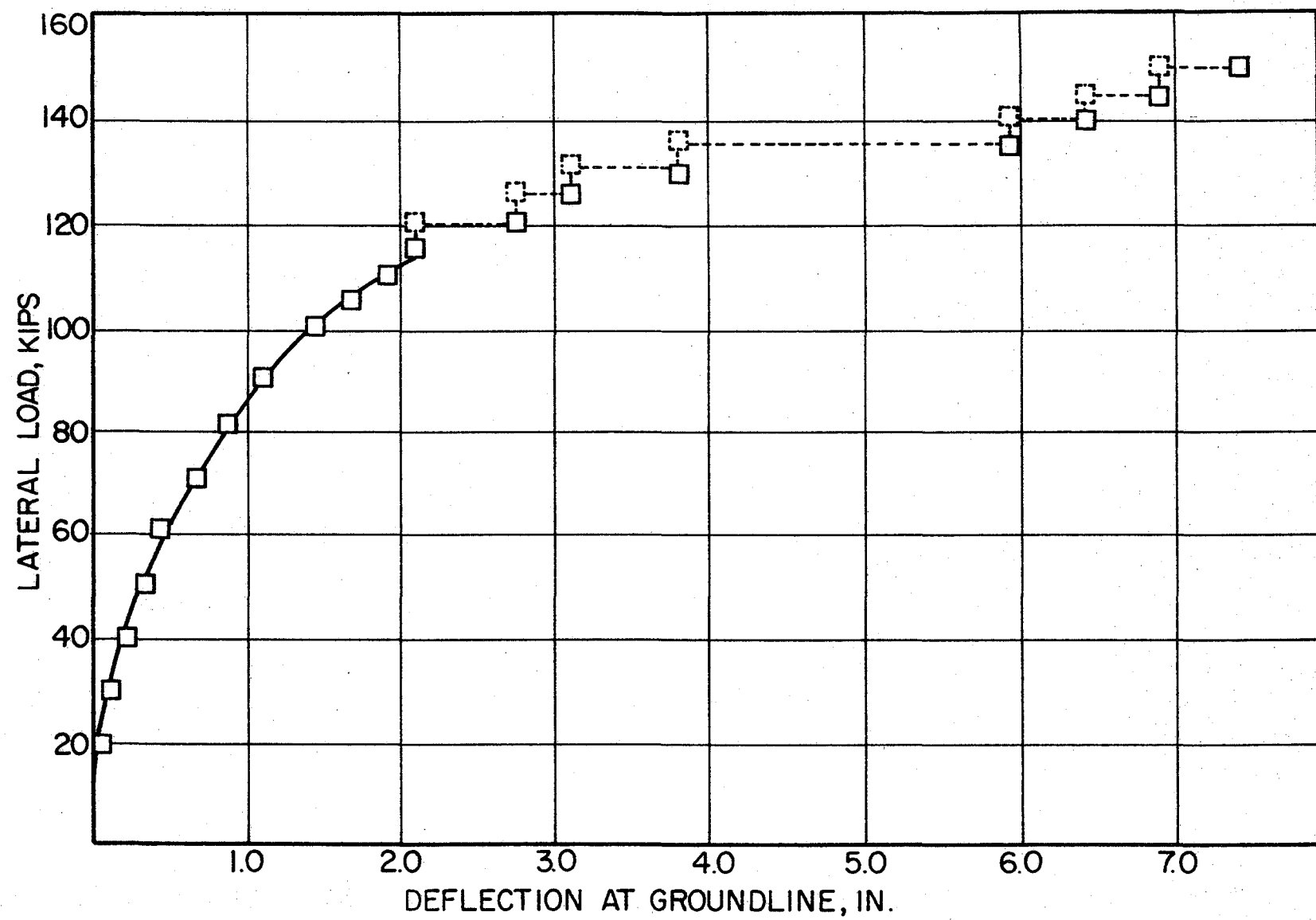


FIG. 29 - LATERAL LOAD VERSUS DEFLECTION AT GROUNDLINE  
1 kip = 4.45 kN, 1 in = 2.54 cm

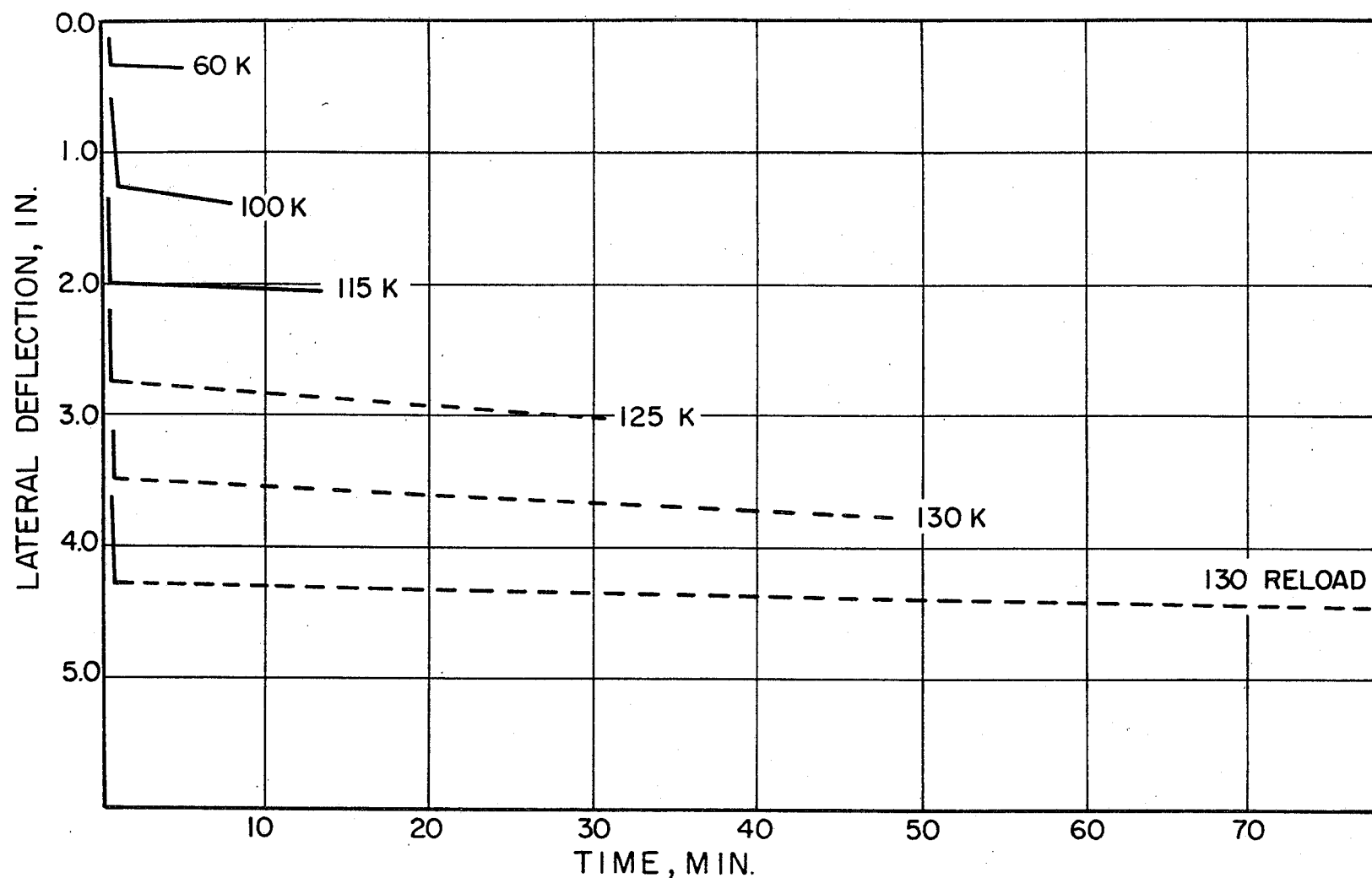


FIG. 30- LATERAL DEFLECTION VERSUS TIME  
1 kip = 4.45 k N, 1 in = 2.54 cm

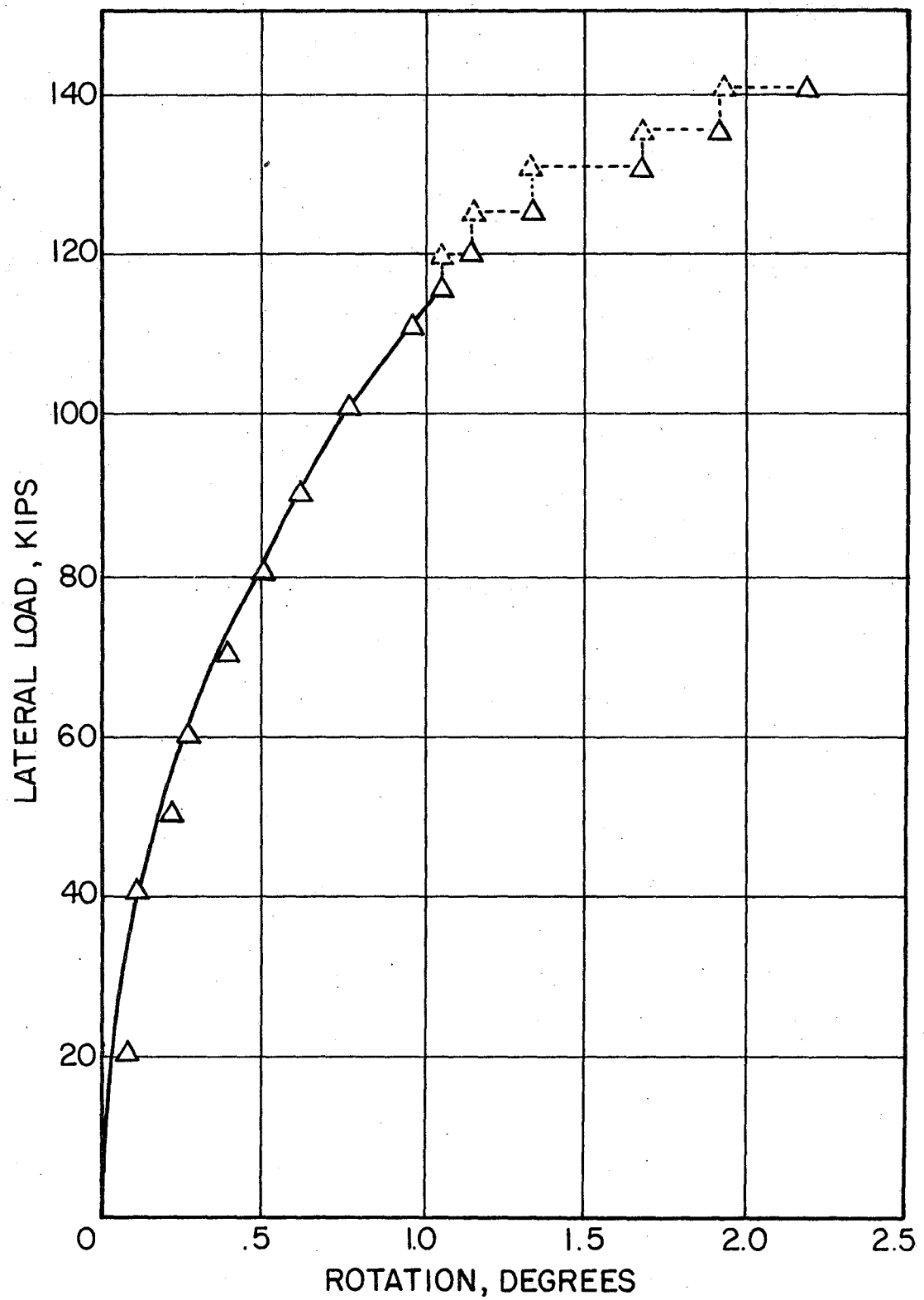


FIG. 31 - LATERAL LOAD vs. ROTATION  
1 kip = 4.45 kN

moment arms is less than 0.2.

The exact location of the point of rotation of the shaft is not well defined. The rotation point indicated by the pressure cell readings seemed to be occurring approximately 10.5 ft (3.2 m) below the ground surface or between pressure cells 886 and 888 (see Fig. 27). However, as the lateral load exceeded 115 kips (512.0 kN), the inclinometer and plumb-line readings indicated that the point of rotation was between 9.0 and 10.50 ft (2.75 m and 3.20 m). These points of rotation were obtained by dividing the measured deflection of the shaft at the ground surface by the tangent of the rotation angle. These measurements along with the point of rotation determined by the pressure cell readings seem to indicate that the approximate point of rotation is close to two-thirds the embedment depth. This agrees well with what other authors (4, 12, 13, 15, 16, 17, 18 and 32) have suggested. Analytical studies by Hays et al. (13) indicated that the rotation point did not remain in the same location but shifted downward from some point below the middle of the foundation element for light loads to a point beyond three-quarters of the embedment depth at failure loads. Table 2 indicates this phenomenon was occurring during this test but the point of rotation never extended beyond the three-quarters point.

#### Ultimate Soil Reaction

The value of 115 kips (512.0 kN) has been defined as the ultimate lateral load for this test shaft. It is felt that at this load level the amount of deflection which was occurring and the rate at which it was occurring would have caused an initial soil failure. It is possible that if the loads had been held for longer periods of time movement may

TABLE 2. - Rotation Point Below the Ground Line

Date	Load kips	Deflection (in.)	Average Rotated Angle, $\theta$ (Min.)	Rotation Point, Ft.	
				Inclinometer	Plumb-Line
5/23	0.000	0.000	0		
24	5.000	0.0035	0		
24	9.966	0.017	02.0	1.68	0.96
24	15.148	0.031	03.0	2.21	2.36
24	20.004	0.051	03.8	2.90	4.37
25	25.295	0.079	04.0	5.21	4.53
25	30.007	0.109	04.2	6.68	4.72
25	35.080	0.151	04.2	9.55	5.98
25	39.791	0.204	06.4	8.38	6.07
26	45.227	0.272	09.0	7.91	5.31
26	50.301	0.333	12.6	6.82	5.93
26	55.012	0.396	13.3	7.47	5.87
26	59.361	0.468	16.0	7.63	6.47
29	64.978	0.592	22.6	6.75	7.17
29	69.870	0.675	23.8	7.37	6.78
30	74.581	0.781	26.0	7.09	7.86
30	80.380	0.882	29.8	7.29	7.73
31	85.091	1.023	33.4	8.02	7.46
31	90.237	1.132	36.4	8.16	7.66
6/1	95.456	1.304	41.2	8.32	7.97
1	99.950	1.440	45.2	8.38	8.01
2	105.458	1.695	52.2	8.55	7.97
5	110.096	1.915	58.0	8.71	7.98
6	115.170	2.103	63.8	8.69	8.42
13	120.425	4.033	69.6	9.33	9.00
13	124.955	4.384	80.0	9.29	9.13
14	129.606	5.066	100.0	9.25	9.22
16	135.102	5.960	115.0	9.91	10.55
16	140.175	6.436	130.0	9.78	10.38

NOTE: 1 kip = 4.45 kN; 1 in. = 2.54 cm; 1 ft = 0.3048 m

have eventually ceased due to soil compression with a resulting increase in soil strength. However, for this test shaft, it is apparent that failure occurred somewhere between 115 and 140 kips (512 kN and 623 kN) because of the excessive amount of movement and rotation which was experienced above the 115-kip (512 kN) load level.

The maximum lateral soil pressure which was recorded by cell 885 (see Fig. 27) in the direction of the applied 115 kip (512 kN) lateral load was 76.4 psi (526.8 kPa). The corresponding value of maximum lateral soil pressure in the direction away from the applied lateral load was recorded by cell 892 (see Fig. 27) with a measured value of 114.5 psi (789.5 kPa). The lateral soil pressure is analogous to soil resistance and will be used hereafter to define pressures which were measured. Soil reaction should not be confused with soil resistance. Soil reaction is the soil resistance multiplied by the diameter of the shaft.

Below the point of rotation for a rigid shaft, the soil reaction is measured in the direction away from the applied lateral load. Therefore, at the point of rotation there is a reversal of soil reaction. This is the assumption made in a number of theories (4, 12, 13, 17, and 32) and is the basis for obtaining the static equilibrium. However, the assumption made in plastic design is that the soil reaction is ultimate over the full length of the cross section of a foundation element.

There are several theories which can be used to predict the ultimate soil reaction. Theories proposed by Rankine (35), Hansen (12), Matlock (23), Reese (28), and Hays (13) will be used to compare the

ultimate soil reaction,  $p_u$ , with the two maximum soil reactions obtained at cells 885 and 892 (see Fig. 15) for the 115 kips (512 kN) lateral load. The equations used to predict the ultimate soil reactions according to Rankine, Hansen, Matlock, Reese, and Hays are:

$$\text{Rankine: } p_u = (\gamma x + 2 C_u) B \dots \dots \dots \dots \quad (1)$$

$$\text{Hansen: } p_u = K_c C_u B \dots \dots \dots \dots \dots \dots \quad (2)$$

$$\text{Matlock: } p_u = \left[ 3 + \frac{\gamma x}{C_u} + \frac{0.5x}{B} \right] C_u B \dots \dots \dots \dots \quad (3)$$

$$\text{Reese: } p_u = \left[ 3 + \frac{\gamma x}{C_u} + \frac{2.83x}{B} \right] C_u B \dots \dots \dots \dots \quad (4)$$

$$\text{Hays: } p_u = 2\eta C_u B + \alpha x \dots \dots \dots \dots \dots \dots \quad (5)$$

The term,  $\gamma$ , is the unit weight of the overburden material and  $x$  is defined as the vertical distance below the ground surface. The term,  $B$ , is the diameter of the shaft and  $\eta$  is a soil strength reduction factor. The term,  $\alpha$ , is the slope of the Hays soil reaction curve (13). The terms  $K_c$  and  $C_u$  have been defined on pages 3 and 10 respectively.

A plot of ultimate soil reaction versus depth as determined by the different theories is presented in Fig. 32. Using the soil reactions obtained at the 2-ft (0.6 m) and the 14-ft (4.3 m) depths for the 115-kip (512 kN) load, the dashed curve in Fig. 32 is defined. This dashed curve seems to correlate rather favorably with the method presented by Matlock (23). The general slope of the curve is almost identical to those presented by both Matlock and Hays. The equation used by Matlock is of the same form that was developed by Reese (28) but has been empirically adjusted using the results of lateral load test on piles in soft clay. The equation used by Hays is basically the same as that used by Matlock except that Hays uses a factor of two times the

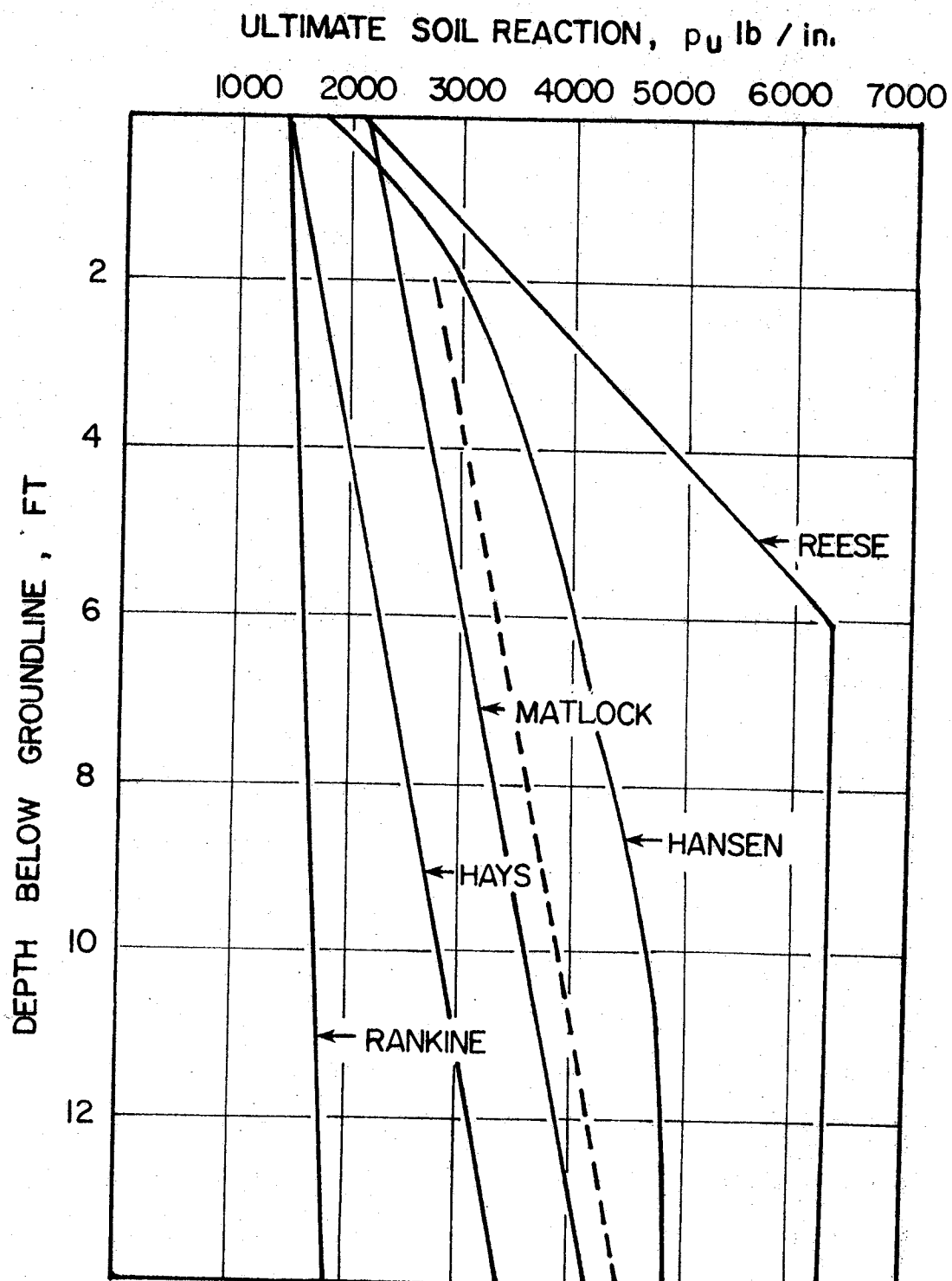


FIG. 32 – ULTIMATE SOIL REACTION VS. DEPTH  
BELOW GROUNDLINE  
1 ft = 0.3048 m; 1 lb / in. = 175 N / m

pile diameter for the ultimate soil reaction at the surface, whereas; Matlock uses a factor of three. In some instances Matlock's equation has predicted satisfactory results for lateral load tests in stiff clay, while Reese's equation has yielded values in excess of those determined experimentally (30, 37). It is possible to conclude that from the data presented and the studies reported by Reese (30, 37) that the Reese method may represent an upper bound for ultimate soil reaction.

The test conducted by Kasch (19) resulted in a structural failure before an ultimate soil resistance could be measured. However, Kasch did verify that the Rankine method was conservative. This fact was also verified by this test as shown in Fig. 32. On the basis of the comparisons discussed above, it seems that the Matlock method most closely predicts the ultimate soil reaction for this particular test site and the Hays method would be conservative. However, additional testing is needed and the correct ultimate load established before it can be determined which method can best predict the ultimate soil reaction.

#### Ultimate Load on Rigid Shafts

The methods previously discussed in the section on rigid behavior of laterally loaded foundations were used to calculate the ultimate loads that could be carried by this test shaft and six other rigid test shafts for which all necessary information was available. The measured ultimate load is the maximum lateral load that can be applied to the test shaft before continued foundation deflection and rotation will occur with no increase in load. A comparison of measured ultimate loads with predicted

ultimate loads for the seven test shafts is presented in Table 3.

Close examination of Table 3 shows that the Hay's (13) method seems to give the best correlation with measured field load for this current test. Also, the Southern California Edison (SCE) shafts 2 and 6 measured loads compare favorably with the loads predicted by the Hay's method. The predicted load for shaft 2 is conservative by 8%, while shaft 6 is conservative by 16%. It should be noted that both shafts 2 and 6 were approximately 15 ft (4.6 m) in depth and 4 ft (1.2 m) in diameter and the lateral load was applied 1 ft (0.3 m) above the ground surface. Shaft 7 was 9 ft (2.7 m) deep and 2 ft (0.6 m) in diameter and the lateral load was applied 1 ft (0.3 m) above the ground surface. For test shaft 7 the Hays method predicted an ultimate lateral load which was approximately 25% less than the measured value. In the paper which Hays et al. (13) published a comparison was made between 15 model tests and the ultimate load solution. From this model study it was concluded that the ultimate load solution was almost always conservative with a predicted mean of 0.61 times the mean of the actual loads. Hays attributed the reason for this conservatism to the relatively low depth to diameter ratio of the model test shafts.

As shown in Table 3, the Bryan and Galveston tests (project 105) produced loads which were higher than all five predicted loads. Hansen's method seems to give the best correlation for both of these tests. The first measured load value was obtained during the initial test both at Bryan and Galveston. A second test was conducted on the same size shaft and in the same soil where 50% of the maximum load was used. The load values from the second test are shown in parentheses.

TABLE 3. - Comparison of Measured Ultimate Loads with Predicted  
Ultimate Loads

METHOD	LOAD TEST						
	TTI Project 2211 (Current Test)	TTI Project 2211 (1977 Test)	TTI Galveston (Project 105)	TTI Bryan (Project 105)	Southern California Edison		
					Shaft 2	Shaft 6	Shaft 7
Measured Load, kips	115-140	169+	5.5 (2.4)*	12.4 (6.2)**	369	375	120
Ivey & Dunlap, with $\phi = 0$ , kips	94	130	1.35	8.72	315	288	80
Ivey & Hawkins, kips	62	89	0.96	5.94	179	166	45
Broms, kips	171	260	1.55	9.54	315	283	112
Hays, kips	131	221	1.75	8.94	341	314	90
Hansen, kips	183	271	2.02	12.4	528	495	116

\*Tested at 50% of load for  $5^0$  overturning rotation predicted by theory until  $2\frac{1}{2}^0$  rotation was obtained.

\*\*Tested at 50% of load for  $5^0$  overturning rotation predicted by theory until  $1\frac{1}{2}^0$  rotation was obtained.

+Ultimate load was not obtained because of structural failure

NOTE: 1 kip = 4.45 kN

These two tests cannot be compared in the same way as the other tests because these shafts were loaded with a constant lateral load over an extended period of time. However, it is interesting to note that the Galveston and Bryan tests reached a rotation of  $1\frac{1}{2}^0$  and  $2\frac{1}{2}^0$  respectively, for the 50% ultimate load.

Dunlap and Ivey (11) stated that the use of this percentage (50%) for long-term loads would probably result in significant rotations, and the engineer should decide what rotation is acceptable for a particular structure. It was also mentioned that if the rotation is limited by functional or aesthetic considerations the use of smaller rotations and loads may be necessary. It should be pointed out that for these two tests (Galveston and Bryan) along with the 15 model tests by Hays et al. (13) that the load was applied at a distance above the ground surface of approximately twice the buried depth of the test shaft. In addition, the depth to diameter ratios were much smaller than the TTI project 211 studies and the Southern California tests.

This information seems to indicate that as the depth to diameter ratio decreases, the Hays method predicts values which are more conservative than for larger ratios. This may possibly be due to the fact that the equation which Hays uses for soil reaction is conservative near the surface. Therefore, a better correlation may be obtained using the Hays method if the ultimate soil reaction predicted near the surface is increased.

The Ivey and Hawkins (17) method as shown in Table 3 which is based on the Rankine passive earth pressure theory consistently yields conservative predictions. This conservatism is also indicated in Fig. 29

since the measured ultimate soil reaction for the present study exceeds the Rankine predicted soil reaction. The method by Ivey and Dunlap is a semi-empirical method which involves the use of a modifying factor that is applied to the Rankine coefficients of passive and active earth pressures. The modifying factor is applied in the use of both the cohesive shear strength and the angle of shearing resistance when determining the ultimate load of a foundation. In order to calculate the predicted values presented in Table 3, the angle of shearing resistance was assumed to be equal to zero and the undrained shear strength was used as reported by the authors. This method (Ivey and Dunlap) seems to work well for small lateral loads but becomes more conservative for the larger lateral loads.

The method proposed by Broms (4) gives predicted loads which are reasonably close to the measured value in some cases. However, there is not a consistent trend in the predicted ultimate loads. Some predicted loads are conservative while others are unconservative. One very significant point concerning the Broms method is that the unit weight of the soil is not used anywhere in the calculations. All the other methods presented in Table 3 include the use of the unit weight of the soil along with the undrained shear strength,  $C_u$ , for calculating the ultimate load on a drilled shaft.

The method which Hansen proposes seems to give predicted loads which are generally unconservative but in a few cases the predicted loads are close to the measured loads. The Hansen method is not easily adaptable to a chart solution but requires only a few iterations for an ultimate load to be obtained. The earth pressure coefficient for

cohesion which is used in determining the soil reaction incorporates both the angle of shearing resistance and depth to diameter ratio. These factors are not included in all the other methods presented in Table 3 for calculating the soil reaction. Three of the methods (Ivey and Dunlap, Broms, and Hays) seem to give predicted values of ultimate lateral load which are close to each other and to the measured values. Therefore, any of the three methods could be used for design purposes, as long as a safety factor is included for added assurance that failure will not occur. However, since the Hays method does seem to correlate best with the load tests presented in Table 3, this method will be used, with a slight modification, as the recommended preliminary design criteria for this current study.

## PRELIMINARY DESIGN PROCEDURE

It is considered appropriate to use rigid foundation design procedures when designing drilled shafts to support precast panel retaining walls. There are several reasons for using the rigid design procedure. In the first place the lateral loads on most retaining walls should not be of such large magnitude as to necessitate a deeply embedded shaft that would require elastic analysis. Secondly, in most instances rigid design procedures are less complicated than elastic solutions because they do not require computer solutions. However, to be reasonably assured of rigid foundation behavior, the depth over diameter ratio of the drilled shaft should be limited to six (19, 38).

There are several other design parameters which must be obtained before the depth and diameter of a shaft supporting a retaining wall can be determined. These parameters include the resultant force acting on the retaining wall, the point of application of the resultant force, the undrained shear strength of the soil, the allowable shaft rotation, and the creep potential of the soil.

### Force Acting on Retaining Wall

The force acting on a retaining wall is the resultant of the lateral pressure in the backfill. Based on the results of a study conducted on an instrumented precast panel retaining wall, Wright et al. (39) developed an equation to predict the resultant force of a level, cohesionless backfill with no surcharge, acting on a retaining wall. The equation developed to predict this is:

$$Fr = 0.25 \gamma h^2 L (K_a + 0.8) \dots \dots \dots \dots \quad (6)$$

where  $h$  is the height of the wall and  $L$  is the length of the panel, pilaster to pilaster. The term  $\gamma$  has been defined in Eq. 1 (p. 59). The expression for  $K_a$  is the Rankine coefficient of active earth pressure, and is defined as follows:

$$K_a = \cos \zeta \cdot \frac{\cos \zeta - \sqrt{\cos^2 \zeta - \cos^2 \phi'}}{\cos \zeta + \sqrt{\cos^2 \zeta - \cos^2 \phi'}} \quad \dots \dots \dots \quad (7)$$

where  $\zeta$  is the angle of the slope of the backfill to the horizontal and  $\phi'$  is the effective angle of shearing resistance of the backfill material.

#### Application Point of Resultant Force

Wright et al. also developed an equation to calculate the location of the point of application of the resultant force,  $F_r$ , of a level backfill with no surcharge. The equation is:

$$H = \frac{h}{2} \cdot \frac{K_a + 0.267}{K_a + 0.8} \quad \dots \dots \dots \dots \dots \dots \quad (8)$$

where  $H$  is the distance from the ground surface to the point where the force is applied above the base of the retaining wall. The terms  $h$  and  $K_a$  were defined in Eqs. 6 and 7.

#### Soil Shear Strength

The State Department of Highways and Public Transportation often uses the Texas Cone Penetrometer Test as the primary means of determining soil shear strength in routine subsurface investigations.

Laboratory testing to determine soil shear strength is often omitted because of the additional expense involved. The TCP test consists of driving a 3.0 in. (7.6 cm) diameter cone attached to a drill rod, with a 170 lb (77.1 kg) hammer. The hammer is dropped 2 ft (0.61 m) for each blow. The cone is seated with 12 blows and the number of blows,  $N$ , required to produce the next foot of penetration is recorded (10).

An improved correlation between the TCP blow count,  $N$ , and the undrained shear strength has recently been reported by Duderstadt et al. (10). The correlation has been reported for highly plastic homogeneous clays (CH) and for homogeneous clays of low to medium plasticity (CL). The results were reported as:

$$\text{Homogeneous CH : } C_u = 0.067N \dots \dots \dots \dots \dots \quad (9)$$

$$\text{Homogeneous CL : } C_u = 0.053N \dots \dots \dots \dots \dots \quad (10)$$

If it is desired by the designer a factor of safety may be applied to the shear strength,  $C_u$ .

#### Allowable Shaft Rotation

If excessive rotation of the drilled shaft were allowed to occur, objectionable deflection of the panel retaining wall in terms of aesthetics and possibly serviceability would result. It is therefore desirable to incorporate a factor of safety to guard against this potential problem.

Based on the finding that the ultimate load of a rigid shaft for minor service structures generally occurs at a rotation of  $5^0$ , Ivey and Dunlap (16) proposed that the following equation be used as a factor of

safety against undesirable rotation:

$$p_{\theta} = \frac{Fr}{1 - \frac{(5-\theta)}{25}} \dots \dots \dots \dots \dots \dots \dots \quad (11)$$

where  $Fr$  is the resultant force transmitted from the wall to the shaft (from Eq. 6) and  $\theta$  is the desired limiting angle of rotation.  $p_{\theta}$  is the force acting at height,  $H$ , necessary to rotate the shaft through the limiting angle of rotation,  $\theta$ . However, the results of this current study indicate that the  $5^{\circ}$  rotation limit is too large for drilled shafts supporting precast panel retaining walls and is not applicable for this case as it was in the case of foundations of minor service structures. Therefore, it is proposed that the  $5^{\circ}$  rotation limit be changed to a value of  $2.5^{\circ}$  rotation. Thus, the equation to be used for factor of safety against undesirable rotation is as follows:

$$p_{\theta} = \frac{Fr}{1 - \frac{(2.5-\theta)^2}{6.25}} \dots \dots \dots \dots \dots \dots \dots \quad (12)$$

The amount of rotation producing undesirable lateral deflection is dependent not only upon the size and configuration of the wall but also upon the location. It was observed during this study that a total rotation of as much as  $2^{\circ}$  could be aesthetically objectionable. The total rotation actually consists of two separate movements after the lateral load is applied. The first is the initial rotation that occurs immediately after the application of the load. The second is a long-term rotation that occurs as a result of soil creep. In view of these considerations it is recommended that  $\theta$  be limited to  $1^{\circ}$  rotation or

less.

### Soil Creep

The time-dependent deformation behavior of a soil mass under a given set of sustained stresses is referred to as creep. There are many factors which probably contribute to creep in soils, but, each specific factor which influences the amount of creep is not completely known or understood. It is generally agreed that creep is a function of several variables including, soil type, soil structure, seasonal variation in temperature and moisture content, and stress history (6, 11). Therefore, the soil in contact with the drilled shaft supporting the panel wall will be subjected to the creep phenomena due to the sustained load being applied to the wall.

Dunlap et al. (11), in a study of sustained loads on drilled shafts, recommended that a factor of safety based on the soil type be applied to account for creep. A factor of safety of 3 is recommended for soft and stiff fissured clays. For stiff non-fissured clays, a factor of safety of 2 is recommended. It was stated that although these safety factors should result in a rotation that terminates, it is likely that the rotation will be significant and in the order of  $1^{\circ}$ . Therefore, if an appropriate safety factor for creep is used in conjunction with a limiting angle of rotation,  $\theta$  equals  $1^{\circ}$  or less, it is likely that the total shaft rotation will be limited to  $2^{\circ}$  or less.

### Drilled Shaft Design Method

Based on the data presented in Table 3, the method proposed by Hays

has been selected as the preliminary design method. However, a modification of the ultimate soil reaction at the ground surface,  $p_{u_0}$ , will be incorporated into the Hays method. This modification will involve an increase from a value of 2.0 to 2.25 for the constant multiplied by the undrained shear strength,  $C_u$ , and the diameter of the shaft,  $B$  (see Eq. 5). In order to expedite the design procedure, a dimensionless design chart developed by Hays (13) will be used as presented in Fig. 33. Since it is impossible to depict accurately all data with a family of curves, it may be necessary to develop additional data points. Also, a computer could be used to determine the exact ratio of  $S_u/p_{u_0}D$  needed in the solution for the ultimate lateral load,  $S_u$ . This would minimize the possibility of error introduced by interpolating. These points can be generated by using the following two equations:

$$S_u/p_{u_0}D = 2K - 1 + \beta (K^2 - .5) \dots \dots \dots \dots \quad (13)$$

$$(S_u/p_{u_0}D)(H/D) = -K^2 + .5 - \beta/3 (2K^3 - 1) \dots \dots \dots \quad (14)$$

$K$  is the ratio of  $x$  over  $D$  and  $\beta$  is a nondimensional variable expressed as the slope of the soil reaction curve times the diameter,  $B$ , and divided by the depth of the shaft,  $D$ .  $S_u$  is the ultimate lateral load and  $H$ ,  $x$  and  $p_{u_0}$  have been defined previously. Eq. 13 can be solved for  $K$  with selected values for both  $S_u/p_{u_0}D$  and  $\beta$ .  $K$  can then be substituted into Eq. 14 and the ratio of  $H/D$  is obtained. This procedure may be followed for different values of  $S_u/p_{u_0}D$  with  $\beta$  being constant until a complete solution is obtained.

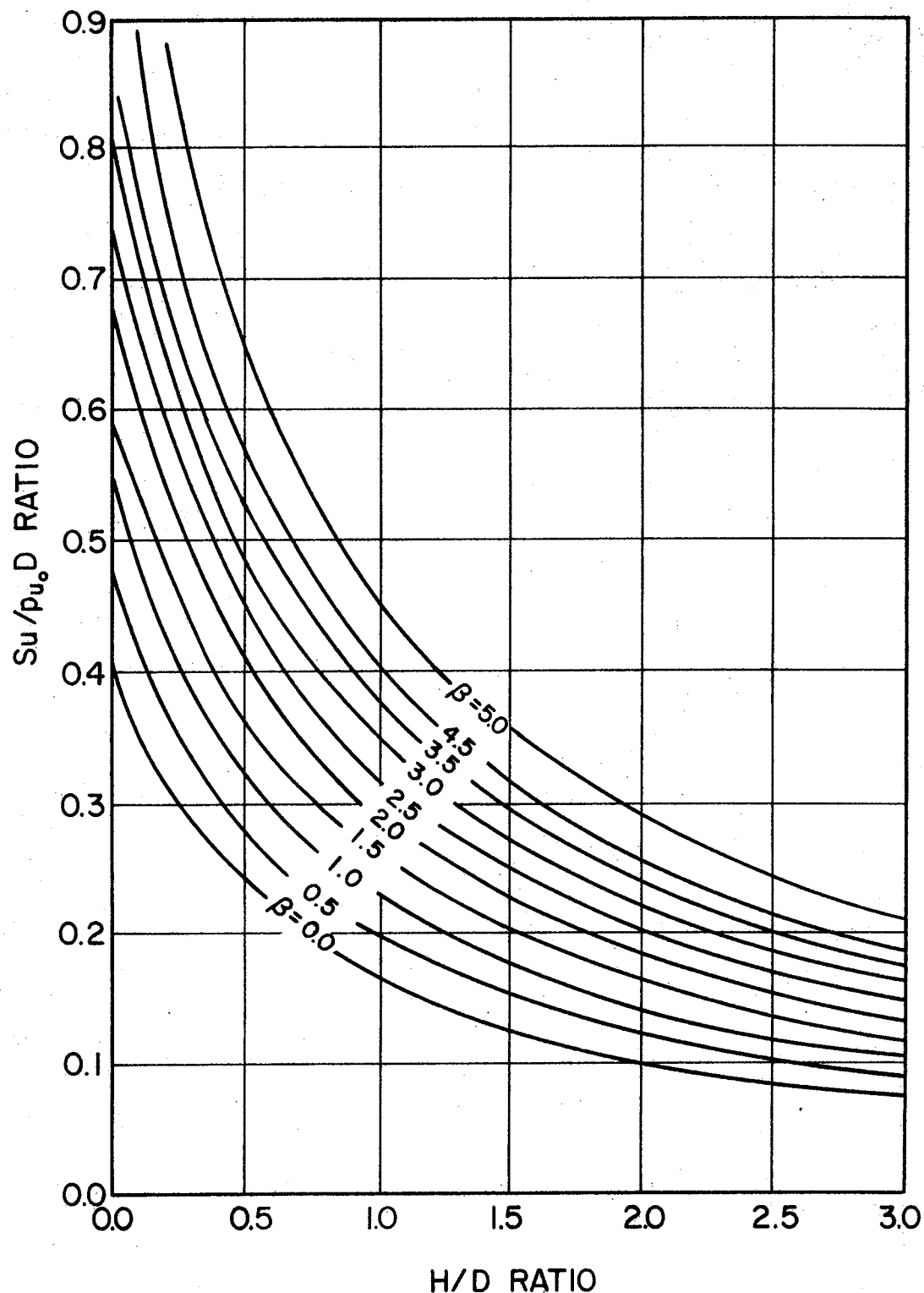


FIG. 33 - DESIGN CHART FOR COHESIVE SOILS  
(AFTER HAYS)

### Proposed Design Procedure

The following procedure is recommended as the preliminary design method for the design of drilled shafts to support precast panel retaining walls:

1. Use Eq. 6 to calculate the force,  $F_r$ , that will be applied to the shaft by the retaining wall.
2. Use Eq. 8 to calculate the point of application,  $H$ , of the force,  $F_r$ .
3. Set  $\theta$  equal to  $1^{\circ}$  or less and calculate the resulting force,  $p_{\theta}$ , using Eq. 12
4. Choose the appropriate factor of safety for soil creep and calculate the design force  $p_d$  as:  $p_d = p_{\theta}$  (F.S.)
5. Determine the undrained shear strength,  $C_u$ , of the soil by use of Eq. 9 or 10. A factor of safety may be applied if desired.
6. Choose a trial value for shaft diameter,  $B$ , and embedment depth,  $D$ .
7. Calculate  $x_r$  using the following operation:

$$x_r = 7 C_u B / (\gamma B + .5 C_u)$$

8. Calculate  $\alpha$  using the following equations:

$$\alpha = \frac{7 C_u B}{D} \text{ for } D > x_r$$

$$\alpha = \frac{7 C_u B}{x_r} \text{ for } D < x_r$$

9. Solve for the soil reaction,  $p_{u_0}$ , at the surface using the

following equation:

$$p_{u_0} = 2.25 C_u B$$

10. Calculate  $\beta$  using the following equation:

$$\beta = \frac{\alpha D}{p_{u_0}}$$

11. Determine the ratio of the height of the applied force, H, to the depth of the shaft, D.
12. Enter the design chart (Fig. 33) with  $\beta$  and H/D to obtain the ratio  $S_u/p_{u_0} D$ .
13. Multiply the ratio  $S_u/p_{u_0} D$  by  $p_{u_0} D$  to obtain the ultimate lateral load,  $S_u$ .
14. Repeat Steps 6-13 until the value calculated for  $S_u$  exceeds the design force,  $p_d$ , calculated in Step 4 by a minimum amount.

#### Example of Design Procedure

The following example is provided as an aid in the design of precast panel retaining wall foundations. A drilled shaft foundation is to be designed for the following situation:

A retaining wall is to consist of panels having a depth of 10 ft (3.05 m) and length of 12 ft (3.7 m). The backfill material will be clean sand having an effective angle of shearing resistance,  $\phi'$ , equal to  $36^\circ$  and unit weight,  $\gamma$ , equal to 115 pcf ( $18.1 \text{ kN/m}^3$ ). The backfill will have no additional surcharge and will have a horizontal slope. The subsoil at the construction site has been classified as a non-fissured

CH. The average N value obtained from the TCP test conducted at the site is 20. The unit weight of the subsoil is 130 pcf ( $20.4 \text{ kN/m}^3$ ). The limiting angle of rotation,  $\theta$ , is  $1^\circ$ .

Step 1a using Eq. 7:

$$K_a = \cos 0^\circ \left[ \frac{\cos 0^\circ - \sqrt{\cos^2(0)^\circ - \cos^2(36^\circ)}}{\cos 0^\circ + \sqrt{\cos^2(0)^\circ - \cos^2(36^\circ)}} \right] = 0.260$$

Step 1b using Eq. 6:

$$F_r = 0.25 (.115)(10)^2(12)(0.260 + 0.8) = 36.6 \text{ kips}$$

Step 2 using Eq. 8:

$$H = \frac{10}{2} \left[ \frac{0.260 + 0.267}{0.260 + 0.8} \right] = 2.49 \text{ ft}$$

Step 3 using Eq. 12:

$$P = \frac{36.6}{1 - \frac{(2.5 - 1)^2}{6.25}} = 57.19 \text{ kips}$$

Step 4: Calculate  $P_d$ ; soil conditions indicate that F.S. = 2.0.

$$P_d = 57.19 (2) = 114.38 \text{ kips}$$

Step 5:  $C_u = (0.067)(20) = 1.340 \text{ TSF} = 2.68 \text{ KSF}$

Step 6: Choose trial depth, D, and diameter, B.

Try:  $B = 3 \text{ ft}$

$D = 15 \text{ ft}$

Step 7: Calculate  $x_r$ :

$$x_r = \frac{7(2.68)(3)}{.130(3) + .5(2.68)} = 32.53 \text{ ft}$$

Step 8: Calculate  $\alpha$ ; the slope of the soil reaction curve:

since  $D < x_r$  then

$$\alpha = \frac{7(2.68)(3)}{32.53} = 1.73$$

Step 9: Calculate  $p_{u_0}$ ; the soil reaction at the surface:

$$p_{u_0} = 2.25 (2.68)(3) = 18.09 \frac{\text{kips}}{\text{ft}}$$

Step 10: Calculate  $\beta$ :

$$\beta = \frac{(1.73)(15)}{18.09} = 1.43$$

Step 11: Divide the distance to the point of application of the resultant force on the wall by the depth of shaft:

$$\frac{H}{D} = \frac{2.49}{15} = .17$$

Step 12: From the Design Chart (Fig. 33):

$$\frac{s_u}{p_{u_0} D} = .49$$

Step 13: Solve for the ultimate load:

$$s_u = (.49)(18.09)(15) = 133.0 \text{ kips}$$

$$133.0 > 114.4$$

∴ This solution is valid. However,  
a more optimum design may exist.

Repeat Steps 6 - 13.

Step 6: Choose a new trial depth, D, and diameter, B:

Try B = 3 ft

D = 14 ft

Step 7: Calculate  $x_r$ :

$$x_r = \frac{7(2.68)(3)}{.130(3) + .5(2.68)} = 32.53 \text{ ft}$$

Step 8: Calculate  $\alpha$ :

since  $D < x_r$  then

$$\alpha = \frac{7(2.68)(3)}{32.53} = 1.73$$

Step 9: Calculate  $p_{u_0}$ :

$$p_{u_0} = 2.25(2.68)(3) = 18.09 \text{ kips}$$

Step 10: Calculate  $\beta$ :

$$\beta = \frac{(1.73)(14)}{18.09} = 1.34$$

Step 11:  $\frac{H}{D}$

$$\frac{2.49}{14} = .18$$

Step 12: Using Design Chart:

$$\frac{s_u}{p_{u_0}D} = .48$$

Step 13: Solve for  $S_u$

$$S_u = (.48)(18.09)(14) = 121.6 \text{ kips}$$

$121.6 > 114.4$  This solution is also valid.

There may still exist a more optimum design, but the value calculated is close enough to the required value to perform satisfactorily with an added assurance of safety. Therefore choose the 3-ft diameter by 14-ft depth shaft.

## CONCLUSIONS AND RECOMMENDATIONS

The second year of a research study on the design of drilled shafts to support precast panel retaining walls has been completed. Progress has been made towards the improvement of design criteria for these drilled shafts. Based upon the analysis of the data obtained from the second lateral load test of an instrumented drilled shaft, the following conclusions and recommendations are made:

### Conclusions

1. Lateral deflections were of such magnitude near the end of the testing program that they would probably be aesthetically objectionable. It is concluded that allowable deflection or rotation rather than ultimate lateral load based on soil failure may be the controlling factor for the design of drilled shafts supporting precast panel retaining walls.
2. Based on the comparison of the measured versus predicted ultimate loads given in Table 3, the Hays method does give the best overall correlation of the different methods which were investigated. Therefore, the Hays method with slight modification is recommended for use as the preliminary design procedure.
3. The Hays method, the Broms method, and the Ivey and Dunlap method with  $\phi$  equal zero, all seem to predict values of ultimate lateral load which are reasonable. Therefore, it is concluded that any of these methods could be used if appropriate safety measures are incorporated into the

particular design method chosen.

4. The Ivey and Hawkins design method, which is based on Rankine's passive earth pressure formula, constantly predicted values of ultimate lateral load which were highly conservative. Therefore this method is not recommended.
5. The Hansen method seems to define an upper bound of values for ultimate lateral load and appear to be generally unconservative. Therefore, this method is not recommended.
6. The available test data which have been published are limited and the proposed preliminary design procedure should be used with caution. Therefore, some degree of conservatism is suggested by using conservative values of the limiting angle of rotation,  $\theta$ ; the factor of safety applied to the undrained cohesive shear strength,  $C_u$ ; and the factor of safety applied for soil creep.

#### Recommendations

1. Additional ultimate load tests should be conducted on shafts of varying depths and diameters.
2. A comprehensive definition of ultimate load based on limiting soil resistance and deformation is needed.
3. A limiting value for total deflection or rotation of a drilled shaft supporting a precast panel retaining wall should be determined.
4. Sustained lateral load tests should be conducted on shafts of varying depth and diameters in order to study the creep

phenomenon.

5. Other lateral load tests should be conducted in other soil types such as sand and silt.

## APPENDIX I - REFERENCES

1. Adams, J. I., and Radhakrishna, H. S., "The Lateral Capacity of Deep Augered Footings," Proceedings, Eighth International Conference on Soil Mechanics and Foundation Engineering, Vol. 2.1, Mockba, USSR, 1973, pp. 1-8.
2. Bhushan, Kul, Haley, Steven C., and Fang, Patrick T., "Lateral Load Tests on Drilled Piers in Stiff Clays," Preprints 3248, ASCE Spring Convention and Exhibit, Pittsburgh, Pennsylvania, April 24-28, 1978.
3. Bowles, Joseph E., Foundation Analysis and Design, 1st. ed., McGraw-Hill Book Co., New York, 1968, pp. 503-512.
4. Broms, Bengt B., "Lateral Resistance of Piles in Cohesive Soils," Journal of the Soil Mechanics and Foundation Division, ASCE, Vol. 90, No. SM2, Proc. Paper 3825, March, 1964, pp. 27-63.
5. Broms, Bengt B., "Lateral Resistance of Piles in Cohesionless Soils," Proceedings of the American Society of Civil Engineers, Journal of Soil Mechanics and Foundation Division, ASCE, Vol. 91, No. SM3, May 1965, pp. 79-99.
6. Broms, Bengt B., "Landslides," in Foundation Engineering Handbook, Winterkorn, Hans F., and Fang, Hsai-Yang (ed.), Van Nostrand Reinhold Co., New York, 1975, pp. 374.
7. D'Appolonia, Elio, D'Appolonia, David J., and Ellison, Richard D., "Drilled Piers," in Foundation Engineering Handbook, Winterkorn, Hans F., and Fang, Hsai-Yang (ed.), Van Nostrand Reinhold Co., New York, 1975, pp. 601-615.
8. Davisson, M. T., and Gill, H. L., "Laterally Loaded Piles in a Layered Soil System," Journal of the Soil Mechanics and Foundation Division, ASCE, Vol. 89, No. SM3, Proc. Paper 3509, May 1963, pp. 63-94.
9. DuBose, Lawrence A., "A Comprehensive Study of Factors Influencing the Load Carrying Capacities of Drilled and Cast in Place Concrete Piles," Texas Highway Department Project No. RP-4, Texas Transportation Institute, Texas A&M University, July 1956.
10. Duderstadt, Franklin J., Coyle, Harry M., and Bartoszewitz, Richard E., "Correlation of the Texas Cone Penetrometer Test N-Value with Soil Shear Strength," Research Report 10-3F, Texas Transportation Institute, Texas A&M University, September 1970.
11. Dunlap, Wayne A., Ivey, Don L., and Smith, Harry L., "Long-Term Overturning Loads on Drilled Shaft Footings," Research Report 105-5F, Texas Transportation Institute, Texas A&M University, September 1970.

12. Hansen, J. Brinch, "The Ultimate Resistance of Rigid Piles Against Transversal Forces," Danish Geotechnical Institute, Bulletin 12, 1961.
13. Hays, C. O., Davidson, J. L., Hagan, E. M., and Risitano, R. R., "Drilled Shaft Foundation for Highway Sign Structures," Research Report D647F, Engineering and Industrial Experiment Station, University of Florida, December 1974.
14. Heijnen, W. J., and Lubking, P., "Lateral Soil Pressure and Negative Friction on Piles," Proceedings, Eighth International Conference on Soil Mechanics and Foundation Engineering, Vol. 2.1, Mockba, USSR, 1973, pp. 143-147.
15. Ivey, Don L., "Theory, Resistance of a Drilled Shaft Footing to Overturning Loads," Research Report 105-1, Texas Transportation Institute, Texas A&M University, February 1968.
16. Ivey, Don L., and Dunlap, Wayne A., "Design Procedure Compared to Full-Scale Tests of Drilled Shaft Footings," Research Report 105-3, Texas Transportation Institute, Texas A&M University, February 1970.
17. Ivey, Don L., and Hawkins, Leon, "Signboard Footings to Resist Wind Loads," Civil Engineering, Vol. 36, No. 12, December 1966, pp. 34-35.
18. Ivey, Don L., Koch, Kenneth J., and Raba, Carl F., Jr., "Resistance of a Drilled Shaft Footing to Overturning Loads, Model Tests and Correlation with Theory," Research Report 105-2, Texas Transportation Institute, Texas A&M University, July 1968.
19. Kasch, Vernon R., Coyle, Harry M., Bartoskewitz, R. E., and Sarver, William G., "Design of Drilled Shafts to Support Precast Panel Retaining Walls," Research Report No. 211-1, Texas Transportation Institute, Texas A&M University, November 1977.
20. Lytton, Robert L., "Design Charts for Minor Service Structure Foundations," Research Report 506-1F, Texas Transportation Institute, Texas A&M University, September 1971.
21. McClelland, Bramlette, and Focht, John A., Jr., "Soil Modulus for Laterally Loaded Piles," Journal of the Soil Mechanics and Foundations Division, ASCE, Vol. 82, No. SM4, Proc. Paper 1081, October 1956, pp. 1081-1 - 1081-22.
22. Mason, H. G., and Bishop, J. A., "Measurement of Earth Pressure and Deflection Along the Embedded Portion of a 40-ft Steel Pile," ASTM Special Technical Publication, No. 154-A, 1954, pp. 1-21.
23. Matlock, Hudson, "Correlations for Design of Laterally Loaded Piles

- in Soft Clay," Preprints, Second Annual Offshore Technology Conference, Paper No. OTC 1204, 1970, pp. 577-594.
24. Matlock, Hudson, and Reese, Lymon C., "Generalized Solutions for Laterally Loaded Piles," Journal of the Soil Mechanics and Foundation Division, ASCE, Vol. 86, No. SM5, Part I, Proc. Paper 2626, October 1960, pp. 63-91.
  25. Osterberg, J. O., "Lateral Stability of Poles Embedded in a Clay Soil," Northwestern University Project 208, Bell Telephone Laboratories, Evanston, Illinois, December 1958.
  26. Outdoor Advertising Association of America, Engineering Manual, Outdoor Advertising Association of America, Chicago, Illinois, 1955.
  27. Prescott, David M., Coyle, Harry M., and Milberger, Lionel J., "Field Measurements of Lateral Earth Pressures on a Pre-Cast Panel Retaining Wall," Research Report No. 169-3, Texas Transportation Institute, Texas A&M University, September 1973.
  28. Reese, Lymon C., Discussion of "Soil Modulus for Laterally Loaded Piles," by Bramlette McClelland and John A. Focht, Jr., Transactions, ASCE, Vol. 123, 1958, pp. 1071-1074.
  29. Reese, Lymon C., Cox, William R., and Koop, Francis D., "Analysis of Laterally Loaded Piles in Sand," Preprints, Sixth Annual Offshore Technology Conference, Paper No. OTC 2080, 1974, pp. 473-483.
  30. Reese, Lymon C., Cox, William R., and Koop, Francis D., "Field Testing and Analysis of Laterally Loaded Piles in Stiff Clay," Preprints, Seventh Annual Offshore Technology Conference, Paper No. OTC 2312, 1975, pp. 671-690.
  31. Reese, Lymon C., and Welch, R. C., "Lateral Loading of Deep Foundations in Stiff Clay," Journal of the Geotechnical Engineering Division, ASCE, Vol. 101, No. 677, Proc. Paper 11456, July 1975, pp. 633-699.
  32. Seiler, J. F., "Effect of Depth of Embedment of Pole Stability," Wood Preserving News, Vol. 10, No. 11, November 1932, pp. 152-168.
  33. Shilts, W. L., Graves, L. D., and Driscoll, G. G., "A Report of Field and Laboratory Tests on the Stability of Posts Against Lateral Loads," Proceedings, Second International Conference on Soil Mechanics and Foundation Engineering, Vol. 5, Rotterdam, Holland, 1948, pp. 107-122.
  34. Stobie, James C., "Pole Footings," Journal of the Institute of Engineers, Australia, Vol. 2, 1930, pp. 58-63.

35. Terzaghi, Karl, and Peck, Ralph B., Soil Mechanics in Engineering Practice, 2nd ed., John Wiley & Sons, Ltd, New York, 1967, pp. 198-200.
36. Vesic, Aleksandar B., "Bending of Beams Resting on Isotropic Elastic Solid," Journal of the Engineering Mechanics Division, ASCE, Vol. 87, No. EM2, Proc. Paper 2800, April 1961, pp. 35-53.
37. Welch, Robert C., and Reese, Lymon C., "Lateral Load Behavior of Drilled Shafts," Research Report 89-10, Center for Highway Research, The University of Texas at Austin, May 1972.
38. Woodward, Richard J., Gardner, William S., and Greer, David M., Drilled Pier Foundations, McGraw-Hill Book Co., New York, 1972, 287 pp.
39. Wright, William V., Coyle, Harry M., Bartoskewitz, Richard E., and Milberger, Lionel J., "New Retaining Wall Design Criteria Based on Lateral Earth Pressure Measurements," Research Report No. 169-4F, Texas Transportation Institute, Texas A&M University, August 1975.

## APPENDIX II - NOTATION

The following symbols are used in this thesis:

B = foundation diameter;

$c_u$  = undrained cohesive shear strength;

D = embedded depth;

Fr = resultant force transmitted from retaining wall to  
drilled shaft;

H = height of lateral load application;

h = height of retaining wall;

K<sub>a</sub> = Rankine coefficient of active earth pressure;

K<sub>c</sub> = earth pressure coefficient;

L = length of precast panel;

N = blow count from TCP Test;

P<sub>d</sub> = design force;

p<sub>u<sub>o</sub></sub> = ultimate soil reaction at groundline;

P<sub>θ</sub> = force acting at height, H<sub>1</sub>, to rotate shaft through  
angle;

p = soil reaction;

p<sub>u</sub> = ultimate lateral soil reaction;

WF = wide flange;

x = depth below groundline;

θ = limiting angle of rotation;

β = nondimensional variable;

ϕ = angle of shearing resistance;

ϕ' = effective angle of shearing resistance;

$\alpha$  = slope of the Hays soil reaction curve

$\gamma$  = unit weight of overburden material

$\zeta$  = angle of slope of backfill to horizontal; and

$\eta$  = soil strength reduction factor.

### APPENDIX III - EXPLANATION OF SPECIAL LOADING PROCEDURES

Due to the design of the loading system and its inherent operating limitations, a constant lateral load was not maintained on the test shaft over an extended period of time. By the time the load had reached 115-kips (512 kN) it was apparent that for any given load the movement was continuing for an indefinite period of time. At this point in the loading procedure the decision was made to measure the length of time the shaft would continue to move under a given load and to determine if the movement would continue at a constant rate. This additional information was needed to determine when it would be reasonable to take representative pressure measurements and inclination readings for a given load. Therefore, two different methods were used in the loading procedure after the 120-kip (534 kN) level had been attained. These two methods were designated the "Constant Time Interval Method" and the "Average Load Method".

The Constant Time Interval Method consisted of two sets of measurements during a five minute period. The first measurement was made as soon as the load was reapplied and brought back up to the specified reading on the Budd indicator. The second measurement was the total movement of the shaft and was made at the end of the five-minute period. These measurements were continued until it was felt that a constant movement rate was obtained (even though the shaft was continuing to move). These movements are shown in Tables III-1 thru III-5 for the reapplication of load from the 120 kip (534 kN) level to that of the 130-kip (578 kN) reload level.

The Average Load Method consisted of setting the Budd indicator 50

TABLE III-1. - Deflections for Constant Time  
Interval (Reload 120 kips)

Time	Time Increment (Min.)	Dial Reading	Movement During	
		1 in.	Load Application	Time Interval Held
1140	5	0.986		
		0.924	0.062	
1145	5	0.914		0.010
		0.898	0.016	
1150	5	0.887		0.011
		0.878	0.009	
1155		0.866		0.012
		0.858	0.008	

NOTE: 1 kip = 4.45 kN; 1 in. = 2.54 cm

TABLE III-2. - Deflections for Constant  
Time Interval (Load 125 kips)

Time	Time Increment (Min.)	Dial Reading	Movement During	
		1 in.	Load Application	Time Interval Held
1210	5	0.834 0.798	0.036	
1215	5	0.761 0.744	0.017	0.037
1220	5	0.709 0.693	0.016	0.033
1225	5	0.659 0.642	0.017	0.034
1230	5	0.610 0.598	0.012	0.032
1235	5	0.573 0.558	0.015	0.025
1240		0.531 0.522	0.009	0.027

NOTE: 1 kip = 4.45 kN; 1 in. = 2.54 cm

TABLE III-3. - Deflections for Constant Time  
Interval (Reload 125 kips)

Time	Time Increment (Min.)	Dial Gage Readings		Movement During	
		1 in.	5 in.	Load Application	Time Interval Held
1105	5	6.372	3.842		
		0.296	3.780	0.076	
1110	5	0.270	-		0.026
		0.257	3.741	0.013	
1115	5	0.241	3.724		0.016
		0.227	3.710	0.014	
1120	5	0.215	3.698		0.012
		0.206	3.689	0.009	
1125	5	0.196	3.679		0.010
		0.186	3.668	0.010	
1130	5	0.176	3.658		0.010
		0.168	3.649	0.008	
1135		0.157	3.639		0.011

NOTE: 1 kip = 4.45 kN; 1 in. = 2.54 cm

TABLE III-4. - Deflections for Constant Time Interval (Load 130 kips)

Time	Time Increment (Min.)	Dial Gage Readings		Movement During	
		1 in.	5 in.	Load Application	Time Interval Held
1156		0.926	3.625		
1158		0.898	3.598	0.028	
1205		0.868	3.568		0.030
1210	5	0.848	3.547	0.020	
		0.834	3.530		0.014
1215	5	0.819	3.513	0.015	
		0.805	3.499		0.014
1220	5	0.789	3.484	0.016	
		0.776	3.469		0.013
1225	5	0.760	3.452	0.016	
		0.743	3.436		0.017
1230	5	0.730	3.422	0.013	
		0.714	3.406		0.016
1235	5	0.701	3.393	0.013	
		0.683	3.376		0.018
1240	5	0.671	3.364	0.012	
		0.658	3.352		0.013
1245	5	0.699	3.337	0.014	
		0.630	3.324		0.014
		0.619	3.312	0.011	
		0.595	3.288		

NOTE: 1 kip = 4.45 kN; 1 in. = 2.54 cm

TABLE III-5. - Deflections for Constant Time  
Interval (Reload 130 kips)

Time	Time Increment (Min.)	Dial Gage Readings		Movement During	
		1 in.	5 in.	Load Application	Time Interval Held
1103		0.478	3.176		
1110		0.420	3.116	0.058	
1115	5	0.405	3.100		0.015
	5	0.392	3.086	0.013	
1120		0.378	3.072		0.014
	5	0.366	3.062	0.012	
1125		0.354	3.050		0.012
	5	0.345	3.041	0.009	
1130		0.334	3.029		0.011
	5	0.326	3.022	0.008	
1135		0.317	3.012		0.009
	5	0.310	3.005	0.007	
1140		0.300	2.994		0.010
	5	0.392	2.986	0.008	
1150		0.277	2.972		0.015
		0.264	2.959	0.013	

NOTE: 1 kip = 4.45 kN; 1 in. = 2.54 cm

micro strains above the desired load and letting it drop to 50 micro strains below the load before reapplying it again. The time for this to occur and the measurement of the deflections between each application was recorded and shown in Table III-6.

As expected, the movement between each reapplication of the load was relatively constant, but the time between each increment was beginning to increase along with the movement between each interval. After two hours significant movements were still being observed at a nearly uniform rate. It was concluded that at this point that the deflection was both a function of the time the load was held and the load itself.

TABLE III-6. - Deflections for  $\pm$  50 Microstrain  
Range (Reload 130 kips)

Time	Time Increment (Min.)	Dial Gage Readings		Movement During	
		1 in.	5 in.	Load Application	Time Interval Held
1430	16	0.221	2.914		0.043
		0.196	2.889	0.025	
1446	26	0.179	2.872		0.017
		0.167	2.861	0.012	
1512	32	0.146	2.840		0.021
		0.136	2.829	0.010	
1544	40	0.114	2.807		0.022
		0.104	2.797	0.010	
1624		0.079	2.772		0.025
		0.069	2.762	0.010	

NOTE: 1 kip = 4.45 kN; 1 in. = 2.54 cm

**NOTES**

